FORSCHUNGSZENTRUM ROSSENDORF

WISSENSCHAFTLICH-TECHNISCHE BERICHTE
**FZR-295**
Juli 2000
ISSN 1437-322X

*Gerhard Brauer (Editor)*

# Construction and use of an Intense Positron Source at new Linac Facilities in Germany

**- Conceptual Report -**

# C O N S T R U C T I O N  A N D  U S E

# of an

# I N T E N S E  P O S I T R O N  S O U R C E

# at

# N E W  L I N A C  F A C I L I T I E S

# in

# G E R M A N Y

## - Conceptual Report -


**Principal coordinator:** G. Brauer (Dresden)

**Editorial board:** G. Brauer (Dresden)
R. Hippler (Greifswald)
R. Krause-Rehberg (Halle/Saale)
K. Maier (Bonn)

**Contributions from:** W. Anwand (Dresden)
V. Baryshevsky (Minsk)
C.D. Beling (Hong Kong)
G. Brauer (Dresden)
R. S. Brusa (Trento)
P.G. Coleman (Bath)
K. Flöttmann (Hamburg)
P. Hautojärvi (Helsinki)
R. Hippler (Greifswald)
G. P. Karwasz (Trento)
G. Kögel (München)
R. Krause-Rehberg (Halle/Saale)
R. Ley (Mainz)
A. Osipowicz (Fulda)
I. Prochazka (Prague)
H. Schneider (Giessen)
D. Segers (Gent)
P. Sperr (München)
H. Stoll (Stuttgart)
A. Zecca (Trento)

# CONTENT

# PREFACE

In 1993, connected with the workout of a "Profile paper" for the newly founded Research Center Rossendorf (FZR, founded 01.01.1992), its Institute of Nuclear and Hadron Physics suggested in 1993 the construction of a superconducting 250 MeV electron LINAC as a future basic instrument. Based on this suggestion and a corresponding recommendation of the scientific council of the FZR, conceptual studies of the "machine technical part" started and have been guided by D.Einfeld. For the "scientific case", a project group guided by H.Prade was constituted (19.01.1994) which mainly had to workout the possible scientific program in the field of nuclear, hadron, and radiation physics but also to show possible applications of such a LINAC for the other institutes of the FZR (Ion Beam Physics and Materials Research, Safety Research, Radiochemistry, Bioinorganic and Radiopharmaceutical Chemistry) as well as other users. In a letter dated 07.02.1994, H Prade kindly invited G.Brauer, head of the "Working Group on Positron Annihilation Spectroscopy" (based but not affiliated at FZR at that time) to contribute to the scientific case by outlining the possible construction of an intense positron source at the future LINAC and its use for the study of near-surface properties of solids.

Based on this invitation, ten institutions and their representatives in Germany, dealing with the use of positrons at that time in Germany, were contacted. Finally, for different reasons, mainly the cooperation with Mainz (R. Ley) and Giessen (H. Schneider) resulted in finishing a substantial chapter for the above mentioned scientific case.

Later in 1994 it became clear that finances for the construction and use of a 250 MeV LINAC at FZR will not become available, i.e. discussions then focused on the realization of its 20 MeV injector machine and their scientific use. Finally, in September 1996, finances have been approved for the construction and use of the superconducting LINAC "ELBE", with mentioning the option to use ELBE for positron production. The general interest of FZR in the use of positrons as a tool for research in three of its institutes has been demonstrated by a seminar series 1998/1999 "Positrons in Materials Science, Medicine, and Technics", including the following speakers for the Materials Science application: K.Schreckenbach (Munich), W.Triftshäuser (Munich), G.Brauer (FZR), A.Manuel (Geneva), K.Maier (Bonn), P.Hautojärvi (Helsinki), and R.Krause-Rehberg (Halle/Saale). The other applications (Medicine, Technics) mainly concerned PET (Positron Emission Tomography, Institute of Bioinorganic and Radiopharmaceutical Chemistry) and industrial applications (Technological applications of PET, Institute for Safety Research).

Since 1996, conceptual work at FZR has been continued in cooperation with colleagues from Mainz (R.Ley), Giessen (H.Schneider), Norwich (P.G.Coleman), Greifswald (R.Hippler), Fulda (A.Osipowicz), Ft.Worth/TX (C.A.Quarles), Minsk (V.Baryshevsky), Hong Kong (C.D.Beling), Prague (J.Kuriplach), and Trento (A.Zecca), and presented to the board of directors of FZR on 14.06.1999.

Independent from the conceptual work at FZR, the University of Halle-Wittenberg (R.Krause-Rehberg), in cooperation with the Tesla Test Facility (TTF) at DESY/Hamburg (K.Flöttmann), in 1999 considered the idea to possibly use TTF to create an European Positron Source for Applied Research (EPOS), too. Therefore, a workshop has been organized at DESY in September 1999 (about 40 participants from 24 facilities of 11 European countries) to discuss this option in more detail. The participants generally agreed that such a positron source would open up new possibilities for the common research field.

The two main directors, F.Pobell (FZR) and D.Trines (TTF), participated in the workshop held at DESY and their opinions have been very valuable for the further efforts towards the realisation of EPOS. It became clear that EPOS should be realized at one location, i.e. Rossendorf or Hamburg, only, and that the first step on the way of realization of EPOS is to fix and submit a "Conceptual Report". This report has now been compiled from contributions of 20 authors from 8 countries and is presented here.

It should be stressed that the report contains not only the outline of obvious applications in atomic physics, materials science, and surface physics but several new methodical developments which will be possible only when having a high intense positron beam at hand. These are e.g. advanced positron lifetime measurements based on multi-detector arrangements, advanced options for a chemical analysis by positrons, and a new methodology to characterize semiconductor defects by P-DLTS. A high positron intensity will also allow for the use and further development of image-creating applications being of special interest for industrial applications.

Gerhard Brauer (Dresden)
Reinhard Krause-Rehberg (Halle/Saale) June 2000

## ABSTRACT

In this conceptual report the idea to establish an European Positron Source for Applied Research („EPOS“) based on new LINAC facilities in Germany (ELBE/Rossendorf or TTF-DESY/Hamburg) is considered. The report contains not only the outline of obvious applications in atomic physics, materials science and surface physics, but also several new methodical developments which are only possible with an intense positron beam. This opportunity will also allow the use and further development of imaging techniques being of special interest for industrial applications.

**Keywords:** positron, intense positron beam, linac, atomic physics, materials science, surface physics, image-creating applications

## 1. INTRODUCTION

P.Hautojärvi (Helsinki)

When positrons enter condensed matter they rapidly loose all their energy. Their annihilation is announced by 511-keV photons whose energies, momenta and time of emission may be measured with high precision. The utility of positron annihilation studies relies on the fact that these annihilation characteristics reflect the electronic and defect structures of the matter.

Because the information is carried out by penetrating gamma radiation, the positron technique provides a nondestructive and noncontact method applicable to all types of materials. Regions from surface to bulk can be probed by varying the initial positron energy.

The positron, as the antiparticle of the electron, was discovered around 1930. The development of the positron annihilation studies began in 1950's, when it was realized that the small deviation from collinearity of two annihilation photons gives the momentum of an annihilating electron. Modern ACAR (Angular Correlation of Annihilation Radiation) measurements with position sensitive detectors have provided valuable and often unique information on electronic sturctures in metals, alloys, semiconductors, and superconductors.

The remarkable sensitivity of positrons to vacancy-type defects was discovered at the end of 1960s. This was attributed to positron trapping. Because of the positive charge, positrons are strongly repelled by the positive ion cores in solids. Atomic-size open volumes like vacancies are attractive trapping centers for positrons giving rise to measurable changes in annihilation characteristics. Especially the increase in positron lifetime due to locally reduced electron density is the fingerprint of a vacancy or vacancy cluster. The positron technique has great advantages in defect spectroscopy. It has specific sensitivity to vacancy-type defects making the identification of such defects straightforward. The technique is well supported by theory, since the experimental signal arising from electrons can be accurately calculated.

The experimental and theoretical basis of the positron spectroscopy of defects in metals was developed in 1970's. Notable successes from this period are the determination of vacancy formation enthalpies in metals and alloys, and the direct observation of vacancy migration at so-called stage III in irradiated metals. In 1980's interest in semiconductor applications started gradually to arise. Due to more complicated positron interactions and defect structures, the sufficient level of understanding has been reached around 1990. As great successes one should note the studies of the role of vacancies in doping and compensation as well as the verification of the vacancy character of the metastable defects EL2 in GaAs and DX in AlGaAs.

The progress in physics and applications of positron annihilation has always been strongly coupled with the development of experimental techniques. Fast solid-state electronics became available in 1960's and made possible to detect the positron trapping at vacancies via the lifetime increase. The high-resolution Ge detector for gamma spectroscopy was developed in the beginning of 1970's and applied immediately to study the Doppler broadening of the annihilation radiation. This became a fast and easy method to trace defects under various conditions and initiated the real positron defect spectroscopy.

Around 1980 the low-energy positron beams opened the avenue to study surfaces, thin surface layers and buried interfaces. The enthusiasm towards experiments on clean metal surfaces was high. Various counterparts to electron spectroscopies were developed in 1980's: low-energy positron diffraction, positron-induced Auger-electron spectroscopy, positron energy-loss spectroscopy, positron and positronium re-emission spectroscopy, and positron microscopy. Unfortunately, much of this activity, although pysically well justified, has faded away because of the low intensity of the available positron beams.

The positron-beam technique is crucial for the today´s defect spectroscopy, because novel materials, like semiconductors and superconductors, are often available only in the form of thin layers. Many groups have their own laboratory beams based on positron-active radioisotopes. The beams have low intensity but are

appropriate for defect studies by Doppler broadening. However, only a few positron lifetime beams exist and thus the lifetime information, which gives directly the open volume of a defect, is practically not available for thin layer investigations.

A high-intense pulsed positron beam would satisfy the current needs of the positron annihilation spectroscopy. It would complement the existing laboratory equipments and put into blossom the sophisticated positron spectroscopies already developed. It would give the opportunity to fully utilize the unique features of positrons in studying both electronic and defect structures of surfaces, surface layers, buried interfaces as well as bulk materials.

## 2. SCIENTIFIC AND INDUSTRIAL DEMANDS

G. Brauer (Dresden)

In September 1999, a workshop has been spontaneously organised at DESY/Hamburg by the University of Halle-Wittenberg to consider and discuss the idea to possibly use the Tesla Test Facility (TTF) at DESY/Hamburg to create an intense European Positron Source for Applied Research („EPOS"). The resonance to this short-term organised workshop has been unexpectedly high and is demonstrated from the attendance of about 40 participants from 24 facilities in 11 European countries. At the workshop it turned out that at Research Center Rossendorf similar plans currently are under consideration by the positron group established there in order to make use of the new superconducting LINAC ‚ELBE' at Rossendorf which is based on the same accelerating structures like the TTF at DESY/Hamburg.

The demand of having an intense positron source for applied research, especially for the development of positron microscopy and new types of surface analysis using positron has been present in the positron community since the eighties when positron moderators of acceptable efficiency were developed to produce monoenergetic positrons.

In the USA this development focussed mainly on two locations: Brookhaven National Laboratory (reactor-based positron production) and Lawrence Livermore National Laboratory (LINAC-based positron production). Although attempts have been made over the last twenty years to still establish other intense positron projects, it has to be stated that since about 1996 only LLNL survived finally. Efforts are undertaken at LLNL to establish there finally a national center for applications of positron beam spectroscopies and to develop a positron microscope based on positron lifetime spectroscopy.

In Japan this development focussed mainly at Tsukuba where different laboratories are grouped at a LINAC used for positron production.

In Europe the situation and development is unsatisfactory. A project started in 1988 to establish an intense positron source for applied research at PSI/Switzerland has been given up after about 10 years. A European meeting organised by the University College London, and held at London in September 1995, just stated the demand of a may be accelerator-based intense positron source but never resulted in any project aiming to start such a business at a (not agreed at that time) place in Europe. Two reactor-based projects for establishing an intense positron source in the frame of a local university center are under development since years in Europe (Technical University Munich/Germany, Technical University Delft/The Netherlands) but their finishing, future operation and public access as a general user facility needs to be demonstrated within the next years.

Therefore, and not unexpectedly, the idea of establishing some LINAC-based user facility either at Rossendorf or Hamburg attracted a lot of attention among the European positron community, and even the groups working on reactor-based projects were attracted and participated in the workshop held recently. Although the discussions at the workshop can not be considered final and satisfactory in all respects towards the aimed goal, it must be stated that there exists sufficient expertise and experience in Europe to finally create and operate the wanted facility. And it is very certain that there would be sufficient demand for beam time to do research at an intense positron source and that there would be no serious competition for getting users if the two reactor-based local facilities will finally start operation one day. Therefore, the option of establishing a LINAC-based positron production and user facility either at Rossendorf or Hamburg should be carefully considered and a project when ready pushed by the community.

This Conceptual Report is aimed at collecting and demonstrating the existing experience and knowledge to realize such a project in the near future. It contains not only the outline of obvious applications in atomic physics, materials science and surface physics but several new methodical developments which will be possible only when having a high intense positron beam at hand. A high positron intensity will also allow for the use and further development of image-creating applications being of special interest for industrial applications.

Materials science is the most important part of applied industrial research. The development of modern materials (metals, semiconductors, plastics, combined materials) using innovative, high efficient processes requires a comprehensive analysis of mechanical, structural and electrical properties in macroscopic as well as in microscopic dimensions. Many experimental methods allow to investigate single phenomena or the behaviour of materials. Today's complex problems of materials science (especially in the semiconductor field) can be solved only by combining various techniques and by co-operation of scientists from academic institutions and industry.

The exploding semiconductor market is driven by the growing demand for wireless communication, powerful illumination by LED's, opto-electronic and LASER applications, high performance computing, solar energy generation etc. Simultaneously, the integration and the power density of the devices increases. Established semiconductors (Si, GaAs) as well as relatively new materials (SiC, GaN, $CuInSe_2$,...) have to be produced with lower impurity contents in order to fulfil the requirements of electronic and opto-electronic devices. Therefore, the importance of intrinsic as well as doping-induced defects strongly increases for all types of applications.

In the last decade, improvements of the theoretical understanding and the experimental techniques of positron annihilation spectroscopy (PAS) made it possible to give reliable qualitative and quantitative information about defects in semiconductors and metals on an atomic scale. Some of the results are even important for industrial research and have supported the development of new technologies and materials.

The disadvantage of the methods of PAS up to now is that mostly "scientific" samples (bulk or specially layered) can usually be investigated. However, today and in future many problems in the semiconductor industry are associated with layered or even laterally structured samples produced by oxidation, ion implantation, epitaxial growth, mechanical, or etch processing etc., which can be investigated by advanced slow positron beams and positron microscopes only. On the other hand, the count rates for laboratory positron sources of such machines is limited. Measurements with a high depth and lateral resolution and the application of advanced coincidence techniques do require a lot of time. Therefore, systematic investigations of the formation, behaviour and annealing of lattice defects in industrial samples are extremely rare. High-intense positron sources offer the way out of this dilemma. These are able to produce a positron beam with a high depth, lateral, time, and energy resolution to perform advanced positron experiments on even industrial samples.

The growth of the innovative high technology industry in Germany, and especially in the regions Saxony (Sachsen), Thuringia (Thüringen), and Berlin is based, and will be based in the future, on the strong scientific background available in basic and applied research at Universities, Max-Planck- and Fraunhofer-Institutes, and other research institutions.

Exemplarily, some of the high-technology semiconductor companies of the regions mentioned above which are developing new technologies and products are listed here:

AMD Dresden (computer processors)
Infineon Dresden (memory chips)
Freiberger Compound Materials (GaAs wafers )
Wacker Siltronic Freiberg (Si wafers)
Bayer Solar Freiberg (solar cells)
Jenoptik Jena (semiconductor optics)
SCHOTT Jena (optics)
OSRAM (LASER)

In the regions of Dresden, Chemnitz, Jena, Halle/Leipzig, and Berlin as well as in Germany and Europe many more small innovative companies exist in the field of electronics, optics, biotechnology, and energy generation. The industrial research is playing a key role for the development of these companies. Therefore, the co-operation with research institutions to solve real problems of materials science in reasonable times will be essential. From this point of view, the construction of a high-intense positron source at Rossendorf, or Hamburg, in order to use the positron annihilation techniques for applied investigations of lattice imperfections of matter is highly desirable.

The phenomenon by which changes are induced in the properties of a material due to the repeated application of stresses or strains is commonly referred to by the term 'fatigue', especially when these changes lead finally to cracking or fracture. In addition, the influence of hydrogen or radiation may play a role. As a first impressive example, image-creation around a crack-tip by a positron microscope has been demonstrated to be extremely sensitive and helpful to enlighten the changes going on in stainless steel AISI 321 after plastic deformation [1]. Such investigations are of very high relevance and highly demanded to safety considerations of construction materials of all kinds. A positron microscope installed at an intense positron source could become a valuable tool for doing such type of studies routinely.

**References**

[1] M. Haaks, K. Bennewitz, H. Bihr, U. Männig, C. Zamponi, K. Maier, Appl. Surf. Sci. 149 (1999) 207

# 3. POSITRON PRODUCTION AND TRANSPORT

## 3.1. POSITRON SOURCE CONCEPT / TARGET REGION

R.Ley (Mainz)

Positrons can be created by weak or electromagnetic interaction only. The positrons from weak interaction usually come from radioactive sources like $^{22}$Na. From an activity of about 100 mCi (3.7 GBq) about $10^6$ moderated slow positrons per second may be extracted. Reactor-based slow positron sources either make use of the weak interaction, e.g. from $^{64}$Cu, or electroproduction from the gamma ray cascade after neutron capture in Cd. About $10^8$ slow positrons per second have been reported up to now (Brookhaven, Garching, Delft). In comparison, slow positron intensities two orders of magnitude higher have been obtained by electroproduction using an electron accelerator. From Livermore about $10^{10}$ slow positrons per second were reported (1, 2), whereas e.g. in Germany the former LINACs at Mainz (3) and Giessen (4-7) delivered up to about $10^8$ slow positrons per second. Compared to reactors, modern electron accelerators reach a high degree of reliability, i.e. more than 5,000 h of operation per year. Therefore, and for other reasons, like a pulse structure to be discussed later, they represent a very useful tool to build an intense positron source.

**- Bremsstrahlung and pair production**

An extremely relativistic electron passing through matter looses its energy mainly by bremsstrahlung. This process can be characterized by the so-called radiation length (rl) which is given by:

$$1\ \mathrm{rl} = (2149\ A) / ((15.80 - \ln Z)\ \rho Z^2)\ [\mathrm{cm}] \qquad (1)$$

with A being the mass number, Z being the element number, and ρ being the density (g/cm$^3$) of the target material. One radiation length is the distance over which a fraction of (1 - 1/e) = 63 % of the electron energy is radiated away. The intensity of the bremsstrahlung spectrum is nearly uniform up to 70 % of the endpoint energy - for a comparison of theory with experimental results see ref.(8). The total energy converted into bremsstrahlung within a given target thickness is proportional to the primary energy $E_e$ of the electrons. The gamma quanta from bremsstrahlung loose their energy $E_\gamma$ by Compton effect and pair production. In a tungsten target the pair production is dominant if $E_\gamma > 6$ MeV and becomes independent of the energy if $E_\gamma > 16$ MeV. The combined probability for primary interactions of bremsstrahlung and the generation of pair production becomes roughly proportional to $E_e$ .

In extremely thin targets, such as entrance windows, only ionization losses are essential. In a thick target, however, the processes of bremsstrahlung and pair production are successively repeated several times, i.e. a shower consisting of gamma rays and electron-positron pairs develops. The number of positrons emerging from a conversion target and their energy spectrum depend crucially on the target thickness and the primary electron energy $E_e$ . As long as the target thickness is small compared with the mean range of the primary electrons, the spectrum of the positrons emerging from the target has a maximum at an energy at about 20 % of $E_e$ (9) (see Fig. 1). The positron spectrum has a steep decrease towards lower energies and a long tail towards higher energies.

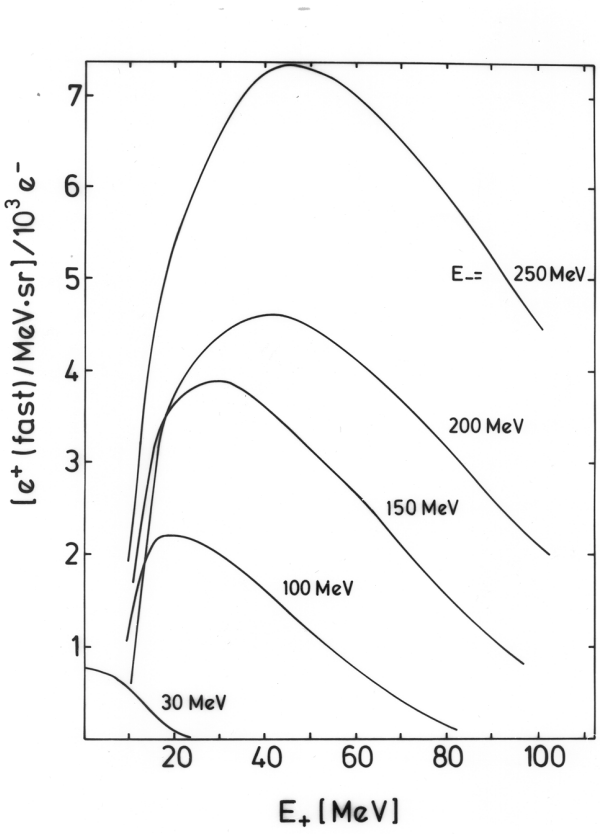


Fig. 1 This figure is redrawn from refs. (9) and (13). Positron spectra for a fixed target thickness equivalent to 4mm tungsten. The primary electron energies taken are 100 MeV, 150 MeV, 200 MeV, and 250 MeV, respectively. The spectrum for 30 MeV is taken from ref.(13) after appropriate re-scaling of the intensity.

An increase of the target thickness to a value which is comparable to the mean range of the primary electrons results in a shift of the most probable positron energy to very low energies and simultaneously the total number of positrons reaches a maximum. Theoretical simulations are able to explain the experimental facts at least qualitatively (10-12). With a further increase of the target thickness the maximum of the positron spectrum remains at very low energies but the number of positrons decreases. This is due to the fact that more positrons are annihilated in the rear parts of the target than are created. It is obvious that an optimum thickness $d^{opt}$ for a conversion target exists at which the highest number of positrons with lowest energies will be delivered.

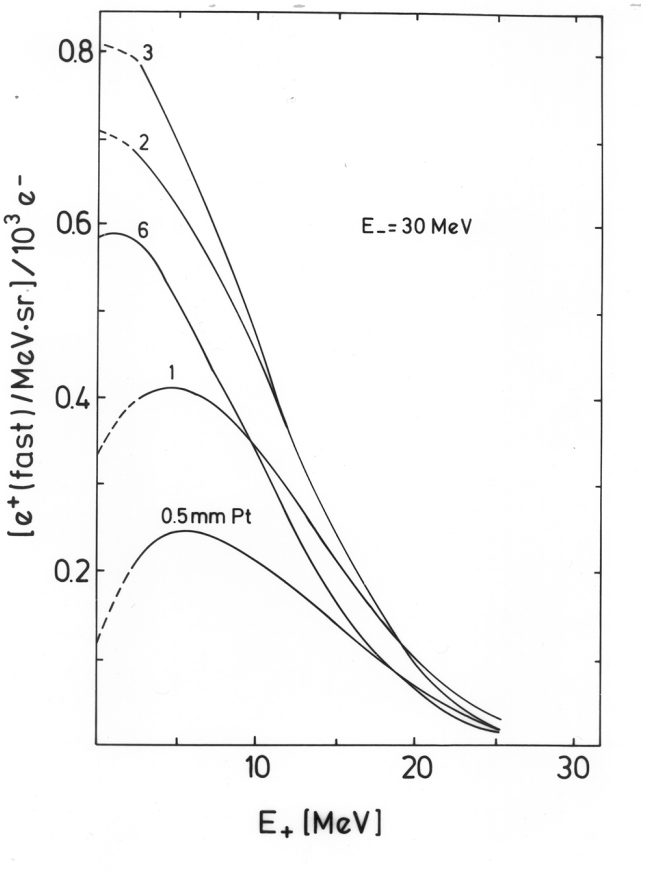


Fig. 2 Taken from ref.(13). Positron spectra for a fixed energy of the primary electrons of 30 MeV. The thickness of a Pt target is varied between 0.5 mm and 6 mm. The optimum thickness of 3 mm Pt is roughly equivalent to 4 mm W.

Experimental values for $d^{opt}$ have been found by a systematic variation of the target thickness at 9 MeV < $E_e$ < 30 MeV (13), at $E_e$ = 75 MeV (14), and at $E_e$ = 100 MeV (1). All these data can be interpolated by the empirical formula for the optimum thickness of a tungsten target:

$$d^{opt}\,[\text{mm}] = 0.670 + 0.0953\,E_e\,[\text{MeV}] \qquad \text{for } 10\text{ MeV} < E_e < 100\text{ MeV}. \qquad (2)$$

Using $d^{opt}$ values from eq.(2), the observed conversion efficiencies Y for moderated slow positrons as a function of $E_e$ may be interpolated by:

$$Y\,[e^+/10^9\,e^-] = 3.319 \times 10^{-4}\,(E_e\,[\text{MeV}])^{3.327} \qquad \text{for } 10\text{ MeV} < E_e < 100\text{ MeV} \qquad (3)$$

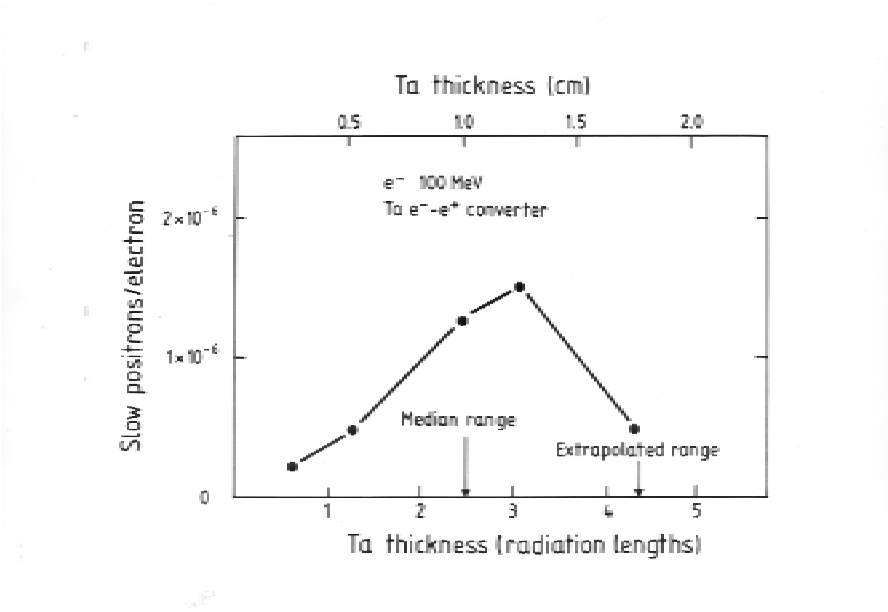


Fig. 3 Taken from ref.(1). For a fixed accelerator energy of 100 MeV the thickness of a tantalum target is varied between 2.5 mm and 17.5 mm. The pronounced maximum at 12 mm, the flat slope towards smaller thickness and the steep slope towards larger thickness are probably due to the good contact between target and moderator, so that a large number of low energy positrons with a high angular spread are collected.

If the electron energy $E_e$ is higher than 100 MeV the formulas (2) and (3) are not longer valid. At $E_e$ = 1 GeV formula (2) would deliver $d^{opt}$ = 100 mm, which is senseless for practical use. From refs. (1) and (3) it is known that for a fixed target thickness of 3 rl (= 10 mm tungsten) the conversion efficiency varies roughly proportional to $E_e$. Extrapolation to 360 MeV and 1 GeV then predicts conversion efficiencies of 5.8 x $10^{-6}$ $e^+/e^-$ and 15 x $10^{-6}$ $e^+/e^-$, respectively. A Japanese group at KEK (19) used a simulation code for the development of the electromagnetic shower in the conversion target. They found an optimum target thickness of 6 rl at 2.5 GeV and a conversion efficiency of 26 x $10^{-6}$ $e^+/e^-$. At 1.6 GeV the conversion efficiency was 18 x $10^{-6}$ $e^+/e^-$. Extrapolation down to 1.0 GeV would then predict a conversion efficiency of 10 x $10^{-6}$ $e^+/e^-$ which is in reasonable agreement with the value of 15 x $10^{-6}$ $e^+/e^-$ obtained above.

For the Tesla Test Facility (TTF) project at DESY in Hamburg/Germany with a time averaged current of 72 μA (= 1 x $10^{-9}$ C/bunch x 7.2 bunches/s) one therefore can predict 2.6 x $10^9$ $e^+$/s at 360 MeV and 4.4 x $10^9$ $e^+$/s at 1 GeV, respectively.

**- Thermal power deposited in the target**

The high energy electrons leave the accelerator beam line through a thin Al window of typical 0.1 mm thickness (about $10^{-3}$ rl), then are travelling through air for about 20 cm before entering the target chamber through another Al window of the same thickness. Every electron will deposit about 1.4 MeV $g^{-1}$ $cm^2$ in the aluminium due to ionization.

For a thick target the energy deposition is not uniform but reaches a maximum at a certain depth. Detailed calculations about the thermal power distribution as a function of depth can be found in ref.(15). The energy deposition averaged over the volume and the temperature rise have been treated in ref.(16). Due to secondary processes the average energy deposition per electron increases for thick targets to:

$$\Delta E = 2\ [(MeV/e)\ /(g/cm^2)] \qquad (4)$$

The total thermal power P generated by an accelerator current I is given by:

$$P\ [W] = I\ [A] \times \Delta E \times d^{opt}\ [cm] \times \rho\ [g/cm^3] \qquad (5)$$

**- Situation at ELBE**

At the Forschungszentrum Rossendorf near Dresden/ Germany a new superconducting LINAC named by the acronym "ELBE" (Electron Source of high Brilliance and low Emittance) is under construction which may be used for the production of an intense slow positron beam (17). Originally planned to deliver a maximum electron energy of about 20 MeV at an average current of 1 mA, it now almost certainly will reach a maximum value of about 40 MeV at the same average electron current. This will allow to produce about $10^8$ slow positrons per second (18). Of course, this value is obtainable only in the $c_w$ – mode of the ELBE accelerator, as planned. For comparison, the 25 Hz – mode of the ELBE accelerator, with a macro-pulse length of 0.1 ms, has a duty cycle of 0.1 ms x 25 Hz = 0.0025 and a time averaged current of 2.5 μA only !

Taking the intended ELBE-LINAC characteristics (40 MeV, 1 mA), the thermal power deposited in the Al windows will amount to about 38 W only which is negligible. However, one obtains P = 17.4 kW for a W target (density $\rho = 19.3$ g/cm$^3$) having the optimum thickness $d^{opt} = 0.45$ cm.

It is supposed to use a disk-shaped W target of diameter $d_2 = 1.5$ cm which is in thermal contact with a surrounding water-cooled Cu block. According to ref.(16), the temperature rise $\Delta T$ in the target is given by:

$$\Delta T = (0.5 + \ln(d_2/d_1)) / (2\pi\lambda) \times \rho \times \Delta E \times I \qquad (6)$$

where $d_1 \simeq 0.5 \times d_2 = 0.75$ cm is the diameter of the electron beam and $\lambda = 1$ W cm$^{-1}$ K$^{-1}$ is the thermal conductivity of tungsten. Inserting all numbers gives:

$$\Delta T = 7.2 \times 10^6 \times I \text{ [A]} \qquad (7)$$

Inserting the nominal accelerator current of 1 mA would result in a temperature far beyond the melting point of tungsten (3683 K). As a consequence, the accelerator beam has to be expended in diameter or lowered in current in such a way that the fraction hitting the W target disk is low enough to guarantee a $\Delta T \leq 2000$ K. This can be achieved using $I \leq 0.28$ mA only or expanding the electron beam to $d_1 = 2$ cm. According to ref.(16), the thermal power deposited by the expanded beam in the water-cooled Cu block is uncritical.

Using the conversion efficiency of 72 $e^+$ / $10^9$ $e^-$ at 40 MeV, a current of I = 0.28 mA will produce about 1.2 x $10^8$ $e^+$ $s^{-1}$.

**References**


1. Howell, R.H., Alvarez, R.A., and Stanek, M., Appl. Phys. Lett. **40**, 751 (1982)
2. Howell, R.H., Cowan, T.E., Hartley, J., Sterne, P., and Brown, B., Appl. Surf. Sci. **116**, 7 (1997)
   Asoka-Kumar, P., Howell, R., Stoeffl, W., and Carter, D., in: AIP Conf. Proc. **475**, 361 (1999)
3. Gräff, G., Ley, R., Osipowicz, A., Werth, G., and Ahrens, J., Appl. Phys. **A33**, 59 (1984)
4. Ebel, F., Faust, W., Hahn, C., Langer, S., and Schneider, H., Appl. Phys. **A44**, 119 (1987)
5. Faust, W., Hahn, C., Rückert, M., Schneider, H., Singe, A., and Tobehn, I., NIM **B56/57**, 575(1991)
6. Schneider, H., Tobehn, I., Ebel, F., and Hippler, R., Phys. Rev. Lett. **71**, 2707 (1993)
7. Hagena, D., Ley, R., Weil, D., Werth, G., Arnold, W., and Schneider, H., Phys. Rev. Lett. **71**, 2887 (1993)
8. Koch, H.W., and Carter, R.E., Phys. Rev. **77**, 165 (1950)
9. Hauptmann, A., Ph.D. Thesis, Inst. für Kernphysik/Univ. Mainz (1972)
10. Katz, L., and Lokan, K.H., NIM **11**, 7 (1961)
11. Sund, R.E., Walton, R.B., Norris, N.J., and MacGregor, M.H., NIM **27**,109 (1972)
12. Segers, D., Dorikens, M., Paridaens, J., and Dorikens-Vanpraet, L., in: AIP Conf. Proc. **303**, 496 (1994)
13. Bernardini, M., Miller, J., Schuhl, C., Tamas, G., and Tsara, C., Frascati Report LNF **62/66** (1962)
14. Takahane, T., Chiba, T., Shiotani, N., Tanigawa, S., Mikado, T., Suzuki, R., Chiwaki, M., Yamazaki, T., and Tomimasu, T., Appl. Phys. **A51**, 146 (1990)
15. Tabata, T., Andreo, P., and Ito, R., Atomic Data and Nuclear Data Tables **56**, 105 (1994)
16. Andreani, A., and Cattoni, A., NIM **129**, 365 (1975)
17. Brauer, G., Wendler, W., Büttig, H., Gabriel, F., Gippner, P., Gläser, W., Grosse, E., Guratzsch, H., Dönau, F., Höhnel, G., Janssen, D., Nething, U., Pobell, F., Prade, H., Pröhl, D., Schilling, K.D., Schlenk, R., Seidel, W., Stephan, J., vom Stein, P., Wenzel, M., Wustmann, B., and Zahn, R., Mat. Sci. Forum **255-257**, 732 (1997)
18. Brauer, G., Ley, R., Schneider, H., and Arnold, W., in: AIP Conf. Proc. **475**, 369 (1999)
19. Asami, A., Enomoto, A., Kobayashi, H., Kurihara, T., Nakahara, K., and Shidara, T., Mat. Sci. Forum **105-110**, 1833 (1992)

## 3.2. MODERATION

D.Segers (Gent)

Slow positrons are produced by bombarding high energy positrons into a material that has a negative positron work function. After the bombardment, the positrons rapidly (~ 10 ps) thermalize, and a fraction of them diffuse back to the surface. Finally, slow positrons with an energy of a few eV, are emitted from the surface. The bulk conditions of the moderator are extremely important, as they control, through $L_+ = \sqrt{D_+ \tau^*}$ (where $L_+$ is the positron diffusion length, $D_+$ is the positron diffusion coefficient and $\tau^*$ is a mean positron lifetime), the migration of thermal positrons to the surface. Therefore, thermal treatments are necessary to anneal structural defects due to cold work.

The selection of the positron moderator material is an important factor for the construction of high intensity slow positron beams. Various positron moderator materials have been proposed for the production of slow positron beams. The historical development of positron moderators has been described in references (1) and (2).

At LINAC based, high intensity slow positron beams, the most widely used material for the primary moderation of the high energy positrons, is annealed tungsten mounted in a “venetian blind” geometry (3-9). A schematic representation of the Livermore set-up (3) is shown in figure 1.

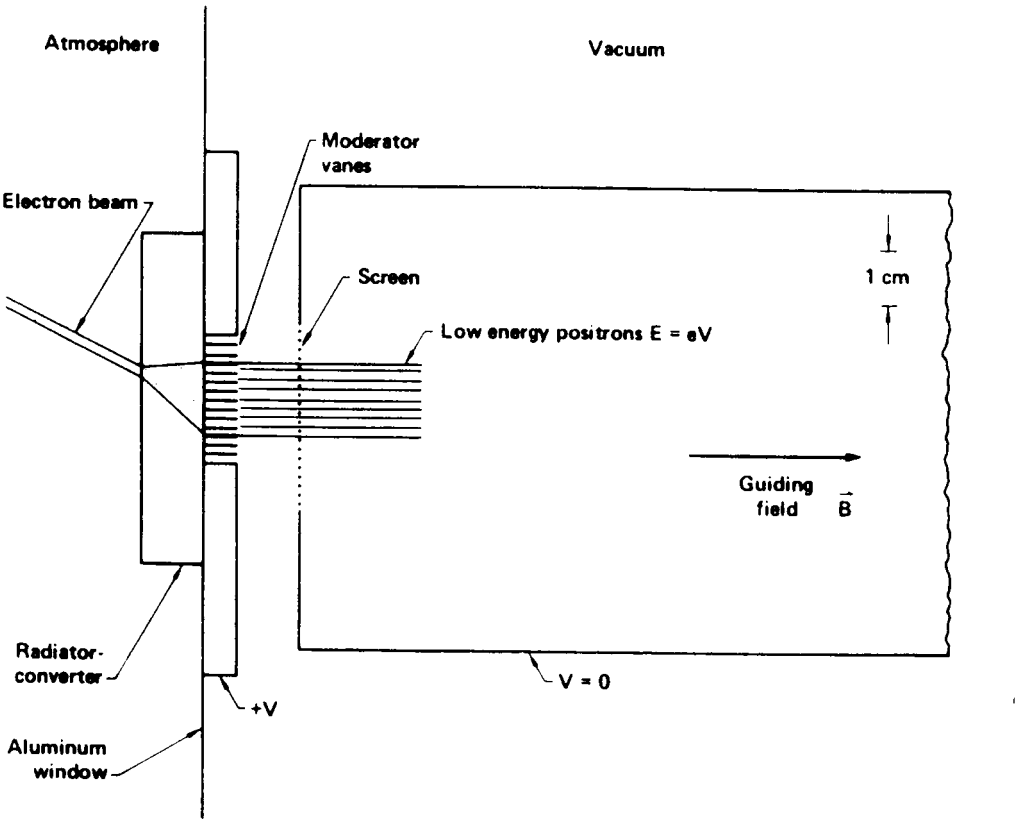


Fig.1 Schematic representation of the front end in the Livermore positron beam system (see ref.(3)).

The moderator vanes have to be placed as close as possible to the electron-positron converter, in order to intercept as much as possible high energy positrons. In the venetian blind geometry, typically 10 tungsten vanes with a thickness varying from 25-250 μm are used. The vanes are chemically cleaned (5) and annealed at ca. 2000°C under high vacuum conditions (< 10-5 Pa).

In a recent study by Suzuki et al. (10) the positron re-emission properties of different moderator materials was investigated in order to improve the positron moderation system at LINAC based high intensity slow positron beams. The investigated moderator materials were: tungsten, SiC, GaN, $SrTiO_3$ and hydrogen-terminated Si. Positron re-emission was studied using a pulsed slow positron beam. From their study it followed that tungsten is still the best material for primary moderation.

One problem of tungsten as the primary moderator is the degradation of the moderation efficiency by irradiation with the LINAC electron beam. The origin of the degradation of the primary tungsten moderator was also investigated (10). Therefore a 25 μm W foil which had been used as one of the moderator foils in a real set-up was investigated using slow positrons and AUGER electron spectroscopy (AES).

In the study described in reference (10), the tungsten foil was initially annealed at 2000°C for 15 min in a vacuum of $10^{-5}$ Pa. During positron production the W foil was kept in a vacuum of $10^{-8}$-$10^{-6}$ Pa. The LINAC energy and current were respectively 70 MeV and 10 μA. The foil was irradiated during 1000h. The moderator assembly was located 10 mm behind a tantalum converter, so that a fraction of the electron beam could go through the converter-moderator assembly. The temperature of the moderator could rise above 400°C. The initial moderation efficiency was ~$2x10^{-7}$ (slow e+/e-). After irradiation for 1000h, the moderation efficiency dropped to one-tenth of the initial value.

The degradation of the moderation efficiency of the tungsten foils is due to:

**1) defect formation**

Positron Doppler-broadening and lifetime studies of the W vane revealed the presence of large vacancy type defects which were created during high energy electron irradiation. The 70 MeV electrons could also produce neutrons, which could create larger vacancy-type defects than electrons. The estimated neutron dose during the 1000h operation was ~$10^{17}$ n/cm$^2$.

**2) surface contamination**

Carbon is one of the major impurities in tungsten. At high temperatures (11) the carbon atoms can diffuse to the surface and accumulate there. AES revealed that the surface of the tungsten vane after 1000h of operation was contaminated with carbon. It is known (12) that a surface contamination with carbon, up to 0.3 mono-layer does not strongly influence the re-emission of slow positrons. The amount of surface carbon on the moderator foil used during LINAC operation was determined and was larger than 0.3 mono-layer. The AES peak shape was more similar to a graphite peak than to a tungsten carbide peak. This suggested that a carbon (graphite) layer was formed by high-energy electron irradiation which also contributes to the degradation of the slow positron re-emission efficiency.

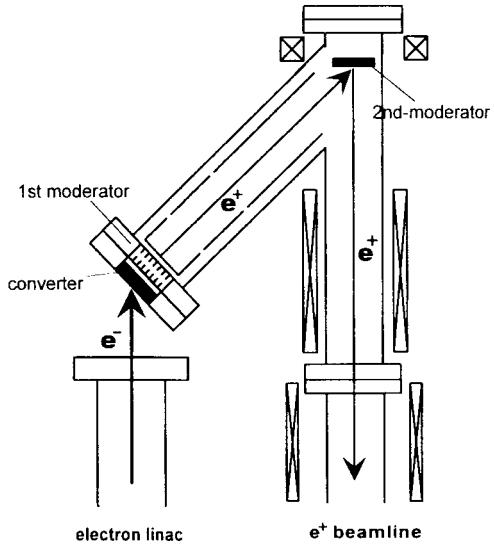


Fig.2 Possible layout for a slow positron beam line with a primary moderation and a remoderation stage (from ref.(15)).

Suzuki et al. (10) also propose an in-situ treatment to regenerate the moderator foils. It is known (13) that the recovery temperature for vacancy-type defects introduced in tungsten by neutron irradiation is ~900°C. It is

also known (12) that oxygen treatment of tungsten at 700-900°C can substantially remove surface carbon. So, an annealing at 900°C in an oxygen atmosphere could be useful to regenerate in-situ the primary moderator foils.

The slow positron beam after the primary moderation mostly has a large diameter (~20 mm or more) and a too large energy spread. To decrease the beam diameter and the energy spread, a re-moderation of the beam has to be performed. In a re-moderation stage, the slow positrons are accelerated to a few keV and focused to a re-moderator onto a much smaller area. Then positrons of a few eV are re-emitted from the re-moderator surface. This is known as the brightness enhancement technique (14). A possible layout for such a beam line is given in figure 2 (15).

Suzuki et al. (10) have pointed out that, for energies below 10 keV for the incoming positrons, n-type 6H-SiC has a higher slow positron re-emission yield than tungsten. So for re-moderation SiC is the best material.

**References**


(1) P.J.Schultz and K.G.Lynn; Rev. Mod. Phys. 60 (1988) 701
(2) Positron solid state physics: Proc. Int. School of physics "Enrico Fermi" course LXXXIII, eds. W.Brandt and A.Dupasquier, Varenna, 1981 (North Holland, Amsterdam 1983)
(3) R.H.Howell, M.F.Fluss, I.J.Rosenberg and P.Meyer; Nucl. Instr. & Meth. B10/11 (1985) 373
(4) G.Gräff, R.Ley, A.Osipowicz and G.Werth; Appl. Phys. A33 (1984) 59
(5) F.Ebel, W.Faust, C.Hahn, S.Langer and H.Schneider; Appl. Phys. A44 (1987) 119
(6) L.D.Hulett, T.A.Lewis, D.L.Donohue and S.Pendyala; in "Positron Annihilation" Proc. of the 8th Int. Conf. On Positron Annihilation 1988, eds. L.Dorikens-Vanpraet, M.Dorikens and D.Segers (World Scientific Singapore) p. 586
(7) J.Paridaens, D.Segers, M.Dorikens and L.Dorikens-Vanpraet; Nucl. Instr. & Meth. A276 (1990) 359
(8) T.Akahane, T.Chiba, N.Shiotani, S.Tanigawa, T.Mikado, R.Suziki, M.Chiwaki, T.Yamazaki and T.Tomimasu; Appl. Phys. A51 (1990) 146
(9) T.Kurihara, A.Shirakawa, A.Enomoto, T.Shidara, H.Kobayashi and K.Nakahara; Appl. Surf. Sc. 85 (1995) 178
(10) R.Suzuki, T.Ohdaira, A.Uedono, Y.Koo Cho, S.Yoshida, Y.Ishida, T.Ohshima, H.Itoh, M.Chiwaki, T.Mikado, T.Yamazaki and S.Tanigawa; Jpn. J. Appl. Phys. 37 (1998) 4636
(11) J.A.Becker, E.J.Becker and R.G.Brandes; J. Appl. Phys. 32 (1961) 411
(12) G.Amarendra, K.F.Canter and D.C.Schoepf; J. Appl. Phys. 80 (1996) 4660
(13) N.Owada, K.Hinode, S.Tanigawa, M.Doyama and S.Okuda; in Proc. 5th Int. Conf. Positron Annihilation, Lake Yamanaka, 1979 (Japan Institute of Metals, Sendai 1979) p.743
(14) A.P.Mills jr.; Appl. Phys. 23 (1980) 189
(15) R.Suzuki, T.Ohdaira, T.Mikado, A.Uedono, H.Ohgaki, T.Yamazaki and S.Tanigawa; Mater. Sc. Forum 255-257 (1997) 114


## 3.3. CONSTRUCTION OF TARGET CHAMBER


A.Osipowicz (Fulda)


The converter-moderator assembly is placed within a vacuum tube (d=300 mm) that is on high positive potential $U_0$ (0-40 kV) and is separated from the ELBE LINAC vacuum (Fig.1). The ELBE electron beam enters the converter/moderator vacuum chamber through a 300 µm Al window and impinges at the converter surface under a 30° angle with respect to the axis of the chamber. To allow for easy access, the converter and moderator are mounted on different flanges.

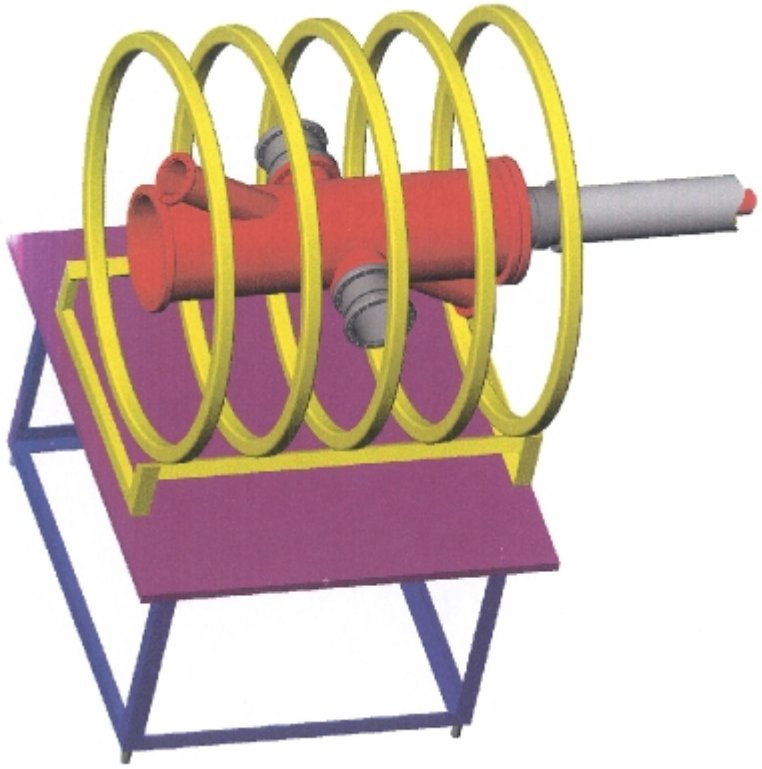

Fig.1 Schematical view of the target chamber (in red), mounted on a free-standing holder (in pink/blue), surrounded by Helmholtz coils (in yellow). See text for detailed description.

The converter consists of a W cube because of its thermal properties and high Z. It is placed in a Cu socket surrounding the cube on 4 sides. A number of tubes is the Cu socket perpendicular to the electron beam allows for a closed-circle water cooling. The thickness of the Cu on the backside of the converter is 2 mm and is designed to shield the moderator vanes against heat damage from the converter.

The moderator is placed immediately behind the converter. In a W socket 10 µm W vanes can be placed in different geometries for a positron beam with different features. For intensive beams a venetian blind geometry which is open in the direction of positron extraction will be used.

A set of Helmholtz coils arranged coaxial along the vacuum chamber provides a homogeneous magnetic field of 100 G well aligned with the axis of the vacuum tube defines the direction of positron beam . To extract the slow positrons from the moderator vanes an electric field is applied across converter ($U_C$), moderator ($U_M$) and two Wehnelt ($U_{W1}$,$U_{W2}$) cylinders so that the downstream Wehnelt potential equals $U_0$. Thus the positrons are accelerated downstream parallel to the magnetic field. Given ideally aligned electric and magnetic fields at the moderator site, the kinetic energy parallel to the magnetic field $E_P$ of the positrons in the transport system is given mainly by the moderator potential $U_M$ and the positron work function $\Phi^+$ and the angle of emission from the moderators.

As the converter area is hazardous due to heavy radiation activation, the slow positrons will be transported to shielded experimental sites by a standard magnetic transport system. A longitudinal magnetic field (B=100G) is produced by a solenoid wound on the outside of a long vacuum tube which is on ground potential. Inside this tube runs a second thin-walled tube that can be electrically connected to $U_0$, the converter/vacuum chamber potential. Thus the energy and the phase space of the positron beam in the magnetic transport system is not affected by a change of $U_0$.

## 3.4. COMPARISON ELBE / TTF

H. Schneider (Giessen)

Currently the two LINACs of Rossendorf/Dresden ('ELBE') and DESY/Hamburg ('TTF') are under consideration for the possible installation of an European Positron Facility (EPF). Both are **pulsed injector machines** with distinct beam features that are given in the table 1 below. The microstructure of both LINAC beams consists of electron bunches of 0.6 ps and 3 ps, respectively, and a bunch separation time of about 100 ns. A number of consecutive bunches form a bunch train. The train length does depend on the number of bunches per train. Consequently, the train separation time does vary accordingly.

1 a

| | TTF | ELBE |
|---|---|---|
| electron energy | 390 MeV (1. Step)<br>1000 MeV (2. Step) | 40 MeV |
| beam power: | max. 72 kW | max. 40 kW |
| bunch load: | ~ 1000 pC | 77 pC |
| bunches per train: | 7200 | min.1176; max.~500 000, (471000) |
| bunch length: | 0,6 ps | (2ps – 10 ps) ~ 3 ps |
| bunch separation: | 100 ns | 77 ns (÷ 13 MHz) |
| repetition rate: | 10 Hz | 25 Hz (max. 100 Hz) |
| mean current: | ~72 µA | ~1 mA |
| train length: | ~0,72 ms | min. ~0,09 ms; max. > ~36,3 ms |
| train separation: | ~2,8 ms | max.< ~39,9 ms; min. < ~ 3,7 ms |
| duty cycle: | ~7 X 10E-3 * | min. ~2,3 X 10E-3; max. ~0,91 + |

* (~4,3 X 10E-8 ≡ 0,6 ps X 7 200 X 10)  + (~3,5 X 10E-5 ≡ 3 ps X 471 000 X 25)

For the present scope it may be also useful to consider the characteristics of an HF-injector that is also planned in the future for the Rossendorf LINAC ELBE (HF fine-structure: 1,3 GHz).

1 b

| | |
|---|---|
| bunch load: | 1,5 pC |
| bunches per train: | (max. 2,7 X 10E6) |
| bunch length: | (8 ps) |
| bunch separation: | ~15 ns |
| rep. rate: | 25 Hz (max. 100 Hz) |
| train length: | min. ~0,1 ms ; max. ~40 ms |
| mean current: | ~0,1 mA<br>(≡ 1,5 pC X 2,7 X 10E6 bunches X 25 Hz) |
| max. beam power: | 4 kW |
| duty cycle: | min. ~2,5 X 10E-3; max. ~1 + |

+ ~0,5 X 10E-3 (≡ ~8 X 10E-12 X 2,7 X 10E6 X 25)

positrons per bunch: ~20  positron mean rate: ~0,5 X 10E8/ s

Short pulses of slow positrons of ~10 ps (= T) length cannot be delivered from the positron facilities at both LINACs directly. The original short pulses of T~0.6 ps or T~3 ps, respectively, are not available because by thermalisation in the multi-foil moderator, and in the corresponding transport system (beam line) the pulses become much longer (see table 2). Therefore, one has to use e.g. in lifetime experiments a buncher or/and (if required) a stretcher (Penning trap), followed by a pulsing system.

Table 2 : $e^+_{slow}$, ~Pulse Widths $\pm\Delta t_0$ (HWHM;ns)+

| $U_{mod.}$* | $\Delta t_0$ | $U_{mod.}$* | $\Delta t_0$ |
|---|---|---|---|
| 50 | 125 | 1 000 | 5 |
| 100 | 36 | 6 000 | 0,8 |
| 300 | 15 | 10 000 | 0,5 |
| 600 | 9,5 | 25 000 | 0,2 |
| *Volt | +without bunching | 100 000 | 0,05 |

To improve the number of registered events at ELBE and TTF, especially with coincidence networks, one may use arrays of several detectors (as usual in nuclear physics; e.g. 200 detectors with corresponding electronic equipments). In coincidence set-up´s the detectors should measure the mutual under 180° emitted γ-rays (511 keV), and in such a manner reduce considerable the measuring time (compare chapters 5.1.3. and 5.1.4.).

Assuming at TTF ~ 1 • 10E4 $e^+_{slow}$/ bunch and at ELBE ~ 20 $e^+_{slow}$/ bunch, the corresponding estimated (registered) ~ counts are given in table 3 a for spectroscopy- and in table 3 b for coincidence- work, respectively (admitted 10% - 15% pile-up at 1 reg. event/ bunch).

Table 3 a: Spectroscopy (ε = det. efficiency; assumed resolving time τ = 10E−7 s).

| LINAC | TTF | ELBE | |
|---|---|---|---|
| bunch/ train | 7 200 | min. 1 176 | > 471 000 |
| ε = 10E−1 | 1 • 10E3* | ~ 2 | |
| ~reg. events | 72 000/ s | 29 000/ s | ~12 000 000/ s |
| ε = 10E−2 | 1 • 10E2* | ~ 0,2 | |
| ~reg. events | 72 000/ s | ~5 800/ s | ~2 300 000/ s |
| ε = 10E−3 | 10* | 0,02 | |
| ~reg. events | 72 000/ s | 600/ s | 230 000/ s |
| ε = 10E−4 | 1 | 0,2 • 10E−2 | |
| ~reg. events | 72 000/ s | 60/ s | 23 000/ s |
| ε = 10E−5 | 0,1 | 0,2 • 10E−3 | |
| ~reg. events | 72 00/ s | 6/ s | 2 300/ s |
| ε = 10E−6 | 0,01 | 0,2 • 10E−4 | |
| ~reg. events | 720/ s | ~1/ s | 230/ s |

*too much!

Table 3 b: Coincidences (fast, constant fraction; $\tau_{coinc.}$ = 10E−10 s).

| ε | TTF | ELBE (minimum) | ELBE (maximum) |
|---|---|---|---|
| 10E−1 | 7,2 • 10E6/ s | 0,6 • 10E4/ s | ~2,3 • 10E6/ s |
| 10E−2 | 7,2 • 10E4/ s | 0,6 • 10E2/ s | 2,3 • 10E4/ s |
| 10E−3 | 7,2 • 10E2/ s | 0,6/ s | 2,3 • 10E2/ s |
| 10E−4 | 7,2/ s<br>432/ min. | 0,006/ s<br>0,4/ min. | 2,3/ s<br>138/ min. |
| 10E−5 | 4,3/ min. | 0,004/ min | 1,4/ min. |
| 10E−6 | 0,04/ min.<br>2,4/ h | 0,00004/ min.<br>0,002/ h | 0,014/ min.<br>0,8/ h |

An increase of the measured counting rates may also be achieved in several cases [by significant factors at spectroscopy- and at coincidence-work; values are f ($U_{mod.}$)] using penning traps to overcome the intervals among the bunches. The improvements are smaller overcoming the breaks between the trains (compare also chapter 5.). In this context one may consider the widths $\pm\Delta t_0$ of the moderated positron pulses.

**Super-conducting LINACs** (as `ELBE´ and `TTF´ *) may also be operated in a `quasi´ **cw-mode**, i.e. with an `infinite´ long train of bunches.[e.g. at ELBE one gets in cw-mode a mean current of 1 mA or 0,1 mA (compare also table 1 a and 1 b), respectively]. It is possible to obtain easy a quasi-continuous beam of slow positrons $e^+_{slow}$ with high intensity [e.g. at Elbe ~ 2 • 10E8 $e^+_{slow}$/ s; compare Appl. Phys. A44, 119 (1987)], and practically without complicated penning-traps. The cw-mode enable `first´ to achieve several experiments.

*not scheduled for cw-mode.

The problems caused by pile-up in the electronic systems (one has to prevent counting errors; see table 4) are greatly reduced in the cw-mode; resulting hence in big advantages for spectroscopy (e.g. in atomic physics; compare chapter 5.3.1.), and especially for working with many coincidence arrangements. For time-of-flight experiments one may, if required, pulse suitable the positron beam. The pulse fine-structure is lost by the moderation.

Table 4: Counting errors in cw-mode. .

| Assumed electronics resolving time: 10E–7 s . | |
|---|---|
| counts | error |
| 10E6/ s | ~ 10 % |
| 10E5/ s | ~ 1% |

## 3.5. POSITRON TRANSPORT ELEMENTS

A.Osipowicz (Fulda)

### 3.5.1. First remoderator stage

To reduce the problems that occur in extended magnetic transport systems, e.g. magnetic gradient drift and transmission losses, it is advisable to enhance the beam brightness and to reduce the beam diameter by a first transmission remoderator before extended transportation. This stage should be located as close as possible to the target chamber. It consists of a 25 µm W foil placed perpendicular to the beam direction. The beam is magnetically focussed and electrically accelerated onto the W foil. The moderated positrons on the backside of the moderator foil are then electrically sucked into the magnetic guiding system. With a significantly smaller diameter the beam can now be transported over a long distance without intensity losses.

### 3.5.2. Magnetic beam switch

Using a magnetic beam switch the positron beam may be fed into 2 tubes leading to different experimental sites. The switch consists of a Y-shaped solenoid system with the positron transport vacuum tube-branching inside. It is operated by an external movable steering solenoid producing a magnetic field that can shift the magnetic flux tube occupied by the incoming slow positrons into either of the two exit solenoids . The magnetic switch can be used to divert the positron beam with the original pulse structure, mainly governed by the LINAC time structure.

### 3.5.3. Transition from magnetic to electrostatic guiding system

The beam is extracted divergence-free from the magnetic field using a ”magnetic spider” into an electrostatic guiding system. The spider essentially consists of a high permeable material and is shaped like the skeleton of an umbrella catching the magnetic flux in its spokes and allowing a large percentage of the positrons to travel to the region of zero magnetic field. This principle has been successfully demonstrated for the first time in the literature /D. Gerola et al., Rev. Sci. Instr. 66 (1995) 3819/.

# 4. POSITRON BEAM MODIFICATION

## 4.1. PENNING TRAP

D.Segers (Gent)

In a LINAC based slow positron beam, the positrons are created during the electron pulse of the accelerator. The main advantage of such slow positron beams is that a huge number of positrons is available.

LINAC's are mostly pulsed and this results in a pulsed positron beam. The pulse length and the repetition frequency are dependent on the particular electron accelerator used. Some relevant data of the ELBE and TTF accelerator, influencing the need for the installation of a Penning trap, are summarised in Table 1.

Table 1: some relevant data, influencing the need for the installation of a Penning trap

| | TTF - DESY | ELBE |
|---|---|---|
| Bunches per train | 7200 | Min.: 1176; max. 471000 |
| bunch length | 0.6 ps | (2 ps – 10 ps) ~3ps |
| bunch separation | 100 ns | 84.6 ns |
| Repetition rate | 10 Hz | 25 Hz |
| train length | ~ 0.72 ms | Min.: 0.099 ms; max.: 39.85 ms |
| train separation | ~ 2.8 ms | Max.: 39.9 ms; min.: 0.15 ms |

The pulsed character of the beam can be an advantage for some kind of experiments; i.e. those experiments where there is a time correlation between the positron beam and the measured signal. Examples of such experiments are the positronium velocity spectroscopy measurements using the time of flight of positronium in vacuum (1).

However for some experiments a quasi-continuous slow positron beam is required. Starting from a pulsed LINAC based slow positron beam, this can be achieved by the use of a so-called Penning trap. The use of such a Penning trap as a storage device for positrons at a LINAC was first proposed by Hulett et al. (2). The idea is based on the trap used by Malmberg and co-workers for the creation of electron plasmas (3). A schematic representation of such a Penning trap is given in figure 1.

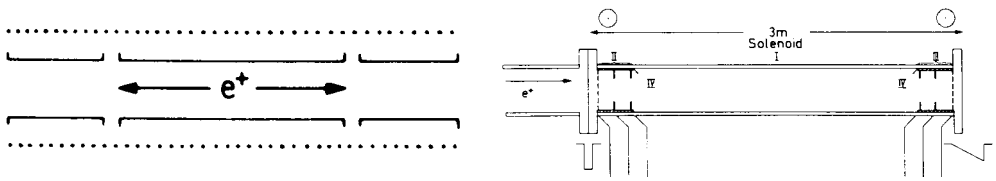


(a) (b)

Fig.1 Schematic representation of the design of a Penning trap for the storage of positrons at a LINAC-based slow positron beam; (a) in the case where an internal drift tube is installed (2), (b) in the case where no internal drift tube is used, and where the entrance and exit gates consist of grids (4).

The basic idea is very simple: The Penning trap consists of a vacuum tube where the positrons are stored. At the entrance and exit, an electrostatic gate is installed. This can be made with cylindrical lenses or grids. When the positron burst reaches the Penning trap, the potential of the entrance gate is dropped to allow the admission into the storage region. The potential of the exit gate is higher than the potential at which the positrons are stored, so that they are reflected back to the entrance gate. In the time required for the burst to return to the entrance gate, its potential will have been reset for trapping. If a drift tube is installed in the vacuum tube (see figure 1a), the stored positrons can be released from the trap during the period in between two accelerator pulses, by raising the potential of the drift tube, so that the positrons can overcome the barrier at the exit gate. If no internal drift tube is installed (see figure 1b), the stored positrons can be released by lowering the potential of the exit grid. Thus, the Penning trap will extend the time frame over which positrons are dispensed, making single particle counting much easier. The axial magnetic field must restrain the positrons from colliding with the walls of the drift tube as they undergo the many thousands of reversals in their flight direction.

Constructions based on these ideas have been tried out by different groups (4-8) with varying degrees of success. The train separation determines the time that the positrons have to be stored. This can be in the micro- or millisecond range. This determines certain requirements at the construction of the Penning trap.

For example, at the former Gent LINAC beam, the repetition frequency was 300 Hz and the pulse length was typically 3 μs (8). This means that the positrons had to be stored for 3.3 ms. The loss of intensity is illustrated in figure 2, where the number of positrons is shown after different confinement times. It was calculated that after a storage time of 3.3 ms a 15% loss of positrons occurred.

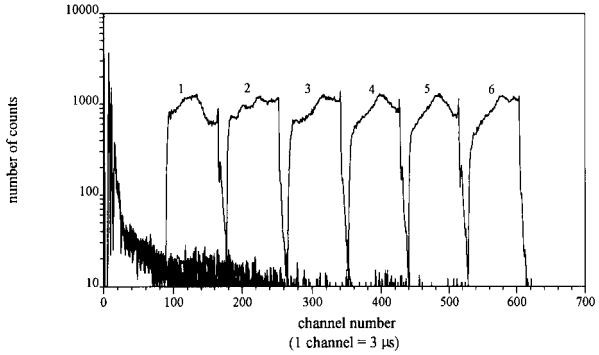


Fig.2 The Penning trap is loaded with positrons during the 3 μs long positron pulse. The positrons are stored for different confinement times (1 = 0.3 ms, 2 = 0.6 ms, 3 = 0.9 ms, 4 = 1.2 ms, 5 = 1.5 ms, 6 = 1.8 ms) and are then released during a time interval of 0.27 ms. No great loss of positron intensity is seen after a confinement time of 1.8 ms (8).

Positron loss mainly appears by scattering of positrons at rest gas molecules. The slow positron intensity I can be described with the de Beers attenuation low, i.e.: $I = I_o\, e^{-\sigma z N}$, where z is the distance travelled, N is the number of residual gas atoms per unit volume and $\sigma$ is the total cross section for positron-gas scattering. A typical value for this cross section is $5x10^{-20}$ $m^2$. For a 30 eV positron, the travelled distance during a confinement time of 3.3 ms is over 10 km. This means that $I/I_o$ drastically depends on the vacuum condition ($I/I_0 = 5.8x10^{-6}$ for a vacuum of $10^{-4}$ Pa and $I/I_o = 0.88$ for a vacuum of $10^{-6}$ Pa). It has also been demonstrated by Surko and co-workers (9), that the confinement time can be drastically influenced by impurity effects. Incorporation of a liquid nitrogen cooled baffle into the vacuum to freeze out impurity molecules drastically improves (by a factor of 20) the confinement time. It was also demonstrated (9) that the confinement time is also very sensitive to the presence of small amounts (as low as $1x10^{-9}$ torr) of turbopump oil. So the installation of cryopumps is a prerequisite.

From the data in table 1, it is clear that for the TTF (DESY) accelerator the installation of a Penning trap is necessary. For the ELBE accelerator, only when it is operated in the mode with the shortest train length (and maximal train separation time), then the installation of a Penning is needed.

A lot of research was done at the university of San Diego, for the creation of positron plasmas (9-12). Positrons were guided in an axial magnetic field (higher than 1 kG). A three stage Penning trap was constructed to store and cool the positrons. In the different stages a different partial $N_2$ gas pressure is present. This is achieved by differential pumping. In the high pressure stage (stage I, $p = 10^{-3}$ Torr) positrons loose energy by inelastic ionization and/or electronic excitation of $N_2$ molecules. The latter stages II and III are designed to operate at energies below the threshold for positronium formation (i.e. 8.8 eV in $N_2$), using vibrational excitation of the $N_2$ gas as an inelastic scattering mechanism. The intrinsic efficiency of the trapping scheme is limited by the positronium formation in region I. A schematic representation of the Penning trap is given in figure 3.

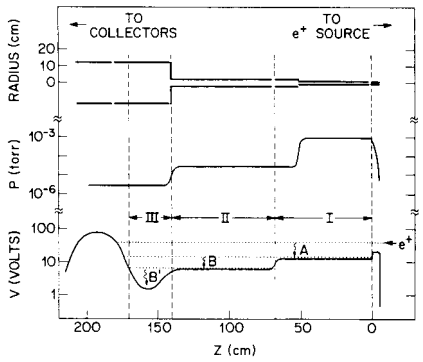


Fig.3 Schematic representation of the Penning trap used to create positron plasmas (9).

Confinement of positrons for days has been achieved in Penning traps operated at low gas pressures of $10^{-11}$ Torr (13). Further, collisional cooling on nitrogen has the advantage of increasing the particle phase space density without the losses of positrons that use of a re-moderation stage would entail (11). This is reflected in the axial energy distribution of the positrons. An energy spread of 0.018 eV (FWHM) is obtained. This is represented in figure 4.

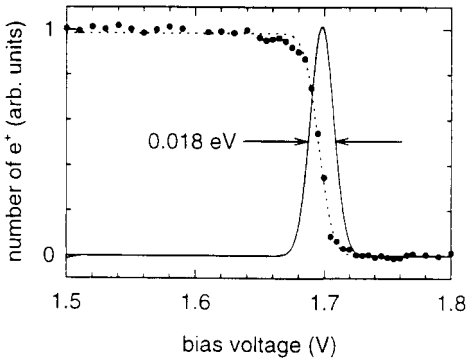


Fig.4 Distribution of the axial energy of the stored positrons (11). A very narrow energy distribution is obtained (0.018 eV FWHM).

In the near future, this type of Penning trap can be obtained commercially (First Point Scientific, Inc., project Director Rod Greaves, greaves@firstpsi.com). This design is maybe the best proposal as a positron storage device at LINAC-based positron beams. It can also be used in a pulsed mode (as short as 150 ps at repetition frequencies of 1 kHz upward).

Furthermoe, as pointed out in section 7.2.1 a more advanced version of a Penning trap (14) (see figure 2 in section 7.2.1) can be used as a storage trap, a variable phase space shifter and beam splitter.

**References**

(1) R.Howell, I.J.Rosenberg and M.J.Fluss; Nucl. Instr. & Meth. 43 (1987) 247
(2) L.D.Hulett, Jr., T.A.Lewis, R.G.Alsmiller, Jr., R.Peele, S.Pendyala, J.M.Dale and T.M.Rosseel; Nucl. Instr. & Meth. B24/25 (1987) 905
(3) J.H.Malmberg and C.F.Driscoll; Phys.Rev.Lett. 44 (1980) 654
(4) F.Ebel, W.Faust, H.Schneider and I.Tobehn; Nucl. Instr. & Meth. A274 (1989) 1
(5) Y.Ito, O.Sueka, M.Hirose, M.Hasegawa, S.Takamura, T.Hyodo and Y.Tabata; Proc. 8th Int. Conf. Positron Annihilation, Eds. L.Dorikens-Vanpraet, M.Dorikens, D.Segers (World Scientific, 1989) p.583
(6) T.Akahane, T.Chiba, N.Shiotani, S.Tanigawa, T.Mikado, R.Suziki, M.Chiwaki, T.Yamazaki and T.Tomimasu; Proc. 8th Int. Conf. Positron Annihilation, Eds. L.Dorikens-Vanpraet, M.Dorikens, D.Segers (World Scientific, 1989) p.592
(7) T.Cowan, R.Howell and R.Rohatgi; Nucl. Instr. & Meth. B56/57 (1991) 599
(8) D.Segers, J.Paridaens, M.Dorikens and L.Dorikens-Vanpraet; Nucl. Instr. & Meth. A337 (1994) 246
(9) C.M.Surko, A.Passener, M.Leventhal and F.J.Wysocki; Proc. 8th Int. Conf. Positron Annihilation, Eds. L.Dorikens-Vanpraet, M.Dorikens, D.Segers (World Scientific, 1989) p.161
(10) C.M.Surko, M.Leventhal and A.Passner; Phys. Rev. Lett. 62 (1989) 901

(11) R.G.Greaves, M.D.Tinkle and C.M.Surko; Phys. Plasmas 1 (1994) 1439
(12) S.J.Gilbert, C.Kurz, R.G.Geaves and S.M.Surko; Appl. Phys. Lett. 70 (1997) 1944
(13) P.B.Schwinberg, R.S.Van Dyck,Jr. and H.G.Dehmeldt; Phys. Lett. 81A (1981) 119
(14) G.Kögel, unpublished results 1995-1999

## 4.2. BUNCHING SYSTEM

P.Sperr (München)

This contribution about a bunching system for a positron lifetime beam is based on discussions with G. Kögel and on the over ten years of experience we have with pulsed positron beams at our institute in Munich.

Electron linacs, which are used to generate the positrons via pair production have an excellent pulse structure with a width in the picosecond range. The question is, if this time structure can be directly used for positron lifetime experiments with low energy (≤ 50 keV) positrons.

1. The low energy positrons are produced by the moderation technique [1]. They are emitted from the first moderator with an average energy of about 2.7 eV (W – moderator). But even from a well annealed moderator foil an energy uncertainty ΔE of about ± 0.2 eV and in a addition a low energy tail is observed [2]. The value of ΔE and the intensity of lower energy positrons depend critically on the treatment and the durability (UHV – conditions) of the moderator.

2. As the first moderator is in a high radiation field, a strong degradation of the efficiency and a considerable broadening of the energy distribution of the emitted positrons occur [3,4 ].

3. In order to obtain as much positrons as possible probably a stack of first moderator foils has to be used. The point of creation is smeered out. Also the primary positron beam from the first moderator is expected to have a diameter in the order of centimeters.

Due to the high radiation field in the environment of the first moderator stage the moderated positrons have to be guided in a beam line over a long distance away from the point of creation. The time spread Δt (FWHM) after a flight path of 10m is shown in figure 1 as function of the extraction energy. In addition it has to be stressed out

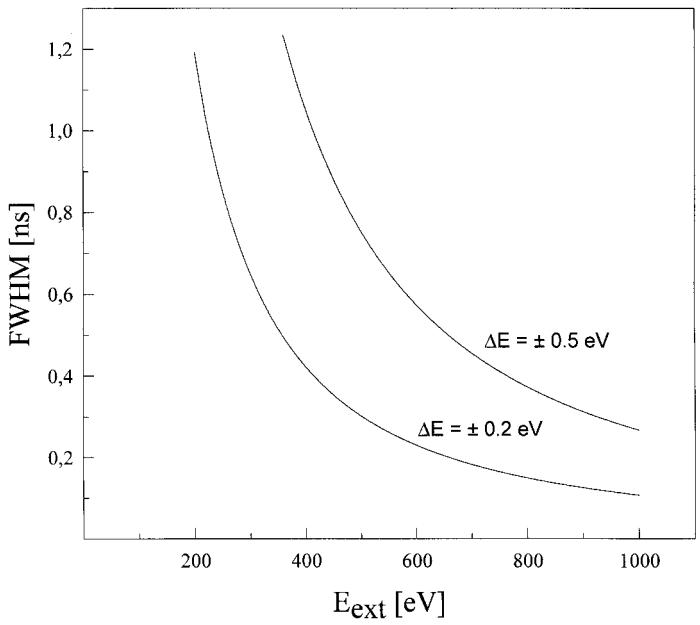


Fig.1 Time spread Δt (FWHM) after a flight path of 10 m as a function of extraction energy.

that the very low energy positrons create a large tail in the time distribution (example is given in [5]). An extended moderator foil stack and the necessity to focus a large diameter beam to a small spot on the target will cause additional time spreads.

The arrangement which is proposed here is shown in figure 2. It is based on the pulse and time structure which is

given e.g. in the information on the TESLA Test Facility (TTF). The bunches of positrons from the first moderator (see contribution of D. Seegers, section 3.2.) are fed into the "lifetime beam line" (2) by a pulsed switching device (1) and focussed onto a remoderator stage (3). The remoderation stage is described in section 4.3. by G. Kögel. With this remoderation the large beam diameter and the energy spread of the positrons is

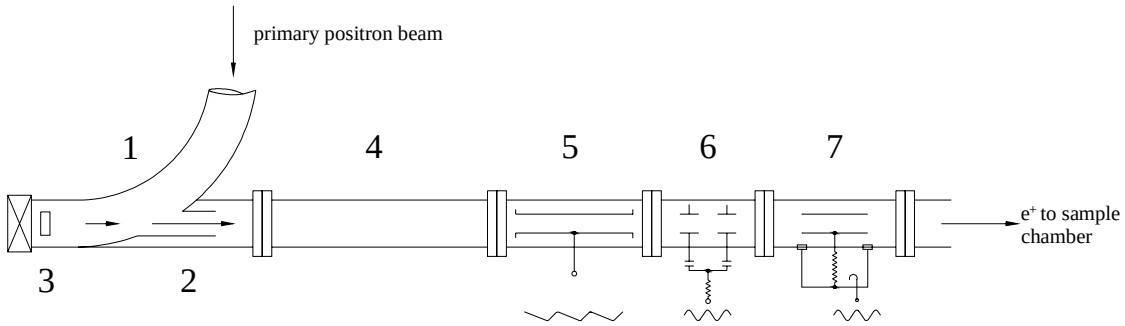


Fig.2 Proposed stage for remoderation and bunching.

considerably reduced [6]. The remoderated positrons (efficiency ≈ 20%) are extracted at low energy (with device (1) "OFF") into a stretcher (4). As the time separation of bunches is about 100 ns, there is enough time to clear the line (2) before the next bunch arrives. The extracted low energy positrons are stored in (4) (penning trap type stretcher) during the whole bunch train (duration ≤ ms). As the repetition rate of the bunch trains is low (10 Hz), there is enough time to clear the trap. The (now dc-beam) of positrons is now bunched again in a prebuncher device (5), e.g. configured as a saw tooth buncher. At a repetition rate of 10 MHz it is possible to get about 80% of the positron s into a bunch with a width of 1 ns (FWHM) [5]. The tails in the time structure of the pre-bunches are cut off by a chopper device (6). This chopper can be made as a double deflection plate system with an external resonator. The final time structure is made in a resonator type main-buncher (7). Due to our experience it is possible to achieve a time structure of about 100 ps (FWHM). The total time resolution of the life time system (about 200 ps (FWHM)) is mainly determined by the resolution of the detector systems for the 511 keV annihilation quanta and not by the pulsing components. After the main-buncher the positrons can be variably accelerated to the desired energy and guided to the target position. Devices like (5), (6) and (7) are successfully in operation in our laboratory [7,8]. This arrangement offers a large flexibility for the demands of new experiments, e.g.

(i) with (5), (6) and (7) "OFF", a very intense dc-beam is available

(ii) with (4) "OFF" and a masterfrequency of 10 MHz (repetition rate of the single bunches) a pulsed beam with good time resolution and with $2x10^4$ positrons per pulse is available (starting with about $8x10^9$ slow positrons/s in the primary beam and a remoderation efficiency of 20%). If in addition such a beam can be focussed down to ~ 1 $\mu m^2$, experiments like implanting large numbers of positrons near to a void will be possible.

(iii) with all components ON and a clearing time of about 0.1 s for the trap one gets about $10^2$ positrons in one bunch.

It is quite obvious that with this high count rate new multi-detector systems have to be concidered. Special care has also to be taken for the giudance of the positron beam (extraction out of or reentry in magnetic field configurations).
The rf-components which are needed in the arrangement as proposed here are state of the art and can be built on customer request. No special development of single components is required.

**References**


[1] P.J. Schultz and K.G. Lynnn; Rev. Mod. Phys. 60 (1988) 701

[2] P. Willutzki, J. Störmer, D.T. Britton, G. Kögel, P. Sperr, R. Steindl and W. Triftshäuser; Proc. SLOPOS 5, Jackson, Wyoming (1992)

[3] R. Suzuki, T. Ohdaira, a. Uedono, Y. Koo Cho, S. Yoshida, Y. Ishida, T. Oshima, H. Itoh, M. Chiwaki, T. Mikado, T. Yamazaki and S. Tanigawa; Jpn. J. Appl. Phys. 37 (1988) 4636

[4] G. Triftshäuser, private communication: W-moderator in the radiation field of a reactor core.

[5] P. Sperr, P. Willutzki and M.R. Maier; Materials Science Forum Vols. 175-178 (1995) 993

[6] A.P. Mills jr.; Appl. Phys. 23 (1980) 189

[7] P. Sperr and G. Kögel; Materials Science Forum Vols. 255-257 (1997) 109

[8] W. Bauer-Kugelmann; Thesis (2000), Institut für Nukleare Festkörperphysik, Universität der Bundeswehr München, and to be published


## 4.3. REMODERATION AND ADIABATIC TRANSFORMATION OF PHASE SPACE


G.Kögel (München)


Besides the flux, I, also the occupied phase space volume, $\Omega$, determines the quality of a positron beam. For rotationally symmetric fields, the transverse phase space, $\Omega_t$, is proportional to the product of beam cross section, Q, and transverse energy spread $\Delta E_t$. The longitudinal phase space, $\Omega_l$, is proportional to the longitudinal energy spread, $\Delta E_l$ and to the duty factor $T_p/T_r$, where $T_p$ denotes pulse duration and $T_r$ pulse separation time. In usual beam systems, $\Omega_t$ and $\Omega_l$ separately are conserved to first order. According to Liouville´s Theorem, only $\Omega_t \cdot \Omega_l$ is strictly conserved under the action of conservative forces.

These beam characteristics are displayed in table 1 for a laboratory beam with radioactive source and beams as expected from the Elbe [1] and TTF accelerators, assuming $\Delta E_t = \Delta E_l = 2$ eV and Q = 4 cm$^2$ together with those for an electron beam from a monoatomic field emission tip [2]. Also the requirements for various positron experiments at the specimen are listed in table 1. Besides the quantities listed in table 1, the following experimental conditions were assumed: detector counting rate 1 MHz, overall detection efficiency 2%, $T_p$ = 100 ps and $T_r$ = 20 ns in lifetime measurements, 5 mm diameter of the analyzed spot, 20 eV kinetic energy and 30 mm distance from the last lens in PAES, 100 eV kinetic energy, 1 mrad beam divergence and $\Delta\lambda/\lambda = 10^{-3}$ in LEPD. Always optimized particle optics without aberration correction is assumed.

**Table 1:** Comparison of relevant beam characteristics for various sources and experiments

| **Item** | $\Omega_t$ **[eV cm$^2$]** | $\Omega_l$ **[eV]** | **I [1/s]** | $\Omega_l \cdot \Omega_t$ **[eV$^2$cm$^2$/s]** | **Remarks** |
|---|---|---|---|---|---|
| Electron source | $2 \times 10^{-16}$ | 0.5 | $10^{10}$ | $10^{-16}$ | |
| Laboratory beam | $6.5 \times 10^{-3}$ | 0.2 | $< 5 \times 10^5$ | $1.3 \times 10^{-3}$ | |
| ELBE | 8 | $4 \times 10^{-3}$ | $5 \times 10^7$ | 0.032 | FEL injector |
| TTF | 8 | $1.1 \times 10^{-5}$ | $10^{10}$ | $10^{-4}$ | |
| Lifetime exp. | 0.05 | 0.025 | $5 \times 10^7$ | $1.25 \times 10^{-3}$ | |
| Microbeam 1 µm | $10^{-6}$ | $5 \times 10^{-3}$ | $5 \times 10^7$ | $5 \times 10^{-9}$ | Pulsed beam for lifetime experiment |
| Microbeam 10 nm | $10^{-11}$ | $5 \times 10^{-3}$ | $5 \times 10^7$ | $5 \times 10^{-14}$ | |
| LEPD | $2.5 \times 10^{-5}$ | 0.2 | $5 \times 10^7$ | $5 \times 10^{-6}$ | |
| PAES | 0.25 | 1 | $5 \times 10^7$ | 0.25 | |

The data in table 1 demonstrate the inferiority of all positron sources as compared to a good electron source as well as the huge difference between the requirements of advanced positron experiments and possible positron sources, particularly in the $\Omega_t$ values. To reduce $\Omega_t$ there are three possibilities. As in electron optics, we could reduce $\Omega_t$ and I together by a *beam aperture*. Because of the small positron flux this is prohibited in all but the simplest experiments. On the other hand, in positron optics we can invoke stochastic forces in the process of *remoderation* thereby circumventing the restrictions of Liouville´s theorem. Finally, we can try to invent *advanced optics* where the loss free reduction of $\Omega_t$ is achieved by an increase of $\Omega_l$ so that the product $\Omega_l \cdot \Omega_t$ remains unaltered.

## Remoderation

A typical remoderation stage is sketched in fig. 1. A primary beam is focussed into a spot area $Q_s$ as narrow as possible on a remoderator. Since $\Omega_t$ is conserved, $\Delta E_t$ must be increased to $\Omega_t/Q_s$ at the spot. The implanted positrons, however, are thermalized and a fraction of about 20% (5 keV implantation energy at W 100) is reemitted from $Q_s$ with near thermal energy spreads $\Delta E_{t,r}$, $\Delta E_{l,r}$.Thus $\Omega_t$ is reduced by a factor of $\Delta E_t/\Delta E_{t,r}$. The reemitted beam must be separated from the primary beam. With magnetic positron optics [3] this can be achieved by a suitable magnetic prism on the common beam axis. Furthermore, magnetic lenses present minimal spherical aberration, which controls the minimal $Q_s$ for a given beam [3]. For the best available magnetic lenses, $\Omega_t$ and $\Omega_l$ are reduced according to

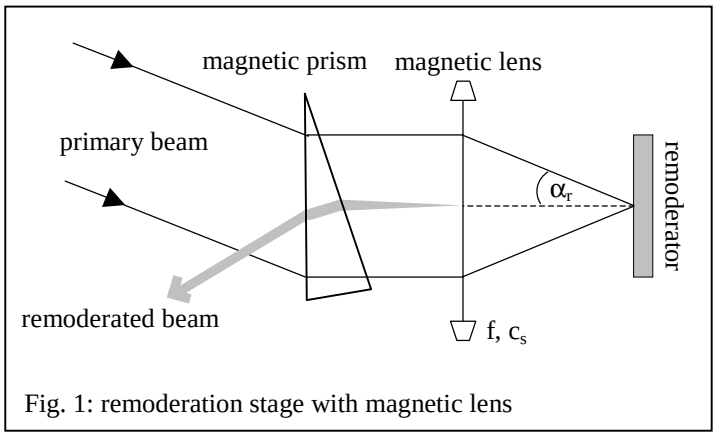

Fig. 1: remoderation stage with magnetic lens

$$\Omega_{t,re\,\mathrm{mod}} = \eta\,\Omega_{\mathrm{t,primary}} \tag{1}$$

$$\Omega_{l,re\,\mathrm{mod}} = \frac{\Delta E_{l,r}}{\Delta E_{l,primary}}\Omega_{l,primary}\,, \tag{2}$$

with $\eta \approx 1.5 \times 10^{-4}$, in perfect agreement with the experimental results [4]. The magnetic remoderation stage has been applied for the first time in the München Scanning Positron Microscope. In this Positron Microscope, the primary beam from a source of about 2 mm diameter, is focussed onto a 20 µm spot (FWHM) at the remoderator. The remoderated beam has an aperture (half cone angle) of 1 mrad at 200 eV kinetic energy. For the intense positron source under construction at the FRM-II reactor at München [5], a large magnetic remoderation stage (15 $cm^2$ primary beam) has been constructed and tested successfully with electrons [6]. Formula 1 is restricted to $Q_s > 10^{-6}$ $mm^2$.

The more traditional remoderation stage, as shown in sec. 3.2, fig. 2 of this report, is based on electrostatic optics. Beam separation is achieved by tilting the axis of the remoderated beam relative to the primary one. Due to this arrangement and due to by orders of magnitude stronger spherical aberrations in electrostatic lenses, the theoretical limit for $\eta$ in eq. (1) is about $1.5 \times 10^{-3}$. So far, this limit has not been achieved in the experiment.

## Advanced Optics

There are difficulties, which prevent us from achieving any reduction of $\Omega_t$ by sufficiently many remoderation stages. Besides the intensity loss of 80% for each stage there is also an increase by about 5 keV in the voltage drop between source and specimen. For a user-oriented installation there is also the disadvantage, that a chain of remoderation stages delivers fixed characteristics $\Omega_t$ and $\Omega_l$, whereas the various experiments demand quite different characteristics, as may be seen from table 1.

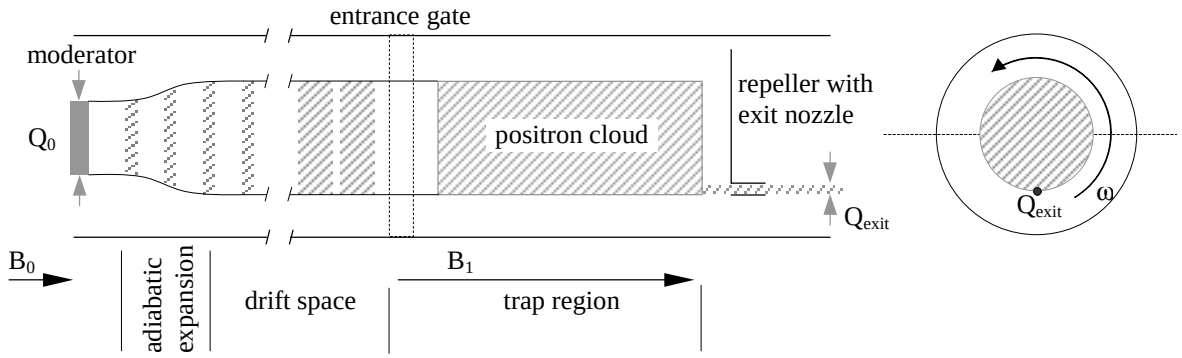


Fig.2: Advanced penning trap for extraction of an adiabatically cooled beam with cross section $Q_{exit}$

Are there further opportunities to reduce $\Omega_t$ which do not suffer from these disadvantages? Yes, the pulsed operation of accelerator-based positron sources offer, at least in principle, such an opportunity if the Penning trap is modified somewhat with respect to the traditional arrangement as displayed in sec. 5.

This modified setup [7] is sketched in fig. 2 Approximate numbers are given for the characteristics of TTF. The guiding magnetic fields for the moderated positrons is lowered

from the starting value $B_o$ at the moderator to $B_1$. Therefore, the cross section of the beam is adiabatically increased from $Q_o$ to $Q_1 = \frac{B_o}{B_1} Q_o$, $\Delta E_t$ is reduced to $\Delta E_{t,1} = \Delta E_t \cdot B_1/B_o$ and $\Delta E_l$ is increased to $\Delta E_{l,1} = \Delta E_l + (B_o - B_1)\, \Delta E_t/B_o$. Then the positrons drift in a flight tube at appropriate kinetic energy so that the pulse width increases from $T_p$ (≈ 150 ps) to $T_r$ (≈ 100 ns) at the entrance gate for the storage region of the Penning trap. Since the most energetic positrons arrive first, with an appropriate periodic sawtooth signal superimposed on the continuously lowered gate voltage, the energy spread at the entrance can be reduced to $\Delta E_{l,2} = \Delta E_{l,1} \cdot T_p/T_r$ (≈ 4 meV). If $T_{fill}$ denotes the total filling time (≈ 720 µs) and $T_a$ the turnaround time (entrance to entrance ) of positrons in the trap, then the final energy spread of the stored positron cloud is $\Delta E_{l,3} = \Delta E_{l,2} \cdot T_{fill}/T_a$ (≈ 1 eV). In contrast to the standard configuration, where a beam of cross section $Q_1$ is extracted by continuously lowering the exit gate over the extraction time $T_{exit}$ (≈ 100 ms), here positrons with energy spreads $\Delta E_{t,1}$ and $\Delta E_{l,3}$ will be extracted through a small exit nozzle of cross section $Q_{exit}$. Obviously $Q_{exit} \cdot T_{exit} \geq Q_1 \cdot T_a$ for complete extraction. Also the trapped positron cloud has to be moved gradually with respect to the nozzle. This can be achieved by weak electric drift fields and by the Brillouin rotation of the positron cloud due to the space charge with angular frequency $\omega_{Brillouin} = \rho/2\varepsilon_o B_1$ ($\rho$ = density of space charge). After some algebra one obtains for the transformation of phase space by the advanced Penning trap [7]

$$\Omega_{t,exit} = \Omega_{t,o} \cdot T_a/T_{exit}, \tag{3}$$

$$\Omega_{l,exit} = \Omega_{l,o} \cdot T_{exit}/T_a + \frac{B_o - B_1}{B_o} \Delta E_t \cdot \frac{T_{fill} \cdot T_r}{T_a \cdot T_p}. \tag{4}$$

The fringing fields of the exit nozzle will cause additional contributions to $\Omega_{t,exit}$ and $\Omega_{l,exit}$. However, this disturbance will be of the same relative order as for the usual extraction from the full cross section $Q_1$, since the exit gate and the exit nozzle present a similar potential distribution. The interaction occurs only once for the exit nozzle, but on the average $T_{exit}/2T_a$ times for the full exit gate [7].

With respect to a remoderation stage, the advanced Penning trap presents considerable advantages. There is neither a potential drop nor an intensity loss. Furthermore, the phase space could be shifted between longitudinal and transverse degrees of freedom depending on the requirements of the actual experiment by the simple control of $T_a$ (see (3) , (4)). Finally, more than one exit nozzle could be implemented in the advanced Penning trap, enabling a continuous, loss free split of the beam for parallel experimentation. For TTF, $\Omega_{t,exit} = 10^{-4}\, \Omega_{t,o}$ should be achieved.

In the case of ELBE, the storage time of the trap cannot exceed 100 ns [1]. The pressure for loss free reduction of $\Omega_t$, however, is even higher because of the comparatively low intensity [1]. A simplified version of the advanced Penning trap may achieve $\Omega_{t,exit} = 10^{-2}\ \Omega_{t,o}$ [7].

**Conclusions**

There are two promising strategies to match the positron beam, as delivered by an intense source, to the specific requirements of advanced experiments. A highly flexible, advanced Penning trap should be placed next to the source. It will serve as storage trap, variable phase space shifter and beam splitter. The remaining compression of $\Omega_t$, if required, must be achieved by remoderation. Here, the design depends on the actual performance of the source and the specific needs of the relevant experiment. To assist the selection, approximate rules (1) to (4) for phase space transformation have been developed.

**References**


[1] The ELBE Radiation source project at the Forschungszentrum Rossendorf, G. Brauer et al. Mat. Science. Forum 255-257, 732 (1997)

[2] Field emission from nanotips, Vu Thien Binh and S.T. Purcell, Appl. Surf. Science 11, 157 (1997)

[3] A through the lens reflection moderator for positrons, K. Uhlmann, D.T. Britton and G. Kögel, Optik 98, 5 (1994)

[4] Rasterpositronenmikroskop, A. David, thesis, Universität der Bundeswehr München, unpublished (2000)

[5] High intense positron beam at the new Munich research reactor FRM-II, C. Hugenschmidt et al., Appl. Surf. Science 149, 7 (1999)

[6] Aufbau eines remoderierten Positronenstrahls, B. Strasser, diploma thesis, Technische Universität München, unpublished (1996)

[7] G. Kögel, unpublished results 1995–1999.


## 4.4. ELECTROSTATIC FOCUSSING


R. S. Brusa, G. P. Karwasz and A. Zecca (Trento)


In the last twenty years, slow positron beams have been demonstrated to be very powerful instruments in solid state and atomic physics. However, it was also realized that the full exploitation of these instruments is limited by the low intensity and low brightness obtainable with laboratory based positron beams.

With a LINAC it is possible to obtain intense positron beams , about $10^8$ e+/s (see paragraph 3.1), and new exciting possibilities in applied and fundamental positron physics could be opened.

However for the major applications it is necessary to have a good quality of the beam, and not only an intense flux of positrons. Some required characteristics are : tunability in a wide low (< 1- 200 eV ) or high (100 eV – 40 keV) energy ranges, low angular divergence, spot diameter in the micron or sub-micron range, pulsing in the nanosecond or picosecond range. Usually different experiments demand a combination of these characteristics. A comparative table of these characteristics for various experiments is given in paragraph 4.3.

The simplest and clear way to obtain these beam characteristics is to implement electrostatic transport and focussing of positrons. The quality of the beam can be expressed by the brightness (B) of the beam per volt, a quantity that is conserved at any section of a beam in presence of conservative forces. $B/V = I/(AV\Omega)$ where I, A, V, $\Omega$, are intensity, area, voltage and solid angle, respectively. In our Trento University Laboratory we have more than thirty years of experience in handling electrons and positrons with electrostatic optics for surface and atomic physics experiments.

We can divide into two classes the positron experiments to be done with an intense LINAC based positron source: a) lifetime experiments in which a pulsed beam (pulse with 100 ps FWHM) is necessary, and b) experiments in which positrons (or positronium) are used as a probe for surface states, surface defects and for

advanced atomic and molecular scattering measurements; in this cases a continuos beam or a beam pulsed at nanosecond is required.

It is well known [1] (see also previous paragraphs), that with high intensity pulsed beams from LINAC, the instantaneous current at the target can be too high to be handled by counting devices and the brightness is very low (spot diameter of the centimeter order). The first problem is solved by a storage system like a trap device from which positrons are spilled, the second one by implementing the brightness enhancement techniques [2], i.e. several re-moderation stages. Since the re-moderation process involves non-conservative forces, positrons out of the re-moderator come from an electron-optical object with higher brightness. A further problem to solve is the extraction of the positron beam from the magnetic field that transports the positron beam from the primary source to the experimental hall.

Now we suppose that positrons are just transported, stretched and spilled from a trap in a field free region. This is demonstrated to be feasible by field terminators [3, 4] (see also paragraph 3.5).

As a consequence of the above considerations about the different requirements of the different experiments, the incoming beam must be splitted at least into two lines. This is achievable with electrostatic transport and switching. The switching, transport and formation electrostatic optics must be accurately shielded ($< 1$ μT) by mu-metal material from the earth and spurious magnetic fields, to maintain the high quality characteristic of the beam.

The next step is the re-moderation of the beam. Two re-moderation modes are possible: in transmission or in backscattering geometry. Our laboratory has good experience in both re-moderation modes; in the following we will address advantages and disadvantages about the two possibilities. The re-moderation in backscattering geometry is the best known but, as will be seen, the re-moderation in transmission geometry can not be discarded for the advantages in the electron optic design and the recent promising results in obtaining good moderation efficiencies.

Beams with re-moderation stages have been realized until now with re-moderation in metal single crystals using complicated geometries in backscattering [5, 6, 7]. Also the lifetime facility at the Lawerence Livermore National Laboratory is intended to use a three re-moderation stage in backscattering geometry, like the design of Ref.6. These geometries worsen the electron-optical quality of the extracted beam and the extracted positrons are more difficult to handle with electrostatic transport. One of the consequences, and increasing complexity, is that to restore the symmetry of the beam, and electrostatic deflector systems are needed, if intensity losses are not acceptable.

Thin film re-moderation allows a more simple geometry, a more compact design of the electron optic system, and lower aberration in the formed beam. Actually, the state-of-the-art in producing thin film moderators is not completely established, and probably for this reason this solution was not yet implemented. However, it has been demonstrated in our laboratory that thin films of Cu and Ni (ref. [8] and references therein), even of not high quality, may reach a re-moderation efficiency comparable with that of a re-moderator in backscattering geometry. These films can be produced by a very simple deposition procedure [8] on sodium chloride crystals (100) surface.

For the first time, a Cu film will be used in a positron beam with a brightness stage for molecule-positron scattering studies : this beam has been just tested in our laboratory [9].

Most probably in the next years, with a small effort, thin re-moderator films of good quality and perhaps of different materials will be produced and tested.

Thin films coupled with simple electron optic devices, like those shown in Fig. 1a and Fig. 1c of Ref. [10], will permit to realize two moderation stages with a demagnification of 30 of the spot diameter for every stage, with only two or 5 electrodes. This device of 4 to 10 cm length could be easily extracted from the system for conditioning simultaneously the two thin films. Another advantage is that the conditioning temperature for these films is only 600 °C and does not need any electron gun for the heating procedure. These films are also very easy to handle being not so brittle as tungsten films.

By focussing a beam with a spot diameter of 2 cm at 5 keV on the first film , a spot of about 20 micron could be obtained as output of the device.

A beam of this dimensions, with very low aberration, can be transported and with suitable electron optics used for surface (PAES, LEPT) and atomic physics experiments.

If a spot diameter less than 1 micron is needed this device can be followed by "traditional" backscattering re-moderation stages or to be constructed with three films in a cascade. The choice can be dictated by the overall design of the facility and from the various experiments. The first choice could be convenient for a lifetime pulsed beam facility, because of the necessity to couple the positron beam with a conventional electron microscope [7].

In all cases the electrostatic electron optic for the formation and the focussing of the microbeam must be designed with particular care to the aberration [11].

In particular, a lifetime positron beam, after the re-moderation stages, pre-bunching, chopping and bunching (see ref. 3, 7 and paragraph 4.2) must be focussed onto a sample at energies ranging from 1 to 50 keV. This is obtainable with electrostatic accelerators with high performances. One accelerator of this type is actually in use in our laboratory for Doppler broadening studies [12,13, 14]. It is composed by six lenses and can produce a spot at a constant position and with a fairly constant size over the large energy range. Starting with a spot size of 20 micron at the re-moderator (two moderator stages only), without any modification, this accelerator can form a constant spot of 6 micron from 1 to 40 keV, at a constant transport efficiency (constant positron flux). This is achieved by varying the potential of three electrodes only. For our purpose the final lens was a long focusing lens; relaxing this condition a smaller spot can be obtained.

This accelerator has also good properties at low positron energies : it transports 70 % of the beam at 10 eV, and at 60 eV is able to form a spot at the target equal in size to the starting beam spot.

**References**


[1] A. Dupasquier and A. Zecca *"Atomic and solid-state physics experiments with low-energy positron beams"* La Rivista del Nuovo Cimento **12**, 1-73 (1985)

[2] A.P. Mills, Jr., Appl. Phys. **23**, 189 (1980)

[3] A. Zecca, R.S. Brusa, M.P. Duarte-Naia, G.P. Karwasz, J. Paridaens, A. Piazza, G. Kögel, P.Sperr, D.T.Britton, K.Uhlmann, P. Willutzki and W. Triftshäuser: Europhys. Lett.**29**, 617 (1995)

[4] W. Stoeffl, P. Asoka Kumar, R. Howell: Appl. Surf. Science **149**, 1 (1999)

[5] R.S.Brusa, W.Raith, A.Schmitt, G.Sinapius, G.Spicher, A.Zecca: EPOS **1986**, Production of Low-Energy Positrons with Accelerators and Applications, Giessen, 25-27 September 1986, International Symposium

[6] T.N. Horsky, G.R. Brandes, K.F. Canter, C. B. Duke, A. Paton, A. Kahan, S. F. Horng, K. Steven, K. Stiles, and A. P. Mills, Jr, Phys. Rev. B **46**, 7011 (1992)

[7] K. Uhlmann, W.Triftshäuser, G. Kögel, P. Sperr, D.T. Britton, A. Zecca, R.S. Brusa , G. P. Karwasz, Fresen. J. of Anal. Chem. **353**, 594 (1995)

[8] R.S. Brusa, W. Deng, R. Checchetto, G.P. Karwasz, A. Zecca : Appl. Phys. Lett. **76**, 1476-78 (2000)

[9] G. P. Karwasz, R.S. Brusa, M. Barozzi, A. Zecca: $10^{th}$ workshop on Low energy positrons and Positronium Physics, KEK, Tsukuba, Japan, July 1999, page.63, Nucl. Instrum. Meth. B (in print)

[10] A.Zecca, R.S.Brusa, Nucl.Instrum. & Meth. **A 313**, 337 (1992)

[11] T. Roach, A. Bakshi, and K. F. Canter: Meas. Sci. Technol. **6**, 496 (1995)

[12] R.S. Brusa, G.P. Karwasz, M. Bettonte and A. Zecca: Slow Positron Beam Techniques for Solid and Surface, SLOPOS-7, Journal Applied Surface Science 116, 59 (1997)

[13] A. Zecca, M. Bettonte, J. Paridaens, G.P. Karwasz and R.S. Brusa: Meas. Sci. Technol. **9**, 1 (1998)

[14] R.S. Brusa, G.P. Karwasz, N. Tiengo, A.Zecca, F. Corni, G. Ottaviani, R. Tonini: Phys Rev. B **61**, 10154 (2000)

# 5. APPLICATIONS

## 5.1. MATERIALS SCIENCE

## 5.1.1. POSITRON DEEP LEVEL TRANSIENT SPECTROSCOPY

C.D.Beling (Hong Kong)

### 1. Introduction.

Most applications of semiconductors involve doping the material with suitable atoms in order to modify the type and magnitude of electrical conductivity to suit the requirements. Whether this be carried out by high temperature diffusion or ion implantation the impurity atoms may reside at non-substitutional sites such as interstitial positions and give rise to deep level states. Vacancies and vacancy complexes may also be formed through implantation damage. The net effect is often a number of localized electronic states within the forbidden gap of the host semiconductor.

The presence of deep levels can be both beneficial and detrimental depending upon the application of the device. For example impurities of Au and Pt are widely used as carrier lifetime quenchers in Si power devices [1], while Cr is added to GaAs to obtain high resistivity substrates [2]. The presence of deep levels, unfortunately, has also, in many circumstances, negative effects, such as the degradation of quantum efficiency in light emitting diodes (LEDs) and solar cells through their contribution to non-radiative decay [3]. These potentially strong influences, together with the fact that in many devices the defect inducing ion implantation technique is required for efficient doping, indicate the clear need to build up a better microstructural understanding of deep level causation.

There exist a number of techniques for providing information on deep levels. There are photoluminescence PL [4] , thermally stimulated current (TSC) [5], thermally stimulated capacitance (TSCAP) [6], and admittance spectroscopy [7] to name some of the more major techniques that have been employed in the literature for the study of deep levels. Each technique has its own disadvantage. The DLTS technique, which was introduced by DV Lang at the Bell Labs, USA in 1974 overcomes most of these [8]. The technique has since its discovery developed into one of the more popular of semiconductor spectroscopies. Indeed the technique dominates in modern semiconductor research when energy levels of deep levels in materials and device structures have to characterized. Commercial instruments are readily available [9].

On the other hand PAS (Positron Annihilation Spectroscopy) has become a powerful technique since the mid 1980s for the characterization of open volume defects in semiconductors. For a review of PAS semiconductor studies the reader is referred to the recent review of Krause-Reberg and Leipner [10]. Unlike DLTS this technique does not seek to provide information on electronic energy levels, but to give structural information on defects present in the material. This is made possible essentially by the propensity of the positron to trap into vacancy related crystalline defects. PAS has been particularly useful in the detection of vacancy defects in compound semiconductors such as GaAs[11] and InP [12], and more recently in GaN [13] and II-VI semiconductors. Metastable DX-like defects have also be studied [14].

With the success of both the DLTS and PAS techniques it is natural to ask why there is any need to develop the admixture of the techniques, namely positron-DLTS. There is in fact a good reason , namely that although DLTS and PAS give information on a particular crystal defect the information from each technique appears at present independent. Stated differently, the microstructure informing PAS signal from a particular point defect, gives no information on the electronic energy level associated with the defect , the latter being an important defect identifier for the device engineer. This statement should be qualified, for there are a class of PAS studies that do relate the positron annihilation signal to particular charge state of a defect. In these studies the Fermi energy is varied either by changing the temperature of the dopant concentration, allowing the defect's electronic charge state to be varied [15]. Such studies are, however, fairly time consuming and seldom carried out. A technique that brings the two spectroscopies together is thus desirable. These sentiments are highlighted by looking at undoped n-type GaAs for which in the DLTS spectrum, apart from the defect EL2 (which is known to be related to the Arsenic antisite) hardly anything but reasoned speculation exists for the microstructures associated with the other defect levels such as EL3 and EL6 [16] .

Founded on the above perceived need, the present proposal, after presenting brief reviews of DLTS and PAS, describes how the two techniques can be amalgamated into positron-DLTS (PDLTS). This is followed by some practical ideas on how a PDLTS spectrometer would look like in practice using the proposed intense beam facility. Some of our present attempts to realize the technique subject to the constraints of low intensity and non-focused beams will also be mentioned. Finally some further useful ideas for PDLTS development will be given. Some of the basic concepts behind PDLTS have already been presented in more rudimentary form elsewhere [17].

## 2. Deep Level Transient Spectroscopy

An understanding of PDLTS is best derived through surveying the essentials of conventional DLTS. Conventional DLTS essentially works through monitoring the capacitance of a junction that has been made to the sample under investigation when deep level traps emit electrons as a result of reverse biasing the junction**.** **Fig. 1** shows the normal sequence of trap filling and emptying . In (a) all the traps in the depletion region are empty as a result of reverse bias. Traps are filled in (b) by reducing the reverse bias to a value close to zero. Electrons rush in from the semiconductor bulk and fill the traps. At time t=0 the system is reverse biased (c) and as time progresses the electrons are emitted into the conduction band. The system finally completes the cycle and returns to (a) at which time (t= $\infty$ ) all traps are empty, having released their electrons. During the emission portion of the cycle (c) the junction (be it a pn junction or a Schottky junction) has blocked the supply of electrons to the conduction band and so the capture rate to the traps is essentially zero. The emission rate $e_n$ is given by:

$$e_n = N_c \sigma v e^{-(E_c - E_T)/kT} \tag{1}$$

where $N_c$ is the effective density of conduction band states, $\sigma$ is the trap's electron capture cross-section, **v** is the thermal velocity of the carriers and $E_C$ - $E_T$ is the energy difference between the trap's ionization energy and the conduction band. The strong exponential temperature dependence of the emission rate as given in (1) is fundamental to the working principle of DLTS, since it allows a capacitance signal:

$$C(t) = C(\infty) + \big(C(0) - C(\infty)\big) e^{-e_n t} \tag{2}$$

derived as a result of trap emission to be monitored on a temperature scan. The normally chosen DLTS signal $\Delta C = C(t_2)$-$C(t_1)$, where $t_2$ is chosen someway towards the end of the emission cycle and $t_1$ somewhere near the beginning, becomes large only if the transient decay occurs within the time frame (rate window) of $t_2$ and $t_1$ . i.e. at a temperature $T_{max}$ such that:

$$e_n(T_{\max}) = \frac{t_2 - t_1}{\ln(t_2 / t_1)} = \text{rate window} \tag{3}$$

At lower temperatures (decay slower) and higher temperatures (decay faster) $\Delta C$ will be smaller than at $T_{max}$. A normal DLTS system thus works by monitoring the $\Delta C$ signal as a function of temperature. A deep level is signatured by a peak. The ionization energy of the level can then be obtained by changing to a number of rate-windows and noting how $T_{max}$ varies. From eqns (1) and (3) it is seen that an Arrhenius plot gives the trap energy ($E_C$-$E_T$).

While DLTS is a powerful technique for detecting deep level defect states, it is not without its limitations. The first limitation is that DLTS can only work for materials that are not too heavily doped (carrier density < $10^{17}$cm$^{-3}$). If a material is of more than this concentration the depletion width at the junction becomes too narrow, the tunneling current becomes too large, and deep levels are prevented from emptying. The second relates to the energy range over which DLTS is sensitive. Here, on the one hand, to get very close to the band edge, low temperatures are required to get within the working time window range available using a typical capacitance meter (~1ms time constant). Such low temperatures normally cause the shallow donors themselves to trap carriers and the resultant loss of electron conductivity up to the depletion zone renders capacitance measurement ineffective. In practice it turns out that energy levels with $E_C$-$E_T$ > 0.2-0.3eV from the band edge can normally be detected. On the other hand it is also difficult to study defects which are too deep in the bandgap, these defects requiring too high a temperature to give them the required transient emission rate. Depending on the sample one is normally limited to looking at defects with $E_C$-$E_T$ < ~1eV.

On a more positive note DLTS has a very high sensitivity to deep level defects. The trap density that may be observed is given by $\beta N_D(\Delta C/C)$ where $\beta$ is a system parameter (of order unity), $N_D$ is the shallow donor concentration and C is the natural junction capacitance. This equation reveals that the lower concentration detectable by DLTS is of ~$10^{-5}N_D$ assuming a 0.001% measurement accuracy of capacitance. Defect densities as low as ~$10^{-11}$cm$^{-3}$ are detectable. Few techniques can boast such a high sensitivity.

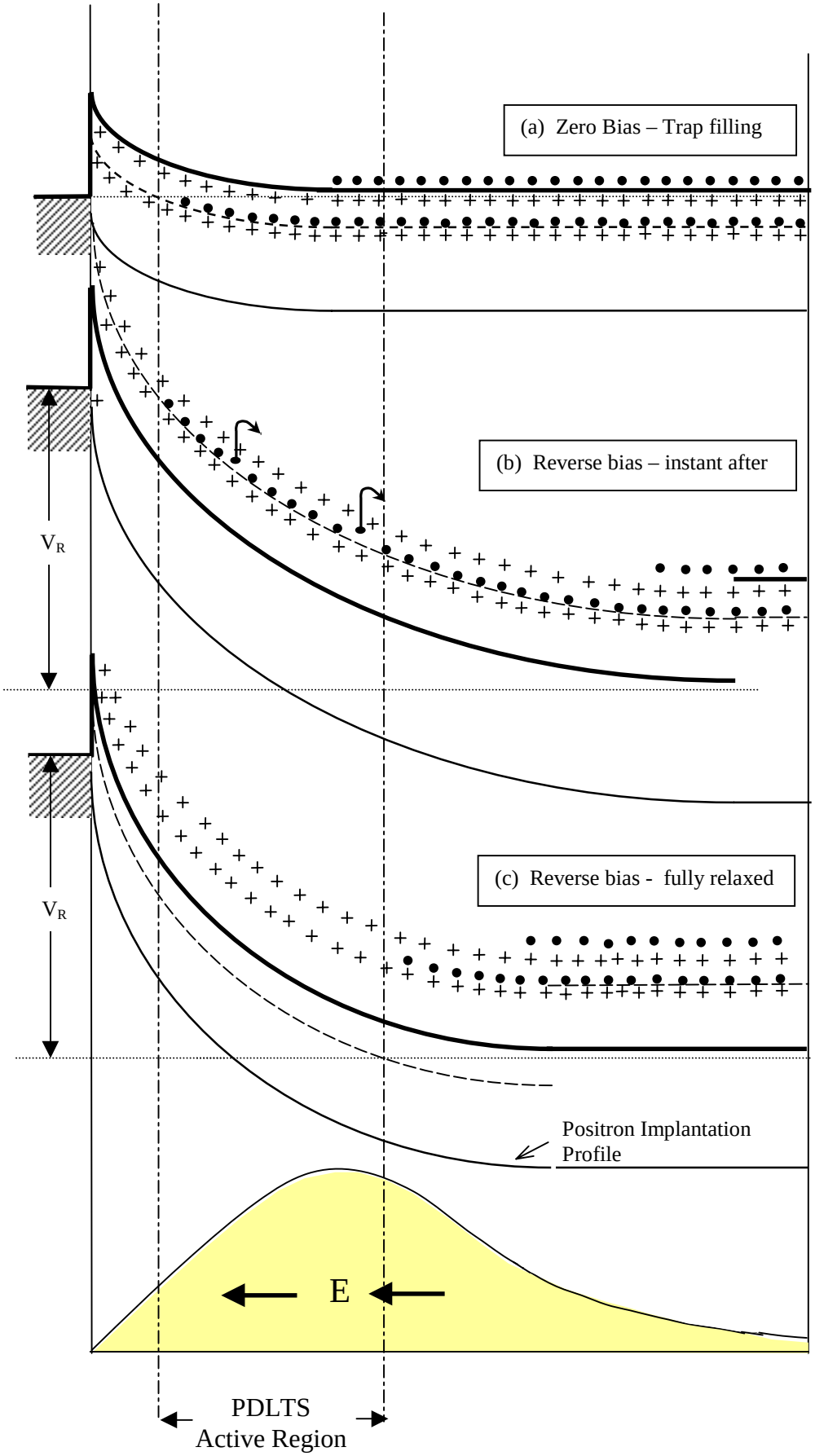


**Fig. 1:** Trap filling and emptying in DLTS and the implantation of positrons to be used in PDLTS

## 3. Positron Annihilation Spectroscopy

Every defect in a semiconductor that traps positrons can be characterized a typical lifetime. The lower electron density experienced by the positron at the open volume site causes a lowering in the annihilation rate and a slightly longer lifetime. This lifetime can now be reliably calculated from theory [18] and thus the LT (lifetime) technique can in conjunction with theory be used to directly identify the basic microstructure of a defect. Such sites are typically open volume defects such as neutral of negatively charged vacancies, divancies or vacancy agglomerates.

In a similar manner the positron-electron momentum distribution changes as a result of the positron experiencing lower momentum electrons of the outer atoms of the defect. Thus positron-electron momentum distribution spectroscopy in the form of either DB (Doppler broadening) [19] or AC (Angular correlation) [20] provides a method of detecting vacancy type defects. Moreover, positron-electron momentum distributions can now be reliably calculated for vacancy defects [21]. Thus DB and AC spectroscopies form potentially powerful tools for assessing defect structures. Except in one or two studies they have not been used in their full form of providing vector information on the electron momentum distribution. This is mainly because it is difficult to separate out the defect distribution from the bulk distribution. Thus it is more common to use single parameter S (valence annihilation) and W (core annihilation) parameters of the material and compare them with the values in a non-defected sample [22].

Generally the trapping model [110] describes the trapping of positrons into defects very well and allows defect concentrations to be determined with some accuracy. Since, however, defect trapping occurs in competition with the annihilation process there is a natural lower limit on the detectable concentration of defects. For example, for the monovacancy in Si the lower limit is ~$10^{15}$cm$^{-3}$ [23]. This is the limit for typical PAS spectra typically containing 1- 5 x $10^6$ events, but it should be noted that this limit is expected to become lower than this for spectra containing $10^8$- $10^{10}$ events or more [as would become possible on the proposed intense positron source] [24].

There is one additional PAS probe that should be mentioned. It is more a technique rather than a spectroscopy, and it is given the name DS (Doppler Shift). In this technique it is not the broadening of the 511keV annihilation line that is of interest, but the small shift ($v_+/2c$) in the centroid position of the line induced by a small drift velocity on the positron. The technique is normally used to measure positron mobilities [25] and is experimentally more difficult than the DB mode requiring the application of an alternating bias of typically 1 Hz frequency to the sample in order to over-ride the more dominant effect of amplifier shift. Interestingly, it was in using DS mode to measure the positron mobility in Semi-Insulating GaAs that the first suggestion of positron-DLTS originated. **Fig 2** shows these mobility measurements as a function of temperature for three

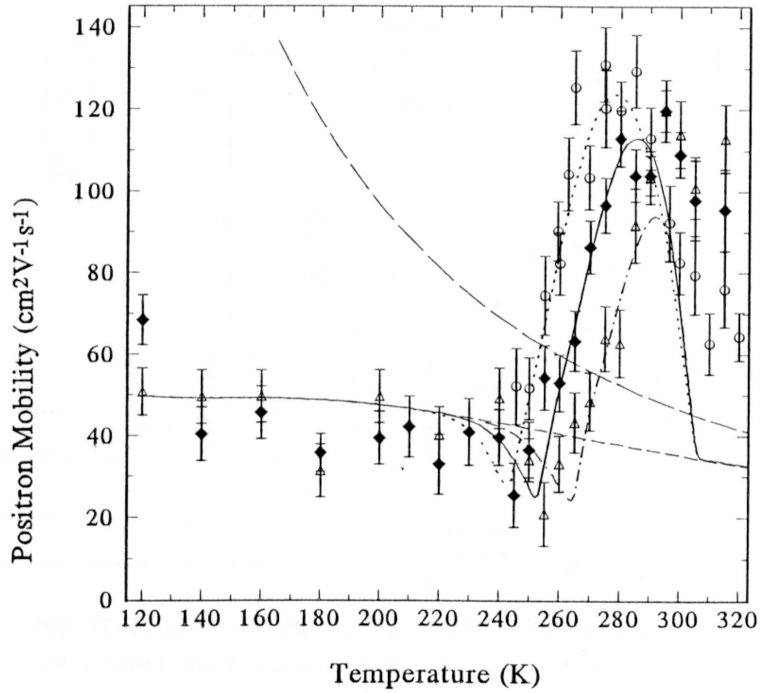


**Fig. 2:** PAS/DS (Doppler Shift) data taken in Hong Kong, showing the transient decay of the EL2 defect as it emits an electron. This is an example of a type II PDLTS spectrum. It took 6 months to collect all the data shown. Rate-windows : open triangles =5Hz, diamonds = 1Hz, circles = 0.25Hz.

different frequencies (rate-windows). The peak in mobility moves with rate-window just as in conventional DLTS, and the explanation is the ionisation produced by the EL2 defect causing the positron to see an enhanced electric field. Arrhenius analysis of the data shows the energy of the defect $E_C$-$E_T$ =0.8eV, thus making a clear identification with the EL2 defect [17].

It is important to note that all the above PAS techniques normally apply to defect studies of bulk crystals in which positrons have been injected from a $^{22}$Na source. In recent years, however, with the development of low energy positron beam technology, it has become very common to study defect structures at surfaces and sub-surface interfaces using SPIS (Slow Positron Implantation Spectroscopy) in which positrons implant a specified depth into a sample which is dependent on the beam energy. The mean implantation depth $\bar{x}$ of positrons of energy $E$ is given by :

$$\bar{x} = \frac{AE^{1.6}}{\rho} \tag{4}$$

where A is usually taken as $4\mu g\ cm^{-2}\ keV^{-1.6}$ and the shape of the positron implantation P(x) is the Makhovian form [26]:

$$P(x) = -\frac{d}{dx}\left[-\frac{x^m}{\bar{x}^m}\right] \tag{5}$$

In the context of the present proposal it is noted that LT, DB and DS techniques can all be implemented as different operational modes of SPIS. This is demonstrated schematically in **Fig 3**. (The PAS-AC technique could also in principle be used but this technique requires a large lateral space, which probably is not available at the proposed facility). It turns out that the ability to exactly "place" stopping positrons according to equations (4) and (5) is important element for implementing PDLTS since as we shall see positrons have to be positioned either in or close to the active depletion region of the DLTS experiment in which traps are being filled and emptied.

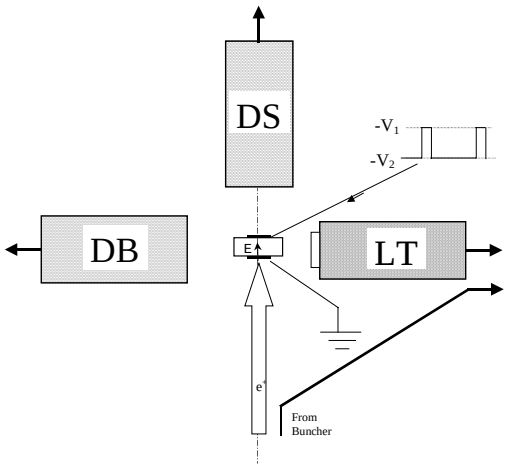


**Fig. 3:** A schematic diagram showing that the three types of PAS spectroscopy mentioned in the text (LT), (DB) and (DS) can be used simultaneously.

## 4. Amalgamation of DLTS and PAS to form PDLTS

As mentioned this proposal seeks to join conventional capacitance DLTS with PAS techniques in a way that should hopefully yield microstructure information on specific deep level defects. This joining of the two techniques, to which we give the name of positron-DLTS (PDLTS), may be done in two different ways. The first (referred to as type I) is that of implanting positrons from a low energy beam into the active depletion region so that positrons sense a time varying ensemble average of defects in different states of electron

occupancy. This is the more important form of PDLTS seeing that in this case both DB and LT techniques, which are sensitive to the vacancy related character of the defects, are employed and thus microstructural information becomes available. The second (type II) relies on the DS alone and utilizes the fact that the positron experiences an increasing electric field as a result of space charge buildup from ionizing defects. This mode appears to give little extra information to that available through conventional DLTS, and it does it at much higher cost (a type II PDLTS spectrum such as that shown in Fig.2 takes typically 6 months with currently available positron information rates compared to typically 1 hour for conventional DLTS !). Nevertheless there are some resistance regimes in which this second sort of PDLTS is operative while its capacitance counterpart is not – such a case seems to exist with semi-insulators – and these could give the technique some significance. These two techniques will be discussed in more detail below, and specifically how they would best be implemented at a high flux LINAC based beam.

**Type-I PDLTS**

As mentioned above the essential feature of this method of observing deep levels is to allow positrons to implant from a positron beam of correctly chosen energy into the part of the depletion region of the reverse biased junction that is emitting its electrons. [Region A-B, **Fig 1**]. At the instance of reverse bias (b) all the vacancy defects in A-B are in a neutral charge state and are thus able to trap positrons, but as time progresses the defects' electrons are emitted leaving the defect positively charged and non-positron trapping. Thus as time progresses we expect to see using the DB PAS mode the valence momentum parameter S start high $S_o$ (b) and then decaying in an approximately exponential form to some lower value ( $S_\infty$ characteristic of the bulk). The same effect will be seen in the mean lifetime $\tau_{av}$ or defect lifetime intensity $I_2$ if LT-PAS is being employed.

The above example of a, $0 \rightarrow +$, transition is an example of the more general case, where a defect with n electrons transits to the same defect with n-1 electrons. The time variation of the generalized PAS parameter P(t) , that results from the competive defect trapping into the two states can be obtained using the two state trapping model [27]. One finds:

$$P(t) = \frac{1}{\lambda_B + \kappa_{n-1} + (\kappa_n - \kappa_{n-1})e^{-e_n t}} \left[ \{\lambda_B P_B + \kappa_{n-1} P_{n-1}\} + \{\kappa_n P_n - \kappa_{n-1} P_{n-1}\} e^{-e_n t} \right] \qquad (6)$$

where trap emission rate $e_n$ is given by eqn. (1), $\lambda_B$ is the bulk annihilation rate, and $\kappa_n$ and $\kappa_{n-1}$ are the trapping rates into the defect states n and n+1 when the states are not competing for positrons. $P_B$ is the PAS parameter in the bulk, while $P_n$ and $P_{n-1}$ are the PAS parameter for positrons trapped in the defects states n and n+1 respectively.

Working from (6) there are two different directions. The first direction is to follow conventional DLTS and define a signal. As mentioned in section 2, conventional DLTS derives its signal usually from the subtraction of capacitance at two different times [ $\Delta C = C(t_2)$-$C(t_1)$,]. This would not be appropriate for the PDLTS signal as it would involved throwing away valuable information from most of the PAS parameter transient. The ideal way is to use a correlator approach by defining the PDLTS signal $\Delta P$ as [28]:

$$\Delta P = \int P(t).(ae^{-e_R t} - b).dt \qquad (7)$$

where $e_R$ is the nominal emission rate window, and $a$ and $b$ are variables that affect the height and zeroing of the signal. As in conventional DLTS $\Delta P$ could be plotted against sample temperature to give a peak representing the deep level. It can be seen from eqn (6) that the variation of $P(t)$ is close to exponential when the trapping rate into the defects is small compared to the bulk annihilation rate. Such a situation is likely to prevail, at least in early PDLTS experiments, because the defect concentration must be less than the donor concentration ~ 5 x $10^{16}$cm$^{-3}$. It is not, however, desirable though to work in this range as a long term goal, where interest might lie in having a high defect annihilation fraction in order aquire a high statistical accuracy on the momentum distribution of a particular defect. The departure of the PAS parameter transient from pure exponential form, however, is not a cause for concern. Departures from pure exponential decay occur in conventional DLTS when the trap density gets close to the dopant density and the standard procedure for dealing with this is to vary the rate window and from the peak maxima make an Arhenius plot (section 2). The Arrhenius plot gives the energy of the trap. In the case of PDLTS changing the rate window would not require further experiments as the nominal rate-window $e_R$ could be varied after data collection. This approach seems on the surface to be doing nothing more than conventional DLTS – namely giving the energy of a deep level. In fact it is doing more, because one only gets a transient and a thus signal $\Delta P$ if:

$$\kappa_n P_n > \kappa_{n-1} P_{n-1} > 0 \tag{8}$$

that is if the initial state of the defect is a positron trap. This in turn means the defect has to be vacancy related. In principle, then a conventional DLTS temperature scan could be performed and compared with a PDLTS temperature scan. Some peaks would coincide – these would show the deep level to come from a vacancy related deep-level, other conventional DLTS peaks would have no counterpart in the PDLTS spectrum and these would either be defects in positively charged states or defects that are not vacancy related.

The first direction outlined above is not the most cost effective. Positron data, even on a LINAC based beam, is limited and there is a need to be economical in the use of beam time. To scan over the whole temperature range looking at all deep levels is a nice idea, but is certainly not economical. It must also be remembered that we are not primarily interested in obtaining the energy of a particular deep level. This can be done much more effectively using conventional DLTS. Our main focus is that of determining the microstructure of a specific defect. It is thus more effective to connect a capacitance meter to the sample and choose a temperature that for the defect in question gives a strong capacitance transient. The emission rate $e_n$ is then

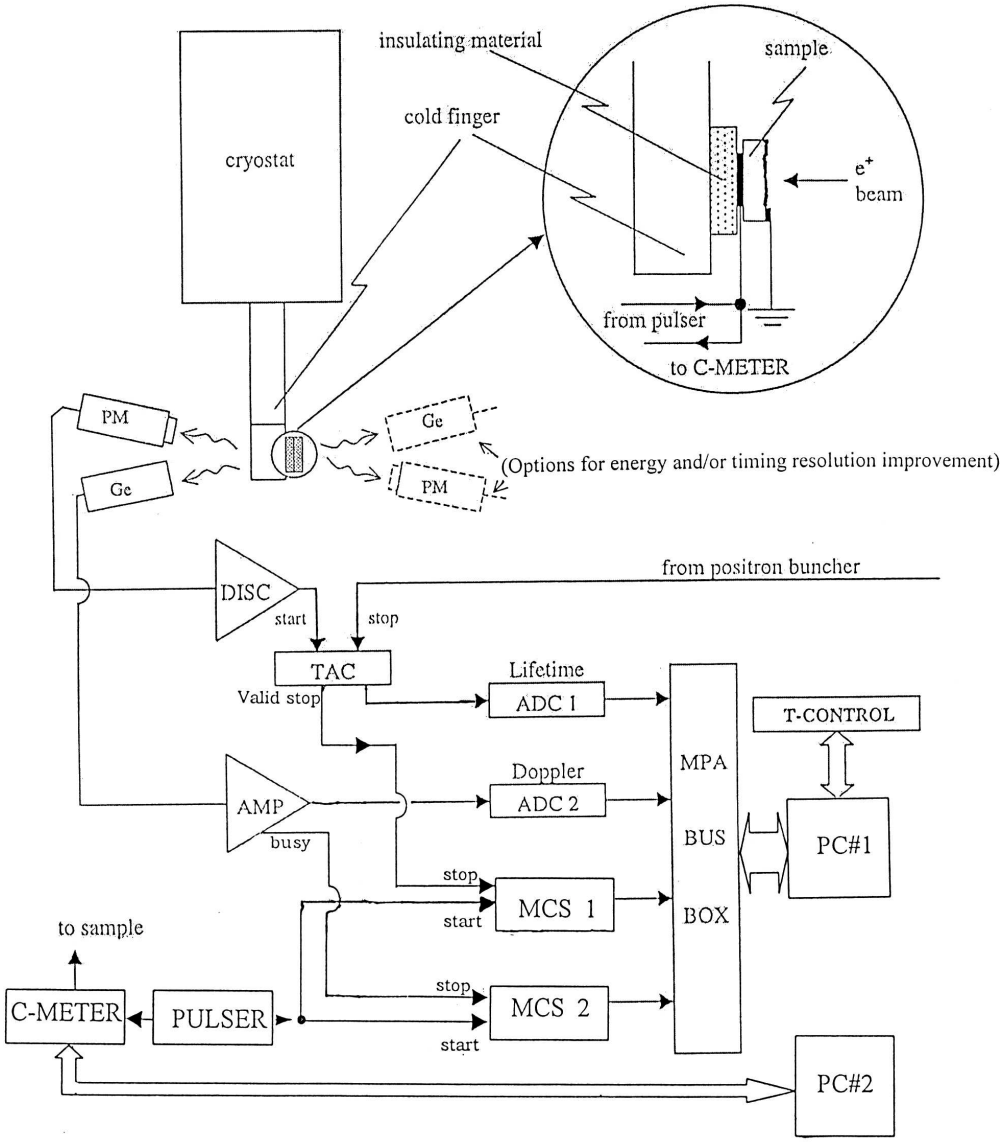


**Fig. 4**. A schematic diagram of a complete PDLTS system, filling in the details of Fig. 3. Note that apart from the on-axis Ge detector and electronics used for DS (optional) and a simple laboratory pulse generator and capacitance meter the PDLTS system has an entirely parasitic operation with regard to the existing detector systems present at a LINAC intense beam facility.

measured and taken as known parameter eqn (6). The next step would be to inspect if there were any transient P(t) at this temperature. The absense of a transient would be evidence that the defect in question was not vacancy related. This could be stated with more certainty if the defect concentration was obtained from the

conventional DLTS data, and known to be above the PAS sensitivity threshold. If, on the otherhand, a transient is found then it would possible to find some fitted values for products like $\kappa_n P_n$ and depending on other information available certain statements about the nature of the vacancy type defect could be made.

A schematic diagram showing a complete PDLTS setup is shown in **Fig 4**. The sample under investigation is mounted on a temperature controlled head with a thin film Shottky or $p^+$ implanted contact facing the beam and earthed. Positrons from the LINAC generated beam implant into the sample's depletion region through the thin contact. As with conventional DLTS a rear ohmic contact is provides the reverse biasing (emission) pulse and the forward biased (filling pulse). A conventional capacitance meter monitors the sample capacitance to ensure that the traps being investigated are indeed emitting electrons at a suitable and known rate. The two separate LT and DB sections of the apparatus are clearly seen and the signal from these digitized and recorded in the computer memory conventionally. The central difference though is that both the LT and the DB signals (or logic pulses deriving from them) are taken to respective MCS (Multi Channel Scaler) units. The reason for this is to provide a stop signal so that all LT or DB measurements are "tagged" with their corresponding "time into emission" (TIE) measurement. The resulting two-dimensional histogram plot, which has the conventional parameter (positron lifetime (LT), annihilation energy (DB)) and the TIE parameter as axes, allows the user to "rebin" the data along the TIE axis into a smaller number of n channels . The resulting n DB (or LT) spectra are then analyzed for S-W (or $\tau_{av}$) parameters.

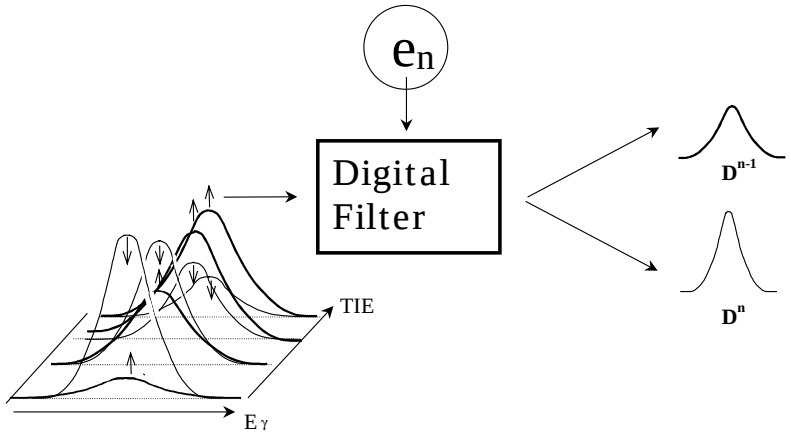


**Fig. 5.** The expected output data from a type I, PDLTS (DB) experiment. Gamma ray energies from the Ge detector are tagged with their TIE (Time Into Emission) signal and displayed on a two dimensional histogram. Data on the TIE axis can be re-binned to give typically 16 DB spectra that can then be subject to S-parameter analysis.

**Fig 5** shows a two-dimensional PDLTS relief plot taken in DB mode, in which the annihilation photon's energy $E_\gamma$ is along one axis with the TIE measurement along the other. Writing the DB spectrum of the defect with n electrons in vector notation $\underline{\mathbf{D_n}}$ and that of the defect with n-1 electrons as $\underline{\mathbf{D_{n-1}}}$ the relief profile shown in Fig 5 can be written as:

$$\mathbf{D}(t) = \frac{1}{\lambda_B + \kappa_{n-1} + (\kappa_n - \kappa_{n-1})e^{-e_n t}} \left[\lambda_B \mathbf{D_B} + \kappa_n e^{-e_n t}.\mathbf{D_n} + \kappa_{n-1}\left(1 - e^{-e_n t}\right)\mathbf{D_{n-1}}.\right] \qquad (9)$$

where g is the positron trapping fraction into the defect state| n> when t = 0. A situation like this could occur during the (O $\rightarrow$ +) transition, in which case $\underline{\mathbf{D_n}}$ and $\underline{\mathbf{D_{n-1}}}$ would be the DB spectra of the neutral defect and the bulk delocalized positron states respectively. In a discrete time sequence such as (7) , and knowing the emission rate constant $e_n$ (again obtained from the capacitance transient), it is possible to employ digital filter techniques to separate the components of each defect charge state [29]. A slightly more complex time variation occurs when the transient is from two positron trapping states (i.e - $\rightarrow$ 0), but the problem can still be formulated to allow separation of components as shown in Fig. 5. Although these techniques still require pioneering, the large benefits from being able to see the momentum distributions from different defects in different charge states can be considered to warrant such an expenditure of effort.

In addition to data processing, successful implementation of PDLTS, has a number of experimental challenges to overcome. The first is that a beam of small diameter and high stability is required. In conventional DLTS spectroscopists normally deal with very small area Schottky diodes made on their material under investigation. Typical the diameter of the diodes is 0.5-1.0mm. This is necessary to prevent leakage currents and problems caused by grain boundary irregularities. If PDLTS is to become acceptable to semiconductor spectroscopists then it can be argued that PDLTS samples should also be of small area. This would mean using beam diameters of 1mm and less. A beam spot size of 0.3 or 0.5 mm would seem advisable to ensure that no positrons are lost from the active depletion region. A secondary advantage of a small area is that it would facilitate on-line capacitance measurement, which as has been pointed out above makes PDLTS signal extraction more reliable. It is not only the beam diameter that has to be considered, but also the long term stability of the spot position. The beam would have to be impacting the Schottky diode area for the whole duration of the experiment which may take as much as 6 hours. Furthermore some method has to tell when the beam spot is actually on the Schottky diode. Perhaps doing an S-parameter rastering of the area around the diode would be the best way of achieving this.

Another important consideration is of what might be called „positron sweep-out". The electric fields present in the active depletion region can be strong enough to drift of positrons out of the "active region". This is, of course, undesirable as such positrons would be unavailable for defect trapping. The situation is better with a p-type sample as in this case the electric field is such as to drift positrons into the active region more effectively. n –type samples, however, are a cause for concern. The critical density of shallow donors $N_D$ above which „sweep-out" becomes appreciable can be easily estimated. The mean electric field over the depletion region is given by $eN_Dd/2\varepsilon$ where $d$ is the depth of the depletion region. Approximating the positron implantion as a square function that is only positive over the depletion region one obtains the rate of positron loss from the depletion region as $\mu_+eN_D/2\varepsilon$ where $\mu_+$ is the positron mobility. By equating this with the bulk annihilation rate one obtains for the critical value of $N_D$

$$N_{D,crit} = \frac{2\varepsilon}{\mu_+ e\tau} \tag{10}$$

Taking a typical semiconductor with a dielectric constant of 12 , a positron mobility of 50 $cm^2V^{-1}s^{-1}$ and a positron lifetime of 200ps, one obtains a value of $N_{D,crit}$ ~$10^{15}cm^{-3}$. This is the present positron sensitivity to defects. Since $N_D$ must be greater than the defect density $N_T$ in order for the carrier to fill up the traps there is a potential problem. The result will be not just an attenuation of the PDLTS signal, but the non-exponential nature of P(t) may increase. The PDLTS signal should , however, still be useable if one operates with a $N_D$ not in excess of $10^{16}cm^{-3}$. The mean positron implantation position, will be important in maximizing the PDTLS signal – since if positron are implanted slightly deeper they will tend to drift into the depletion region. This is why the positron implantatio profile peak in Fig. 1 has been drawn deeper than the middle of the „active region." Another solution to the „seep-out" problem is not to rely on doping and electrical pulsing to fill up the traps so that $N_D<N_T$ . This could be done by optical excitation from the valence band, although some of the defects present in conventional DLTS may be absent due to hole recombination. The prefered solution to getting a clear PDLTS transient is to aim at getting positron sensitivity into the $10^{13}cm^{-3}$ to $10^{14}cm^{-3}$ range – which is where overlap with conventional DLTS is greatest anyway. This can only be done with spectra having many orders of magnitude more events.

Type-II PDLTS

Type II PDLTS does not work through positron trapping signal as in type I. In contrast it utilizes the fact that when defects are emmitting electrons a space charge transient is formed and this causes an electric field transient, which in turn, through the positron's mobility produces a positron velocity transient [17]. The positron velocity transient can then be detected using the DS-PAS mode. It could be considered that type II PDLTS is not such a useful technique as type I, since it conveys no more information than conventional DLTS. [Indeed the electric field as sensed by DS scales in direct proportion to the junction capacitance [17]]. Type II's only claim to usefulness is that it can work on materials where the trap concentration exceeds the donor concentration, a situation existing in semi-insulators. The other reason that may be forwarded for establishing a Type II PDLTS system, would be the fact that with only very small alterations – mainly in the type of pulse used – the system could be configured for measuring positron mobilities.

**Fig 6** shows the essential apparatus which is envisaged as being entirely separate from the apparatus required for Type-I PDLTS. Unlike type I PDLTS the Ge detector has to be along the beam axis, since the

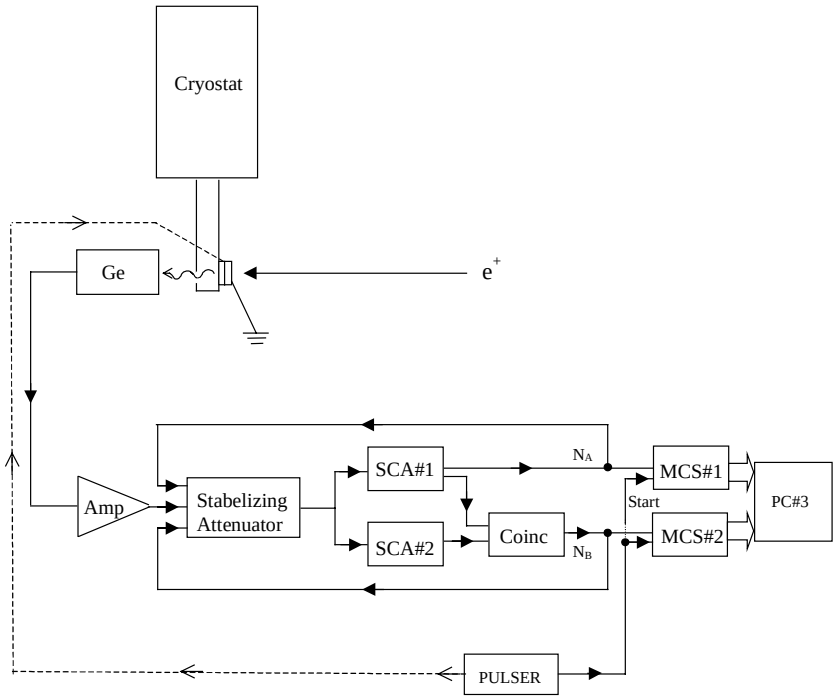


**Fig. 6.** A schematic diagram of a type II –PDLTS system. Positrons implant into the ionizing depletion region where the positron experienes the space charge transient. The Doppler shifted annihilation photons are detected with a Ge detector. The amplified signal is then bisected using to SCAs (Single Channel Analysers). $N_A$ and $N_B$ are the count rates into the lower half and upper half of the peak respectively. These count rates negatively feedback into a stabelizer unit so as to keep the annihilation line accurately bisected over long times ~ 100s. Fast space charge transients, however, cause fast transients in $N_A$ and $N_B$ that are recorded in the PC.

normal to the sample and hence electric field is along the beam axis. The signal from the detector is amplified conventionally, but then the 511keV line is bisected by two SCAs. The two outputs then feed into two MCS units and the data logged into the computer. The two outputs are also fed back into the stabelizer unit, that adjusts the signal attenuation so as to keep the two count rates $N_A$ and $N_B$ equal over a time constant of ~100s thus preventing any long term departure from perfect bisection. Fast transients due to trap emission occur on the millisecond – second time scale for which the stabilizer is essentially of fixed attenuation. The positron velocity is then obtained using:

$$v_+(t) = \alpha \frac{N_B(t) - N_A(t)}{N} \qquad (11)$$

where $\alpha$ is a calibration factor and N is the total count rate into the annihilation line (i.e. $N_A(t) + N_B(t)$).

**Fig 7** has been constructed to show the regions in which various techniques operate as function of both the dopant density and the trap density. The main regions to consider are those of conventional DLTS, PDLTS – type I, and PDLTS – type II. It is seen that there is only a small triangular region, where at present conventional DLTS overlaps with PDLTS – type I. This is unfortunate, but, as mentioned above, it is hoped that in future this region may be significantly widened. It is not essential to operate PDLTS-typeI with conventional DLTS, but it certainly has the big advantage of knowing the emission rate of the trap, and as we have seen this gives much greater confidence and reliability in deciphering the PDLTS signal. Our present efforts to conduct a successful PDLTS-type I measurement are on n-type Si with a $N_D$ of $10^{16}$cm$^{-3}$ (~0.1Ωcm). It is planned to make a thin $p^+$ contact with a 6mm diameter. Si vacancy defects to the level of $5x10^{15}$cm$^{-3}$ will then be introduced using high energy electron bombardment.

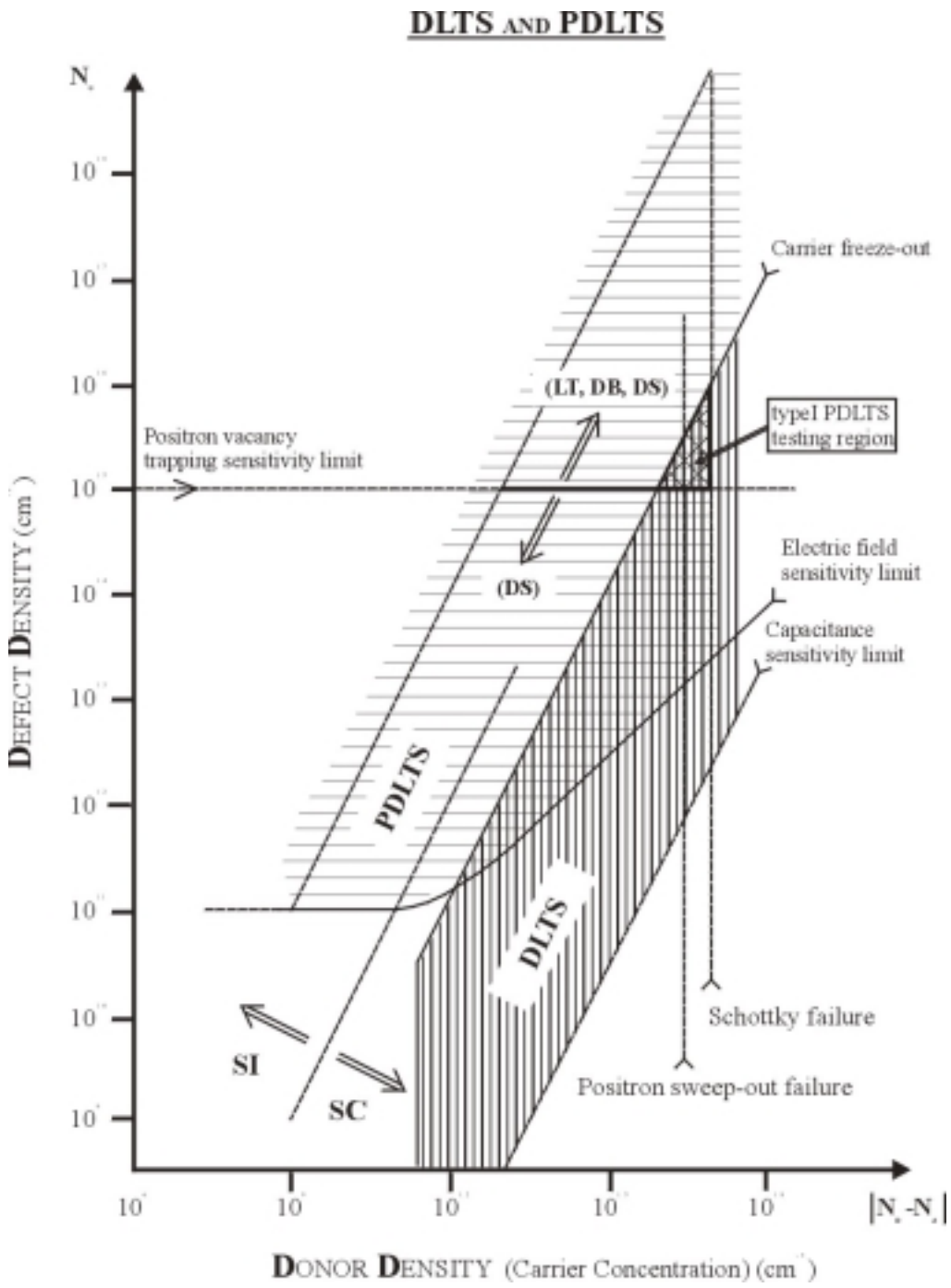


**Fig. 7.** Diagram showing the different regions of operation for DLTS, PDLTS-type I and PDLTS- typeII.

**5. Advantages of PDLTS**

As has been described the main advantage of PDLTS over other spectroscopies is its capability of giving structural information on the defect responsible for a specific deep level. It is true, of course, that there are other techniques such as EPR (Electron Paramagnetic Resonance) that can give structural information, but EPR is often not possible in III-V or II-IV compound semiconductors. EPR is also not particularly energy selective. The conclusion is that the combination of the structure determining PAS and the energy selective DLTS in PDLTS could give the technique that many people have been seeking in illucidating the origins of various mid-gap energy levels.

There other advantages, though, which are worth mentioning. One is that the positron is a much faster sensor than a capacitance meter. Capacitance meters normal operate by applying a low voltage AC signal of megahertz frequency to the sample as a test signal. The requirement of balancing a capacitance bridge limits a capacitance meter to bandwidths of ~1kHz. Trap emissions faster than 1ms cannot normally be studied. On the

other hand the positrons annihilation rate is typically ~0.2ns in most materials. The transient is sampled extremely quickly in PDLTS. The benefit is that one can observe traps much closer to the conduction band. In some cases it may even be possible to "see" the emission from the shallow (or not so shallow) donors that give rise to the materials conductivity. This is an exciting prospect.

Another advantage of PDLTS that may be valuable under some circumstances, is the techniques ability to look at material that is not doped, and that may even be semi-insulating. True in this case, when the material has a trap concentration below $10^{15}cm^{-3}$ it cannot detect vacancy defects, but through the build up of space charge in the semiconductor it can detect the presence of deep levels as per example the data in Fig. 7

Conventional DLTS is not usually able to say whether a trap is a single donor or a double donor. PDLTS may be able to give additional information to solve some of these puzzles of deep level spectroscopy. In PDLTS strong positron trapping occurs when the trap is negative, and moderate trapping with a neutral trap. There is no trapping from a positively charged trap. During the PDLTS cycle traps either go negative to neutral, neutral to positive. The presence or absence of positron trapping and the rate of positron trapping could help elucidate many charge assignment questions.

## 6. The need for an intense beam

In developing PDLTS into a realistic spectroscopy, it is necessary to consider the time taken to build up a spectrum containing sufficient information. As mentioned above the PDLTS technique when used with PL can take months to finish. A PDLTS experiment planned with a positron beam of intensity $10^4 e^+ s^{-1}$ operating in DB mode can take as much as two weeks to produce data of necessary information content. The reason for these long times is two fold. (i) the positron experiments collect data slowly, and (ii) in a PDLTS experiment there has to be a third parameter – the TAF (Time after filling) parameter. Instead of the standard 1D experiments of conventional PAS (PL) and PAS (DB) we are now dealing with a 2D measurement – each positron measurement having to have its associated TAF measurement simultaneously recorded.

We note, however, that the above data which employed PAS (PL) using a conventional $^{22}Na$ source took some 4 months to take and is not a particularly cost effective form of P-DLTS.

Perhaps the only way at this time to envisage putting DLTS on the market for semiconductor spectroscopists is to speed up the rate of acquiring positron data. Here a high intensity beam would be indispensable. With an intense beam Ge detectors could be operated at their maximum information rate $10^5$ pulses/sec, and the PAS-LT mode can be operated even faster [ limited only by the digitization time of ADCs – perhaps $10^7$ TAC events per second]. These improved information rates would cut down to hours what presently takes days and weeks in a PDLTS measurement.

## References


1. B. J. Baliga and E. Sun, *IEEE Trans. On Electr. Dev*. **ED-24**, (1977) 685
2. A. L. Lin and R. H. Bube, *J. Appl. Phys.*, **47** (1976) 1859
3. L. Forbes, *Solid-State Elect.*, **18,** (1975) 635
4. A. A. Bergh and P. J. Dean, *Proc. IEEE*, **60** (1972) 156
5. C. T. Sah and J. W. Walker, *Appl. Phys. Lett*., **22** (1973) 384
6. C. T. Sah, W. W. Chan, H. S. Fu and J. W. Walker, *Appl. Phys. Lett*, **20** (1972) 193
7. W. G. Oldham and S. S. Naik, *Solid-State. Elect*, **15** (1972) 1085
8. D. V. Lang, *J. Appl. Phys*., **45** (1974) 3023
9. Reference to the BioRad system
10. R. Krause-Rehberg and H. S. Leipner, *Positron Annihilation in Semiconductors*, Springer Series in Solid-State Sciences **127** (1999)
11. G. Dlubek and R. Krause. *Phys. Stat. Sol* (a) **107** (1987) 443
12. P. Hautojärvi, J. Mäkinen, S. Palko, K. Saarinen, C. Corbel, L. Liszkay , *Mat. Sci. Eng*. B **22** (1993) 16
13. K. Saarinen, T. Laine, S. Kuisma, J. Nissilä, P. Hautojärvi, L. Dobrzynski, J. M. Baranowski, K. Pakula, R. Stepniewski, M. Wojdak, A. Wysmolek, T. Suski, M. Leszczynski, I. Grzegory, S. Porowski, *Phys. Rev. Lett* **79** (1997) 3030
14. R. Krause. K. Saarinen, P. Hautojärvi, A. Polity, G. Gärtner and C. Corbel, *Phys. Rev. Lett* **65** (1990) 3329
15. C. Corbel, M. Stucky, P. Hautojärvi, K. Saarinen, P. Moser, *Phys. Rev*. B **38** (1988) 8192
16. C. V. Reddy, S. Fung and C. D. Beling, *Phys. Rev. B* **54**, (1996) 11290
17. C. D. Beling, S. Fung, H. L. Au, C. C. Ling, C. V. Reddy, A. H. Deng and B. K. Panda, *Appl. Surf. Sci.* **116** (1997) 121
18. B. Barbiellini, M. J. Puska, T. Korhonen, A. Harju, R. M. Nieminen, *Phys. Rev* B **51** 4176

19. L. Liskay, C. Corbel, L. Baroux, P. Hautojärvi, M. Bayhan, A. W. Brinkman and S. Tararenko, *Appl. Phys. Lett* **64** (1994) 380
20. R. Ambigapathy, A. A. Manuel, P. Hautojärvi, K. Saarinen and C. Corbel, *Phys. Rev* B **50** (1994) 2188
21. W. LiMing, S. Fung, C. D. Beling, M. Fuchs and A. P. Seitsonen, *J. Phys.: Condens. Matter* **10** (1998) 9263
22. M. Hakala, M. J. Puska, R.M. Nieminen, *Phys. Rev*.. B **57** (1998) 7621
23. R. Krause-Rehberg, H.S. Leipner: *Appl. Phys.* A **64**, (1997) 457
24. To be published.
25. H. L. Au, C. C. Ling, B. K. Panda, T. C. Lee, C. D. Beling and S. Fung, *Phys. Rev. Lett* **73** (1994) 2732
26. S. Valkealahti, R. M. Nieminen, *Appl. Phys.* A **35** (1984) 51
27. P. Hautojärvi and C. Corbel, International School of Physics, Course CXXV (1995) 528
28. O. Breitenstein, Private Communication
29. L. B. Jackson, *Digital Filters and Signal Processing, 3rd addition*, Kluwer (1996)

## 5.1.2. Age-Momentum Correlation (AMOC)

H. Stoll (Stuttgart)

### Introduction

The two quantities which can be observed by annihilation of an individual positron in condensed matter are the *positron age* $\tau$ which is the time interval between implantation and annihilation of the positron, and the *momentum* $\boldsymbol{p}$ of the annihilating positron-electron pair. Correlated measurements of these quantities (Age-Momentum Correlation, AMOC *) are an extremely powerful tool for the study of reactions involving positrons. It not only provides the information obtainable from the two constituent measurements but allows us to follow directly, in the time domain, changes in the positron-electron momentum distribution of a positron state (e.g., thermalization, cf. Sect. 3.4) or transitions between different positron states (e.g., trapping of positrons, cf. Sect. 3.2, chemical reactions of positrons and positronium, cf. Sec. 3.1, or self-localization of positronium from a metastable positronium state in liquid rare gases, cf. Sect. 3.3). So far AMOC measurements have only been performed at MeV positron beams [1,2]. It is highly recommended that the advantage of the beam-based AMOC technique should be applied to keV positron beams, too.

### **1** AMOC Relief, Lineshape Function, and "Tsukuba Plot"

Since both 511 keV photons resulting from a 2-gamma-annihilation event transmit equivalent information, one photon may be used to determine the age of the annihilation positron and the other one to deduce information on the momentum of the annihilating positon-electron pair by measurement of the Doppler shift of the photon energy. As an example, Fig. 1 shows the so-called AMOC relief of fused quartz. The number of triple-coincidence counts is plotted on a logarithmic scale versus the positron age and the energy of one of the annihilation quanta. Sections of constant positron age represent energy spectra at different positron ages. The well-known positron lifetime spectrum or the Doppler broadening spectrum may be obtained by summation over all channels with constant energy or constant positron age, respectively. For visualization of the AMOC data a time dependent S-parameter, the so-called lineshape function $S^t(t)$ (Fig. 2a) has been found to be particularly useful especially to demonstrate changes in the population of different positron states as a function of positron age (cf. Sect. 3). Plots of the mean positron lifetime $\bar{\tau}$ as a function of the photon energy (Fig. 2b) are another simple visualization possibility ("Tsukuba Plot") [3].

---

* The name "Age-Momentum Correlation" appears to have been invented by MacKenzie and Mc Kee [4]. The synonym AMOC was introduced by Stoll, , Wesolowski, Koch, Maier, Major, and Seeger [5] at the suggestion of P. Wesolowski.

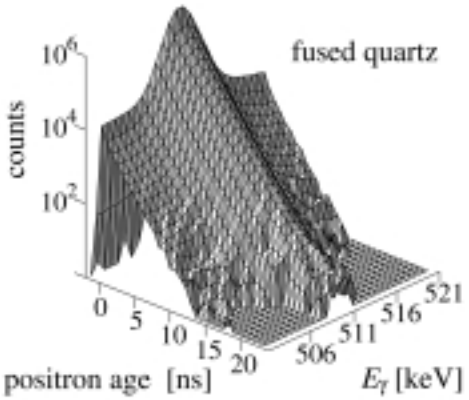


Figure 1: AMOC relief of fused quartz at room temperature

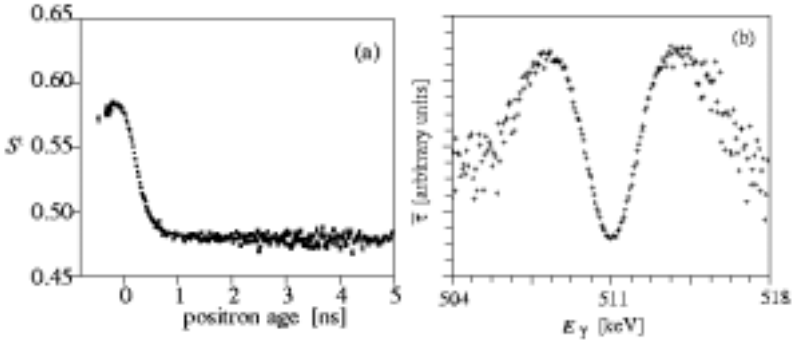


Figure 2: (a) Lineshape function $S^t(t)$ and (b) mean lifetime $\bar{\tau}$ vs. $E_\gamma$ ("Tsukuba Plot") of fused quartz derived from the AMOC relief shown in Figure 1 (for details see text).

## **2** Two-Dimensional Data Analysis

Full use of the two-dimensional AMOC data is made by fitting a two-dimensional model function to the AMOC relief directly. The fitting consists in developing models for the processes under investigation, solving the appropriate system of rate equations with suitable initial conditions, calculating the AMOC relief, and convoluting it with the time and energy resolution function of the set-up [6,7]. In this way fits to the measured AMOC reliefs can be made without prior data reduction. Parameters derivable from such two-dimensional data analysis are: (i) the annihilation rates and the Doppler broadening linewidths of all positron states involved, (ii) the transition rates between distinct positron states, and (iii) the fraction of positrons forming positronium.

## **3** Selected Experiments

### **3.1** Positronium Chemistry

In the field of positronium chemistry AMOC combines the ortho-positronium (o-Ps) sensitive lifetime measurement with the Doppler broadening measurement which is suitable for the observation of the para-positronium (p-Ps) state with its characteristic narrow momentum distribution ("intrinsic" annihilation of the positron of positronium with it "own" electron). In addition AMOC allows time-domain observations of the occupations and transitions of different positron states tagged by their characteristic Doppler broadening. Thus, in contrast to conventional positron lifetime and Doppler measurements AMOC allows us to observe the transitions more directly and to differentiate between distinct reactions. Chemical reactions of positronium "atoms" such as oxidation, complex formation as well as spin conversion and inhibition of positronium formation have been studied by beam-based AMOC [8,9]. E.g., spin conversion of o-Ps to p-Ps in the presence of the free radical HTMPO (4-hydroxy-2,2,6,6-tetramethylpiperidine-1-oxyl) causes an increase of $S^t(t)$ at long positron ages

(Fig. 3 right side) since long-lived o-Ps is converted to p-Ps showing its characteristic small Doppler broadening (corresponding to a large S-lineshape parameter) of the annihilation radiation. The lifetimes of bound states between positrons and halide ions could also be measured for the fist time by beam-based AMOC [9,10]).

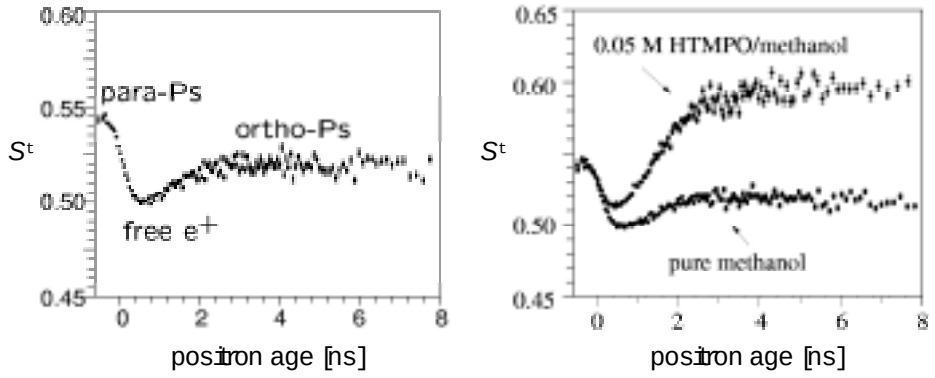


Figure 3: *Left side*: Lineshape function of methanol. The time-dependent S-parameter is determind by the narrow momentum distribution of short-lived para-positronium, the momenta of the electons annihilating with positrons not forming Ps (free $e^+$), and the "pick-off" annihilation of long-lived ortho-positronium (annihilation of the positron of o-Ps with a "foreign" electron).
*Right side*: The free radical HTMPO dissolved in methanol causes a significant increase of $S^t$ at old positron ages since long-lived o-Ps is converted to p-Ps showing its characteristic small Doppler broadening (corresponding to a high S-parameter) of the annihilation radiation.

## **3.2** Trapping of Positrons at Defects

As an example of AMOC investigations of positron trapping at defects Fig. 4 shows the room-temperature lifetime spectrum and lineshape funktion of a natural type IIa diamond [11]. Other diamond were investigated, too [11-13].

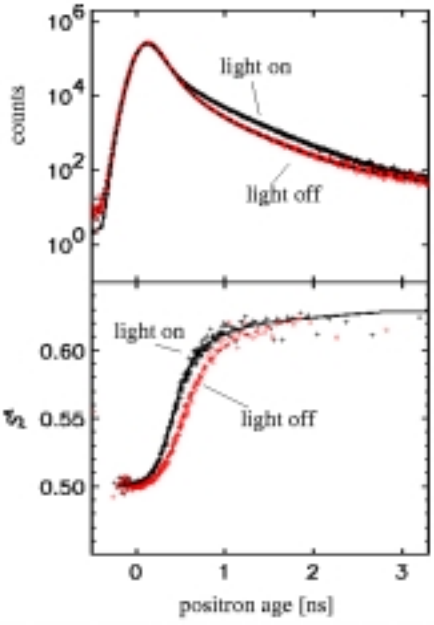


Figure 4: Positron-lifetime spectrum (upper diagram) and lineshape lunction $S^t$(t) (lower diagram) of a natural type IIa diamond. Influence of white light. The solid and dasched lines represent fits of a two state trapping model. Parameters are given in Table 1.

| | $K[10^9/s]$ | $\tau_f$ [ps] | $\tau_t$ [ps] |
|---|---|---|---|
| light on | 1.4 | 115 | 386 |
| light off | 0.7 | 115 | 358 |

Table 1: Parameters of a fit to the diamond AMOC data: Positron trapping rate *K*, lifetime of the free and trapped positrons, $\tau_f$ and $\tau_t$ .

Young positrons annihilate from a delocalized state showing a large Doppler broadening. A narrowing of the annihilation photon line is observed at higher positron ages caused by trapping of positrons at defects. Parameters obtained by fitting a simple two state trapping model to the AMOC data are shown in Table 1. The trapping rate is almost doubled when the diamond is illuminated by white light. This is explained by charging of the defects involved [11].

### **3.3** Positronium States in Condensed Rare Gases

Positron-lifetime and AMOC spectra were measured on Ne, Ar, and Kr in the liquid and in the solid states [7]. The measured o-Ps lifetimes of 2.4 ns in solid Ar at 16 K and of 2.1 ns in solid Kr at 50 K are accounted for pick-off annihilation of o-Ps. The much longer o-Ps lifetimes in the liquids (15.7 ns in Ne at 26 K, 7.0 ns in Ar at 87 K and 5.7 ns in Kr at 120 K) and are explained by o-Ps annihilation in long-lived self-localized states, the socalled “Positronium Bubbles” [14]. The fact that a long o-Ps lifetime component has been found in solid Ne (5.3 ns at 15 K) suggests strongly that here positronium bubbles are formed, too.

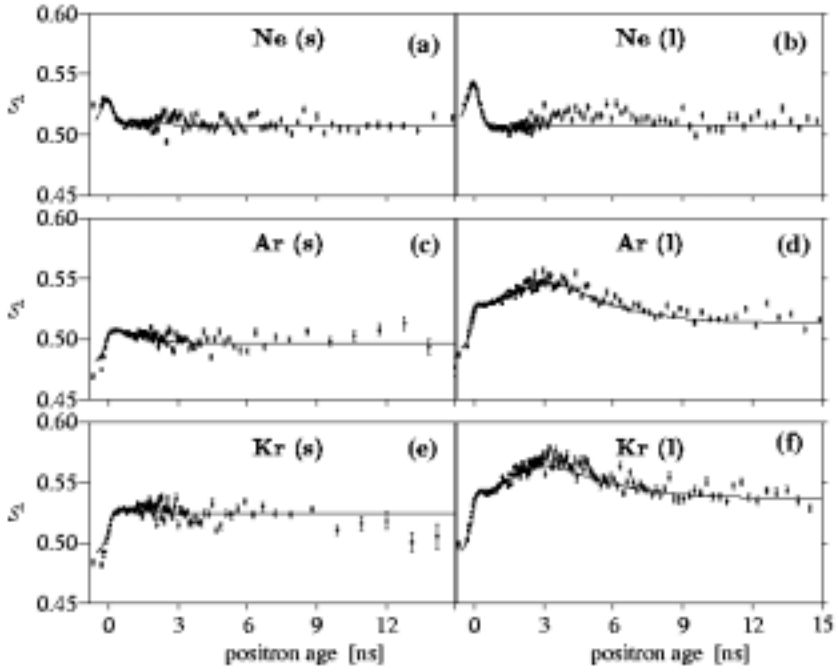


Figure 5: Lineshape functions $S^t(t)$ calculated from AMOC data and model functions (solid lines) for condensed rare gases: Solid Ne at 15.2 K (a), liquid Ne at 26.0 K (b), solid Ar at 83.3 K (c), liquid Ar at 86.3 K (d), solid Kr at 50.0 K (e), and liquid Kr at 120.0 K (f).

The lineshape functions of Ar and Kr in the liquid state showed a surprising maximum at positron ages of about 3 ns (Figs. 5d and 5f}. Analysis of the AMOC data obtained on liquid Ar and Kr revealed for the first time that the positronium bubbles are formed from an additional delocalized, metastable o-Ps state [7,15]. The lifetime of the metastable o-Ps states in the liquids were found to be about the same as the o-Ps lifetimes in the solids in the vicinity of the melting point. The transition rate to the longer-lived and apparently more stable o-Ps bubble states in liquid Ar and Kr is about $3 \cdot 10^8$ $s^{-1}$ [7]. A lower limit of the height of the energy barrier between the two different o-Ps states of about $10^{-1}$ eV is estimated by assuming that the barrier is overcome by overbarrier jumps with an attempt frequency of $10^{14}$ $s^{-1}$. A bump in the lineshape function of liquid Ne may also be possibly visible at positron ages of about 4 ns to 6 ns (Fig. 5b) indicating that a metastable Ps state may be formed in Ne, too.

### **3.4** Positronium Thermalization

Beam-based AMOC allowed us to investigate Ps thermalization in condensed matter for the first time. For all Ps-forming solids and liquids investigated so far [7,16,17] a decrease in the $S^t(t)$ values has been found at young positron ages as shown for TMS (tetramethylsilane) in Fig. 7. This juvenile broadening has never been

observed in materials for which there is no evidence for Ps formation (e.g., see Al results, Fig. 7). When positrons form Ps, the creation of electron-hole pairs as an effective mechanism of losing kinetic energy ceases to operate. In materials with optical phonon branches the dominate slowing-down process for Ps is thought to be the transfer of kinetic energy to the lattice via collision with optical phonons [18,19].

The AMOC data of the juvenile broadening have been analysed in terms of a two state model [7] which approximates the Ps energy loss via interaction with phonons by allowing for transitions between epi-thermal Ps and thermalized Ps. A better analysis of AMOC data on Ps thermalisation is suggested by Seeger [20]. Room temperature thermalization times $t_{th}$ between 10 ps and 40 ps and initial kinetic energies $E_o$ of Ps between 3 eV and 6 eV are obtained by this procedure for materials with optical phonon. The values obtained for $t_{th}$ have a higher reliability than those for $E_o$, which appear to be more model-dependent.

The hypothesis of Ps thermalization via optical phonons predicts that in positronium forming materials without optical phonons much longer Ps thermalization times should be found. This may be tested by AMOC measurements in solid rare gases, crystallizing in the face centred cubic (fcc) structure which, being a Bravais lattice, does not have optical phonon branches.

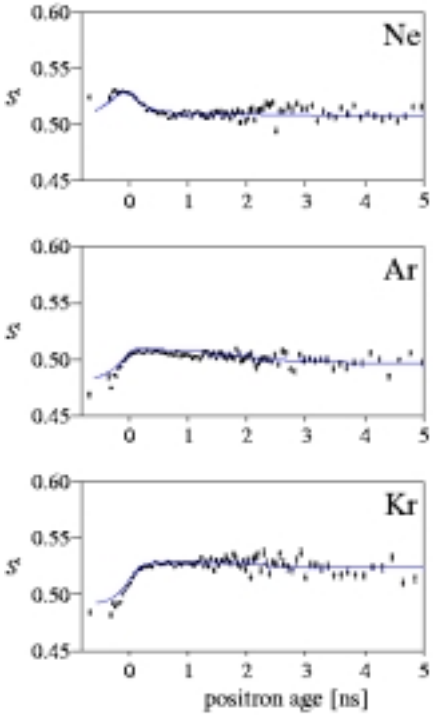


Figure 6: Lineshape functions $S^t(t)$ of solid rare gases (data points with error bars). The solid lines have been calculated from the two-dimensional AMOC data and are not fits to the data points.

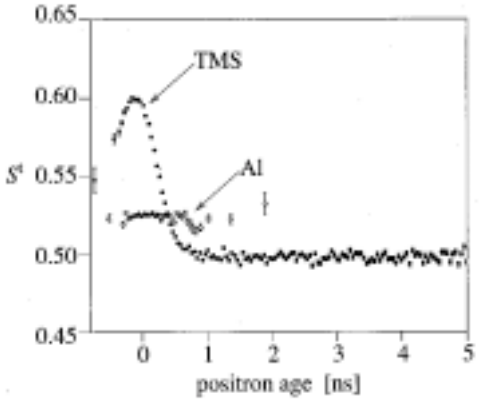


Figure 7: Lineshape function of TMS (tetamethylsilane) and Al at room temperature

In Ar and even more pronounced, in Kr, the lineshape functions $S^t(t)$ show indeed a clear shift of the juvenile Doppler broadening to higher positron ages (Fig. 6). The narrowing annihilation of thermalized p-Ps giving a high S-parameter value has vanished completely showing that most of the p-Ps annihilates from an epi-thermal state. This indicates Ps thermalization times $t_{th}$ in the order of the p-Ps lifetime. The analysis based on the two-state model mentioned above (solid lines in Fig. 6) yields thermalization times $t_{th}$ of 125 ps to 250 ps for solid Ar, and of 400 ps to 600 ps for solid Kr [7,17]. They do not differ very much from those for the liquid states.

The lineshape function $S^t(t)$ of solid Neon (also presented in Fig. 6) shows a maximum similar to TMS (Fig. 7). The thermalization times $t_{th}$ according to the two state model analysis are in the range of 20 ps to 40 ps [7] and thus are similar to $t_{th}$ in materials with optical phonons.

The rather long Ps thermalization times $t_{th}$ observed in Ar and Kr are in agreement with the idea that Ps cannot lose energy by generating electron-hole pairs and, since in the rare gases studied there are no optical phonon branches, the Ps energy can only be transferred to acoustic phonons which is significantly less effective than the transfer to optical phonons. The process responsible for the shorter thermalization times in Ne is not yet fully understood and requires further study.

## References


1. H. Stoll, M. Koch, K. Maier, and J. Major, *Nucl. Instr. and Meth*. B **56-57**, 582 (1991).
2. H. Stoll, *MeV Positron Beams*, in: *Positron Beams and Their Applications*, ed. P. G. Coleman, (World Scientific, Singapore, 2000) p. 237.
3. Y. Kishimote and S. Tanigawa, in: *Positron Annihilation*, eds. P. G. Coleman, S. C. Sharma, and L. M. Diana, (North-Holland, Amsterdam, 1982) p. 168, p. 404, p. 790, p. 815.
4. I. K. MacKenzie and B. T. A. McKee, *Appl. Phys.* **10**, 245 (1976).
5. H. Stoll, P. Wesolowski, M. Koch, K. Maier, J. Major, and A. Seeger, *Materials Science Forum* **105-110**, 1989 (1992).
6. H. Schneider, A. Seeger, A. Siegle, H. Stoll, P. Castellaz, and J. Major, *Appl. Surf. Sci.* **116**, 146 (1997).
7. A. Siegle: Positronenzerstrahlung in kondensierter Materie - eine Untersuchung mit der Methode der Lebensalter-Impuls-Korrelation, Dr. rer. nat. Thesis, Universität Stuttgart, (Cuvillier, Göttingen, ISBN 3-89712-129-8, 1998).
8. H. Schneider, A. Seeger, A. Siegle, H. Stoll, I. Billard, M. Koch, U. Lauff, and J. Major, *J. Physique IV* **3**, C4 69 (1993).
9. P. Castellaz: Untersuchung von chemischen Reaktionen des Positrons und des Positroniums in Flüssigkeiten mit Hilfe der Lebensalter--Impuls--Korrelation (AMOC), Dr. rer. nat. Thesis, Universität Stuttgart, (Cuvillier, Göttingen, ISBN 3-8958-934-2, 1997).
10. P. Castellaz, J. Major, C. Mujica, H. Schneider, A. Seeger, A. Siegle, H. Stoll, and I. Billard, *J. Radioanal. Nucl. Chem.* **210**, 457 (1996).
11. U. Lauff, R. W. N. Nilen, S. H. Connell, H. Stoll, K. Bharuth-Ram, A. Siegle, H. Schneider, P. Harmat, P. Wesolowski, J. P. F. Sellschop, and A. Seeger, *Appl. Surf. Sci.* **116**, 268 (1997).
12. H. Stoll, M. Koch, U. Lauff, K. Maier, J. Major, A. Seeger, P. Wesolowski, I. Billard, J. Ch. Abbe, G. Duplatre, S. H. Connell, J. P. F. Sellschop, E. Sideras-Haddad, K. Bharuth-Ram, and H. Haricharun, *Beam--Based Age--Momentum Correlation Studies of Positronium Spin-Conversion in Paramagnetic Solutions and of Positron Trapping at Defects in Diamonds*, in: Proceedings of the Fifth International Workshop on Slow-Positron Beam Techniques for Solids and Surfaces, eds. E. H. Ottewitte and A. Weiss (American Institute of Physics Conference Proceedings 303, New York, 1994) p. 179.
13. R. W. N. Nilen, U. Lauff, S. H. Connell, H. Stoll, A. Siegle, H. Schneider, P. Castellaz, J. Kraft, K. Bharuth-Ram, J. P. F. Sellschop, and A. Seeger, *Appl. Surf. Sci.* **116**, 198 (1997).
14. R. A. Ferrell, *Phys. Rev.* **108**, 167 (1957).
15. A. Seeger: *Evidence for the Existence of Two Kinds of Orthopositronium in Condensed Rare Gases and for Irreversible Transitions between them*, in: *Radiation Physics and Chemistry* (Proc. of the 6th Int. Workshop on Positron and Positronium Chemistry, Tsukuba, Japan, 1999) in press.
16. H. Stoll, M. Koch, U. Lauff, K. Maier, J. Major, H. Schneider, A. Seeger, and A. Siegle, *Appl. Surf. Sci.* **85**, 17 (1995).
17. A. Seeger, *Materials Science Forum* **255-257**, 1 (1997).
18. A. Seeger, *Appl. Surf. Sci.* **85**, 8 (1995).
19. A. Seeger, *J. Phys.: Condens. Matter* **10**, 10461 (1998).
20. A. Seeger*: Slowing-Down of Positronium: Analysis of the Age-Momentum Correlation*, in: *Radiation Physics and Chemistry* (Proc. of the 6th Int. Workshop on Positron and Positronium Chemistry, Tsukuba, Japan, 1999) in press.

## 5.1.3. DETECTOR SYSTEMS

R.Krause-Rehberg (Halle/Saale)

## 5.1.3.1. ADVANCED POSITRON LIFETIME SPECTROSCOPY

### 1. Introduction

The positron lifetime spectroscopy is the most powerful positron technique with respect to defect investigation [1-3]. It will be the most important technique of the planned EPF system.

### 2. Setup of a positron lifetime spectrometer at a LINAC-based positron source

Without a LINAC, the experiment is usually performed using $^{22}Na$ $\beta^+$ sources. This setup has the advantage that the $\beta$ decay supplies a 1.27 MeV gamma quantum which indicates the "birth" of a positron. The lifetime of an individual positron can thus be measured as the time difference between the appearance of this 1.27 MeV quantum and the 0.511 MeV annihilation quanta. This allows a relatively simple time spectrometer setup (for more details see [2]). Because of the uncorrelated appearance of the positrons in the sample due to the radioactive decay, only weak sources can be used. This is due to the demand that the time between the generation of two positrons must be distinctly larger (a factor of $10^3$ to $10^4$) than the individual lifetime. Only this ensures that the unwanted background in the lifetime spectra is not too high.

This disadvantage can be overcome by using a discontinuous positron beam where the positrons reach the samples as bunches to well defined times. Thus, the time-zero signal for the lifetime measurement will be generated by the bunching system as a sharp electronic signal. The positron source (radioactive isotope or pair production site) is well separated from the sample chamber, and thus only annihilation events from the sample material will be observed. This is a further advantage over the "sandwich technique" where the isotope source is placed between two identical samples, so that the annihilation events in the source itself must be subtracted. Additionally, a positron beam allows the moderation of positrons, i.e. the formation of a monoenergetic beam. Thus, by changing the beam energy, defect depth profiling can be done.

The simple lifetime setup at a positron beam uses a time-to-amplitude converter (TAC) which is started by a signal generated in the bunching electronics, and which is stopped by one of the two annihilation $\gamma$ quanta. This quantum is detected by a fast scintillator / photo multiplier (PM) setup. The amplitude of the output pulse of the TAC is then proportional to the time difference between start and annihilation pulse, i.e. the positron lifetime. The positron lifetime in solids is in the order of 0.1 to 1 ns, so that a repetition rate of the bunched positron pulses of 100 ns is ideal for fast data collection. This can hardly be achieved in a normal electron LINAC where repetition rates of about $10^3$ $s^{-1}$ are available. However, the FEL-LINAC's planned at DESY or at Rossendorf will have repetition times of about 100 ns, which suits very well to the requirements of the positron lifetime spectroscopy. Although a theoretical data collection rate of $10^7$ $s^{-1}$ seems thus to be possible, the realistic rate to be obtained by a single PM detector is much smaller. There are two reasons for this. The first is obvious: the photomultiplier tube has a maximum average current (for the XP 2020: 200 $\mu$A; for good stability only 10 $\mu$A). This limits the maximum number of detected $\gamma$ quanta to about $5\times10^4$ $s^{-1}$.

A possible way to increase the count rate is to disconnect the last dynodes of the PM and to use a fast preamplifier instead. This reduces the problems with power dissipation in the PM distinctly. However, there is another physical limit for the count rate at a single detector: In the case that in every positron bunch several annihilation events are detected, the positron lifetime spectrum will be strongly distorted, since the long lifetimes will be suppressed. This is due to the dead time of the PM detector, i.e. the first incoming annihilation $\gamma$ quantum will stop the individual lifetime measurement. Longer lifetimes will hardly be detected when the product of N (number of positrons per bunch) and $\alpha$ (the detection efficiency of the PM) $N\alpha > 1$. Therefore, $N\alpha$ should be about $10^{-2}$ to $10^{-3}$ $s^{-1}$ in order to avoid this problem, i.e. only every $10^2$ to $10^3$ bunch will supply an registered event. Thus, the count rate of the lifetime measurement is limited to about $10^4$ to $10^5$ $s^{-1}$. This can only be overcome by using a multi-detector system where the stop event is detected by a larger number of PM detectors. But even in this case, a correction of the lifetime spectrum with respect to long lifetime components seems to be necessary.

### 2. Advanced positron lifetime spectroscopy

The conventional lifetime experiment uses only one of the two annihilation $\gamma$ quanta as the stop signal. The measurement suffers from a relatively bad time resolution and a poor peak to background ratio in a surrounding

with a relatively high radiation level like the experimental hall of a LINAC. Both disadvantages can be reduced by the use of the second annihilation γ quantum.

Since the second quantum appears exactly at the time as the first, the measurement of the lifetime can be improved by the simultaneous detection of both times and the subsequent calculation of the arithmetic average of the two values (Fig. 1). This can improve the time resolution of the system and may reduce the FWHM of the Gaussian resolution function by the factor of $1/\sqrt{2}$ (see discussion below). This was found by Monte-Carlo simulations and by an experimental test setup using a conventional $^{22}$Na source [4]. There is another advantage when detecting the second γ quantum: one can subtract both lifetimes from each other. This gives a delta function since the γ quanta appear exactly at the same time. Due to the limited time resolution, the two registered times will deviate, and the difference of many events will give a distribution around zero: the delta function is folded with the time resolution function, giving the time resolution function itself. However, a possible time spread due to the incoming positron beam cannot be detected this way. This is especially important when a conventional β source shall be used. In this case the start signal must be detected by another PM detector, and consequently only the fraction of the time resolution which originates from the stop detectors can be improved and monitored. Thus, the advanced lifetime technique is especially suitable for a LINAC-based system with a small time spread of the incoming slow positron beam. In this case, the difference spectrum can be used to monitor in a simple way already during the running measurement the stability of the time-zero channel of the spectrum and the time resolution of the system.

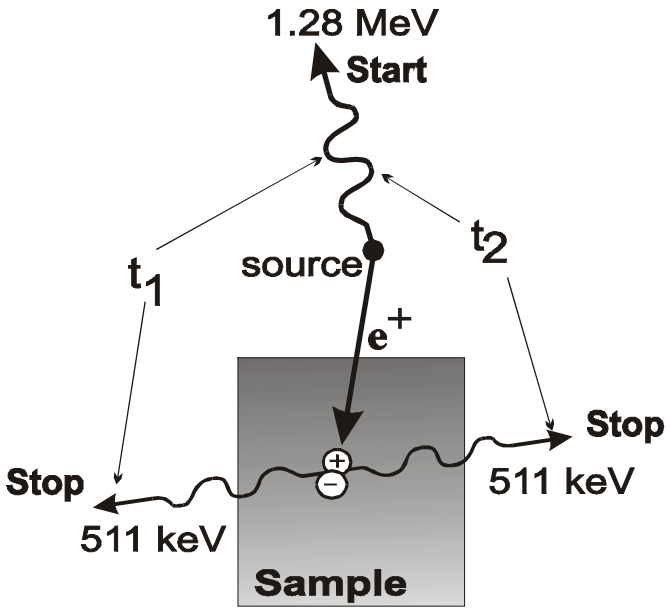


**Fig.1:** The conventional positron lifetime spectroscopy detects the time difference between the start pulse (either obtained from the 1.28 MeV γ quantum of the $\beta^+$ decay of a radioisotope or by the bunching system of a positron beam) and one of the two annihilation γ quanta. The advanced positron lifetime spectroscopy makes use of the second annihilation quantum in a coincidence measurement. The average of the two times ($t_1 + t_2 / 2$) improves the time resolution of the system and significantly reduces the background. The difference $t_1 - t_2$ gives directly the resolution function (more detailed description in the text).

### 3. A possible multi-detector setup of the advanced positron lifetime spectroscopy at an FEL-LINAC

Fig. 2 shows the scheme of a possible realization of the advanced positron lifetime setup. The start signal will be
taken from the last stages of the bunching system of the electron LINAC. In case a remoderation stage with an additional buncher will be realized for the positron beam, this signal will be generated there. All TAC's will be started by this pulse. The stop pulse is obtained from both annihilation  quanta by PM detectors with subsequent differential constant-fraction discriminators (CF). The energy window of the CF's can be set by remote control from the system PC by digital-analog converters (DAC). For this purpose, the pulse height spectrum of the PM output pulse can be measured by analog-digital converters (ADC) in coincidence or anti-coincidence with the energy window. This allows the automatic adjustment of the energy windows for the whole system, which seems to be important for a multi-detector setup and for the operation from a remote site via the internet.

The analog output pulse of the time-to-amplitude converter (TAC) is converted to a digital signal by very fast ADC units. Such integrated circuits with a resolution of 14 bit and a conversion rate of 100 Ms are available for a moderate price. The fast conversion is necessary since the next event can occur after 100 ns (although this must be a rare event, see the discussion above). The result of the conversion is temporarily stored in dual-port RAM's, which will be read out by the system controlling PC.

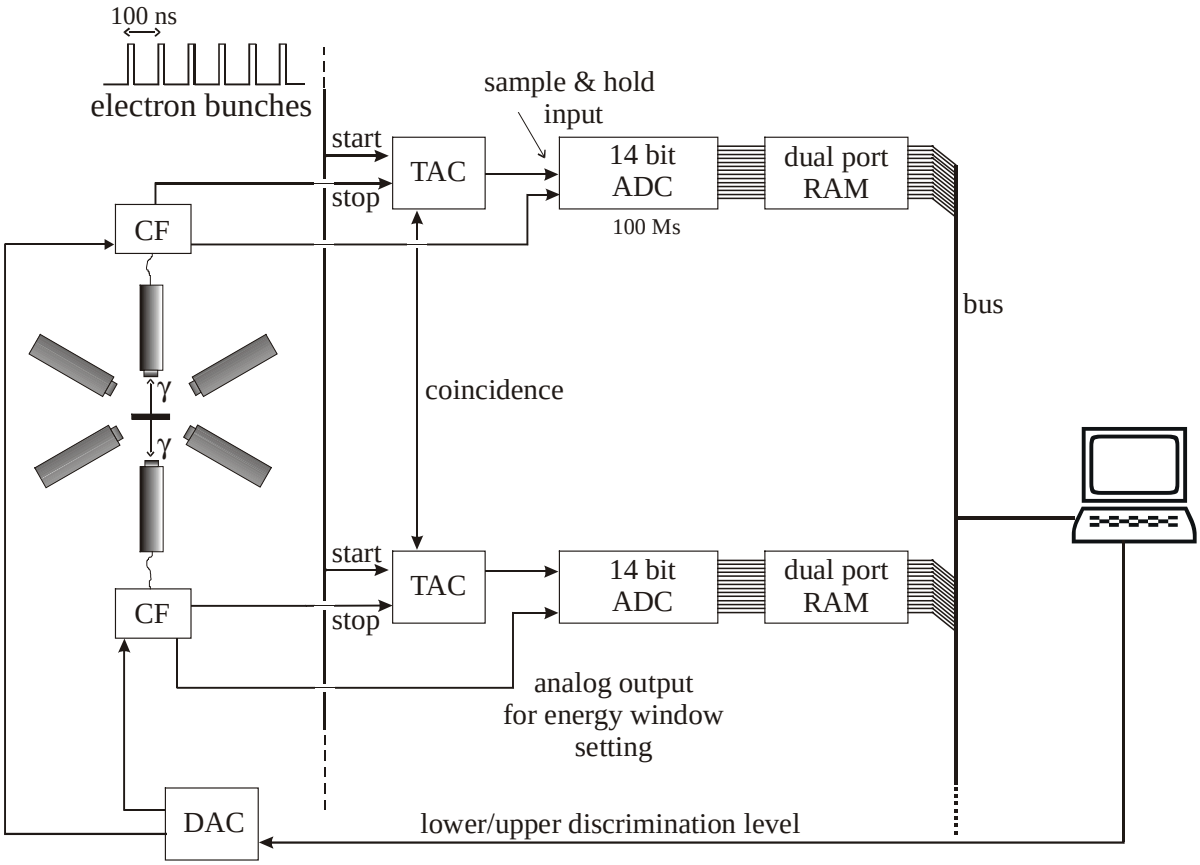


**Fig. 2:** Scheme of the advanced positron lifetime system for the application in a multi-detector setup at a FEL-LINAC-based positron beam. The start pulse for the lifetime measurement is obtained from the bunching electronics of the electrons. The two collinear annihilation γ rays are detected by two scintillator / photomultiplier detectors. The output pulses are maintained by constant-faction discriminators (CF) and stop the time measurements in the time-to-amplitude converters (TAC). Fast analog-digital converters deliver the time information to a dual-port RAM which acts as intermediate memory for the data transfer to a PC. The energy window of the CF is remote controlled by digital-analog converters.

The data registration must be organized in such a way that all events are stored in both channels, i.e. also the single channel events will be stored. The data analysis will then provide the two normal lifetime spectra and the coincidence spectrum (the single channel spectra have a much higher statistics, although the time resolution and the background will be worse). The coincidence must be realized by a coincidence unit that may be triggered from the two TAC outputs. For this purpose, the data collection must be done in the "list mode", i.e. the two lifetimes of a annihilation event must be stored together. This is also important for a later data re-analysis. Thus, pairs of two lifetimes are stored, where mostly a zero time is paired off with a certain lifetime value (single-channel events) and only about in 5 to 10% of the stored events both lifetime values are valid (the detector efficiency is about 5 and 10% depending on the scintillator size and material). Thus, a coincidence lifetime spectrum with about $10^7$ events will correspond to a list file size of about 500 Mb. It is collected in a single detector pair in about 2000 sec (see the discussion above about the count rate).

However, in a multi-detector setup using 20 pairs of detectors, the data collection time is reduced to about 100 sec. In case, only normal lifetime spectroscopy is required, the time of a single lifetime measurement is reduced to 10 sec, and when only the average lifetime shall be used (statistics of $10^6$ events), 1 sec measuring time is sufficient. However, the data analysis will become very time consuming, because in a multi-detector setup the individual lifetime spectra can only be summed up, when the time-zero channel was determined before. Nevertheless, the multi-detector setup is the only way to make use of the high number of positrons available at an FEL-LINAC.

The automation of the beam system must be done in such a way that all function (programming the measurement with corresponding modes, temperatures, times, etc.) can be set by the IC/PIP internet protocol. This enables users from a remote site to operate the positron beam system. A technician in the lab is only responsible for the mounting of the sample to the sample roundabout in the sample chamber and for the service of the equipment. So it will become possible that experienced users may do experiments without traveling to the lab (important for a European facility).

The main part of the data analysis (formation of the final lifetime spectra from the list files) must be done at the system PC or another PC directly in the lab (due to large size of the list file). The lifetime spectra, however, can easily be transported via the internet.

**4. Summary**

The positron lifetime spectroscopy is the main technique which will be applied for defect studies in solids. With a multi-detector setup the data collection time can be reduced to about 1 sec for normal lifetime spectra. The application of the new advanced positron lifetime spectroscopy will significantly improve the quality of the spectra. The background will be reduced distinctly (more than one order of magnitude) and the time resolution can be improved by a factor of $1/\sqrt{2}$ at the maximum. The difference spectra can be used for online monitoring of the system stability. An automation system will allow the remote control of the measurement via the internet.

## 5.1.3.2. TWO-DIMENSIONAL DOPPLER-BROADENING COINCIDENCE SYSTEM

**1. Introduction**

Recently, it has been shown that the high momentum part of the positron-electron annihilation momentum can be used to identify the chemical surrounding of the annihilation site [5-10]. This is based on the fact that tightly bound core electrons, owning high momenta, retain their element-specific properties even in a solid. In particular, the method can be used to identify the sublattice of a vacancy in a compound as well as vacancy-impurity complexes [5, 6]. The technique itself is based on the coincident detection of both 511-keV annihilation γ quanta from a single annihilation event. This allows the observation of the high-momentum annihilation distribution due to a strong reduction of the otherwise disturbing background.

Using a single high-purity Ge detector (HP-Ge) in coincidence with another γ-sensitive detector (such as a NaI scintillator) improves the peak to background ratio from about $10^2$ up to $10^4$ compared with a measurement using a single detector [5, 9]. However, a superior technical realization of a coincidence experiment is the use of two HP-Ge detectors (Fig. 3) registering the energy of both annihilation quanta [7]. This results in a peak-to-

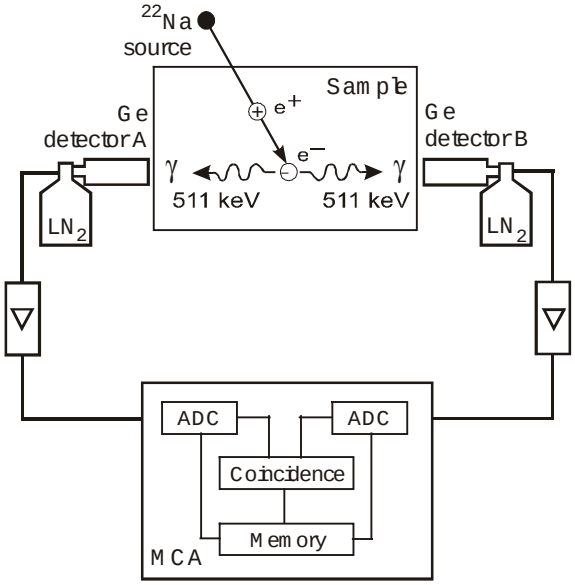


**Fig. 3:** Scheme of the Doppler-broadening coincidence spectroscopy. Both collinear γ quanta are detected by two energy dispersive systems (Ge detectors). A coincidence unit ensures that only those events are stored in the memory that are due to the same annihilation event.

background ratio of about $10^5$ and an improvement of the resolution function by a factor of $\sqrt{2}$ [11]. Nowadays, the setup of such a two-detector measurement is quite simple due to the availability of versatile computer-based multiparameter systems which can process the resulting two-dimensional data arrays and realize the time coincidence as well. In an earlier case study [12] the FAST-ComTec MPA-Win system was used which turned out to be in the moment a standard among the positron groups world-wide.

## 2. Experimental method

### 2.1 Setup

The experimental setup consists basically of two high-purity Ge detectors aligned in collinear geometry, corresponding amplifiers and analog-to-digital converters (ADC). The ADCs are connected to a busbox which contains the coincidence electronics. The busbox is fed to a PC running the multiparameter software which stores the event in a two-dimensional array. The energy resolution of these Ge detectors is about 1.2 to 1.5 keV (FWHM). Using conventional $\beta$ sources, the distance between the source and each of the detectors is about 30 cm. At a LINAC-based source with a higher positron intensity, the distance must be higher in order to reduce the total number of counts (see discussion below). In a test setup, a final count rate of 230 $s^{-1}$ was obtained in the 511-keV peak by using a 40 µCi $\beta^+$ source. In a typical measurement, about $1x10^7$ events should be collected in the 2-dimensional spectrum. However, in some cases statistics had to be increased to be about $4x10^7$ in order to reveal small differences.

### 2.2 Data treatment

Using two Ge detectors it is possible to detect simultaneously the energies $E_1$ and $E_2$ of both annihilation $\gamma$ quanta which originate from the same annihilation event. The sum energy $E_1+E_2$ then equals $2m_0c^2 - E_B$ with $m_0$ being the electron rest mass, $c$ the velocity of light, and $E_B$ the binding energy of the electron and positron in the solid. The difference energy $E_1 - E_B$ is equal to $p_Lc$ with $p_L$ being the momentum component of the annihilating pair in the direction of the detector 1. The energy of the detected $\gamma$ quanta is then up(down) Doppler-shifted by an amount of +(-) $p_Lc/2$ (see, e.g. Refs. [5, 7, 10, 11]).

The essence of the method lies in the possibility to take a diagonal cross-section of the two-dimensional spectrum considering only events which fulfill the condition $E_1+E_2=2m_0c^2$ (Fig. 4). The result is a practically background-free, symmetric spectrum. A peak to background ratio of $>10^5$ was found (Fig. 5) in agreement to

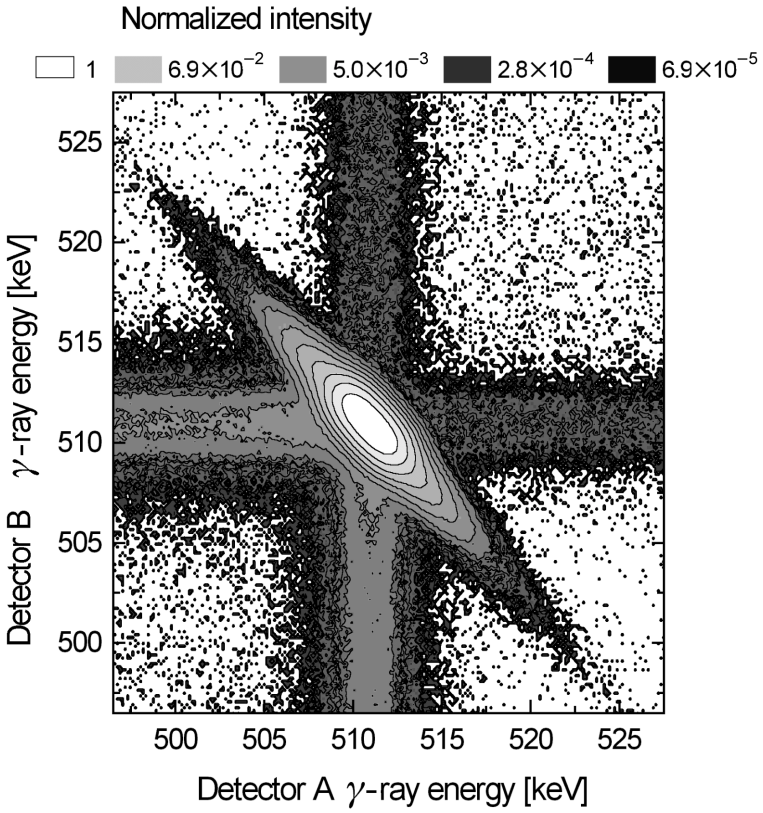


**Fig.4** The spectrum as measured by two Ge detectors in a Doppler-broadening coincidence setup according to Fig. 3. The normalized pulse height is shown as a contour plot as a function of the energy axis of both detectors in the range of the annihilation energy, 511 keV. The diagonal spectrum follows the equation: $E_1 + E_2 = 2m_0c^2 =$ 1022 keV. It exhibits an improved energy resolution and peak-to-background ratio.

other results [7, 10] in the above mentioned test setup [12]. No further attempt was necessary to remove remaining background which was found to have only negligible intensity. This background is mainly due to the Compton scattering of the 1.28 MeV γ quanta from the $\beta^+$ source. Thus, it will be further reduced in a positron beam system where the 1.27-MeV quanta are not present. A cross section along the other diagonal ($E_1$ - $E_2$=0) gives a good approximation of the energy resolution $\Delta R$ of the system [10]. In practice, the cross section is taken within a small width δ according to ($2m_0c^2$ - δ < $E_1$+$E_2$ < $2m_0c^2$ + δ) [7, 10]. The optimum width of the cross section must be optimized because a too small δ will waste statistics whereas a too high δ will fail to remove all the unwanted background.

After taking the cross section, the symmetrical spectra were normalized to unit area, shifted to a central peak channel (shifting was found to have no influence on the peak shape), folded around $E_1$ - $E_2$ = 0, and averaged. Folding is equivalent to an improvement of the statistics by a factor of two. Data smoothing should be avoided since is was found to falsify sometimes the effects in the spectra, in particular if differences are small.

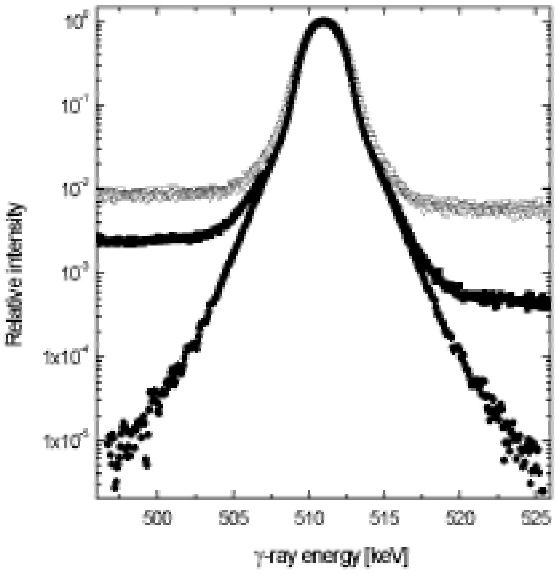


**Fig. 5:** Doppler spectra as obtained by the conventional Doppler-broadening spectroscopy (∇), by a simple coincidence where the second detector serves only to improve the background, and the diagonal spectrum of Fig. 4 (•).

### 3. Application of the technique at an intense FEL-LINAC-based positron source

The use of a slow-positron beam gives the possibility to avoid the simultaneous detection of the annihilation radiation with the gamma radiation of a $\beta^+$ source [7, 10]. This increases the peak-to-background ratio distinctly. In addition, a LINAC-based positron source may provide a very large number of positrons. Since Doppler-broadening spectroscopy is especially useful in simultaneous combination with positron lifetime spectroscopy, the measurement has to be performed using a pulsed positron beam. Although each of the bunches may contain a large number of positrons, the detectors can only register a single event per bunch. This is due to the extended dead time of such detectors. Moreover, the number of events to be detected must be further reduced to about $10^5$ counts per second to avoid a detector overload, pile-up effects, and the worsening of the energy resolution. The second detector of a coincidence system will reduce the count rate of the system by its own detection efficiency which is of the order of 30%. Thus, only a count rate of about $3\times10^4$ $s^{-1}$ will be available. Since the comparison of experimentally observed high-momentum spectra with corresponding calculated spectra requires a high statistics (>$10^7$ counts per spectrum), the Doppler-coincidence technique cannot be applied as a standard technique together with positron lifetime spectroscopy (see chapter 5.1.3.1) which will be much faster. Thus, only selected positron lifetime experiments can be accompanied by Doppler-coincidence measurements.

Opposite to the planned multi-detector lifetime setup, the overall count rate of the Doppler system can hardly be increased by the establishment of a multi-detector arrangement of Ge detectors. This is due to the high costs of such a detector and the fact that the solid angle around the samples will be almost filled by the lifetime detectors. However, for many applications the recording of “normal” (non-coincident) Doppler spectra will be very useful. This gives two independent Doppler spectra with a total count rate of about $2\times10^5$ /s. Since an analysis of these spectra using simple lineshape parameters requires only a medium spectra statistics (about $10^6$

registered events), the collection time will be rather short. Thus, the measurement automation system should allow lifetime measurements without Doppler-broadening experiments for highest data rates and lifetime spectroscopy correlated either with coincident or non-coincident Doppler-broadening spectroscopy.

**4. Summary**

The Doppler-broadening spectroscopy provides an additional source of information about the defect structure under investigation which complement positron lifetime spectroscopy. Thus, positron lifetime experiments should always be accompanied by Doppler-broadening spectroscopy. The total count rate of Doppler measurements will be distinctly smaller compared to lifetime data collection, so that the Doppler system will be active for only a part time of the experiment. The Doppler-coincidence technique decreases drastically the background of the Doppler spectrum around the 511 keV gamma line. This is of particular importance in a surrounding of relatively high radiation background like the laboratory at an FEL-LINAC. Only this background reduction makes it possible to get information of the high-momentum region of the Doppler spectrum. Furthermore, the coincidence technique leads to a significant improvement of the energy resolution, and thus to more detailed Doppler spectra. Therefore, the Doppler-coincidence technique is state-of-the-art of modern positron laboratories, and will be an essential part of the detector system of a possible FEL-LINAC-based positron source.

**References**


1. P. Hautojärvi (Ed.): *Positrons in solids* (Springer, Berlin 1979)
2. R. Krause-Rehberg and H.S. Leipner: *Positron annihilation in semiconductors,* (Springer-Verlag, Berlin 1999)
3. M.J. Puska and R.M. Nieminen: Rev. Mod. Phys. **66**, 841 (1994)
4. R. Krause-Rehberg, S. Eichler, F. Börner, and F. Redmann: Nucl. Instr. Meth. Phys. Res. to be submitted (2000)
5. M. Alatalo, H. Kauppinen, K. Saarinen, M.J. Puska, J. Mäkinen, P. Hautojärvi, and R.M. Nieminen: Phys. Rev. B **51**, 4176 (1995)
6. M. Alatalo, B. Barbiellini, M. Hakala, H. Kaupinen, T. Korhonen, M.J. Puska, K. Saarinen, P. Hautojärvi, and R.M. Nieminen: Phys. Rev. B **54**, 2397 (1996)
7. P. Asoka-Kumar, M. Alatalo, V.J. Ghosh, A.C. Kruseman, B. Nielsen, and K.G. Lynn: Phys. Rev. Lett. **77**, 2097 (1996)
8. S. Szpala, P. Asoka-Kumar, B. Nielsen, J.P. Peng, S. Hayakawa, K.G. Lynn, and H.-J. Gossmann: Phys. Rev. B **54**, 4722 (1996)
9. U. Myler and P.J. Simpson: Phys. Rev. B **56**, 14303 (1997)
10. A.C. Kruseman, H. Schut, A.v. Veen, P.E. Mijnarends, M. Clement, and J.M.M.d. Nijs: Appl. Surf. Sci. **116**, 192 (1997)
11. D.T. Britton, W. Junker, and P. Sperr: Materials Science Forum **105-110**, 1845 (1992)
12. J. Gebauer, R. Krause-Rehberg, S. Eichler, and F. Börner: Appl. Surf. Sci. **149**, 110 (1999)

## 5.1.4. SYSTEM OPERATION AND CONTROL

I.Prochazka (Prague)

**Introduction**

Various experimental techniques of positron annihilation spectroscopy (PAS) were proposed to be implemented on the new positron facility. All these techniques require an intense variable-energy, and pulsed in addition for the lifetime measurements, produced from the LINAC high-energy electron beam (see Section 5.1.3 for detailed discussion). In the present paragraph, common features of the proposed techniques are outlined and specific requirements, which should be taken into account in the control and data collection process, are pointed out. In the next two paragraphs, the hardware and software for solving the control and data collection tasks, respectively, are treated.

Most of the new PAS techniques proposed rely upon the two basic kinds of PAS measurements: (i) the measurements of Doppler broadened spectra of annihilation radiation (PAS/DB) and (ii) positron lifetime spectroscopy (PAS/PL). Both these kinds of measurements are nowadays well-developed in the conventional PAS with radioisotope positron sources and widely used in that field.

Under circumstances of a LINAC based positron beam facility, however, new possibilities of obtaining useful information are provided as well as new requirements occur compared to the conventional PAS. First, the high-energy electron beam utilized for production of positrons as well as the process of formation and guiding the pulsed slow-positron beam of adjustable energy are to be controlled and monitored during the experimental run. The PAS/PL or PAS/DB spectra are always measured as functions of the positron energy and, in sample scanning experiments, also as functions of an adjustable position at which the beam hits the surface of the sample target. In case of PAS/PL, the start timing signal for the TAC is derived from the positron beam pulse while the stop signal comes from the detector registering annihilation photons. It means that positron beam parameters should be controlled during the experiment and recorded together with accumulated spectra. Similarly to the case of the conventional PAS, moreover, other external parameters characterizing the state of the sample (e.g. sample temperature) may be varied in a controlled manner and thus they are needed in measurement and control during the experiment, too. All these factors need to be taken into account in the design of a system for control of in-beam PAS experiment and data acquisition.

Further obvious steps in the development of PAS/PL and PAS/DB methods, especially important for in-beam experiments, consist in building up multi-detector configurations. These bring not only a considerable increase in rates of data accumulation but, above all, allow for a significant improvement of the quality of experimental information: improving the time resolution in PAS/PL measurements and direct obtaining the instrumental resolution function using timing information on both annihilation photons registered in coincidence (these aspects of the advanced PAS/PL method were discussed in Section 5.1.3.1 in detail); a substantial background suppression in the two-detector coincidence mode of PAS/DB measurements (Sect. 5.1.3.2) which can make feasible experimental information on high-momentum components of the electron momentum distributions in solids [1,2]; measurements of the age-momentum correlation can be involved.

The planned high intensity of the positron beam (more than $10^8$ positrons/s) should allow for a high rate of data accumulation so that a sufficient statistical accuracy of accumulated spectra can be reached within measuring times as short as few minutes. Thus, despite of limitations on count rates discussed in Section 5.1.3, up to several hundreds of spectra could be collected per day in a typical PAS experiment on this facility. Simultaneously, the analysis of data from a multi-detector setup will become more time consuming than in conventional PAS. This means that a sufficiently fast and efficient system of data storage and transmission to other remote sites for data evaluation is needed.

Since the LINAC itself is a large-scale and complicated facility, the in-beam PAS experiments require more labor than the conventional PAS experiments with radioisotope positron sources. Therefore, to perform the positron experiments on the EPOS facility more effectively and conveniently, and to avoid man-made mistakes in operating the facility and handling the large-scale experimental data, a system of computerized and highly automated control of the device as well as data acquisition according to a pre-selected program is strongly required. Such a system should involve full control and monitoring of the positron beam, automated collection and storage of the measured spectra as well as preliminary ‘on-line’ evaluations of spectra being collected. The latter function was involved because of possible operator-made interrupts of the current run and subsequent modifications of further steps of the program controlling the measuring cycle. The decision to make such

changes have to be based on the results of such a preliminary analysis of spectra measured in the preceding steps.

**Hardware**

From what has been said in the Introduction, it is obvious that the complete task of computerized control of in-beam PAS measurements can be divided into several various subtasks which would be executed on individual modules, provided that a necessary communication between the modules is satisfied. Another role of the system would consist in enabling communication and data transmission via the Internet to external laboratories (including e.g. even control of the experiments from remote laboratories as considered in Section 5.1.3). Therefore, the computer system of control and data acquisition (see Figure) is proposed to consist of six personal computers (PCs) which are connected to a local area network (LAN). Each PC of the LAN (denoted as PC#1, …, PC#6) is dedicated to one of the different subtasks, which are explicitly listed below, and equipped with necessary ports and interface cards for two-ways communication with the corresponding part of the facility:

PC#1 The LAN server.

PC#2 Remote control and monitoring of the LINAC electron beam.

PC#3 Adjustment, control and monitoring of the pulsed positron beam.

PC#4 Changes and control of the positron beam parameters (energy, position at the sample surface) during the experiment. Communication with electronic modules for spectra collection (ADCs), control of data acquisition, providing the histogram memory for spectra being currently accumulated. Preliminary on-line analysis of spectra, visualization of measured spectra and results of such an analysis. Operator-made interrupts and modifications of the programmed measuring cycle.

PC#5 Monitoring and control of measuring devices for adjusting sample temperature and the other external parameters, not related to the positron beam.

PC#6 Storage of spectra on a large-volume hard disk. Final analysis of experimental data using a high-sophisticated software.

**Software**

Software system for computer control of PAS experiments will consist of several programs grouped into the following three levels (see Figure).

*Level 1*

The level-1 programs are designed to work as an interface between PCs and the other hardware devices. They will acquire and visualize monitor signals from and output control signals to the devices. The control of data acquisition using the computer memory and according to a pre-selected sequence of steps will also be performed by means of these programs. The level-1 programs will be machine dependent and executed using PC#2, PC#3, PC#4 and PC#5 computers.

*Level 2*

The level-2 programs are required to provide an user interface and will be executed on PC#4 computer. These programs will perform preliminary analysis of measured spectra. In case of PAS/DB, the shape parameters S and W will be determined. In case of PAS/PL, the average positron lifetime will be evaluated, or lifetimes and intensities of the individual components will be deduced from the fit of a simple model to the experimental data. Visualization of the measured spectra as well as the preliminary results of preceding steps will be involved in programs of this level, too. The level-2 programs are also assumed to allow for an operator interrupt of the run and modification of the further flow of the cyclic measurement.

Commercially supplied software for operating the PC cards for communication with surrounding devices is assumed to serve as the basis for developing programs of levels 1 and 2. However, it is necessary that the software supports calling user-defined command files and subprograms.

*Level 3*

For running the level-3 programs, the PC#6 machine will be exploited. These programs are supposed to perform detailed final analyses of measured spectra using the software of higher degree of sophistication. Most cases of interest can nowadays be covered with a variety of freely distributed or commercially available packages of programs which were originally developed for conventional PAS with radioisotope sources and are easily executable even on current PCs. For the decomposition of positron lifetime spectra into discrete components, programs PATFIT-88 [3], LIFESPECFIT [4], LT [5] and others are well-examined and widely used. In case of continuous distributions of positron lifetimes, the programs CONTIN [6], MELT [7] and [8] are now routinely used in the world. The PAS/DB experiments and depth profiling of defects can best be analyzed in the frame of VEPFIT [9] or POSTRAP [10] codes. Contrary to the conventional PAS, however, data taken in in-beam PAS experiments will require modifications of some of the above algorithms to take into account specific conditions of these experiments (multi-detector setup, correction of PAS/PL spectra with respect to the long-lifetime part, as discussed in Section 5.1.3.1)

For the sake of a better reliability of results, it may appear useful to perform the final analyses of PAS data by means of various approaches to the same problem and, therefore, it would be convenient to have all the programs listed above implemented in the system as the level-3 programs. As some of these programs may use different data formats, it turns desirable to include in the system flexible format conversion routines.

**Conclusions**

In building up the above proposed system of computerized control and data acquisition for PAS experiments at the new positron facility, wide expertise acumulated to date by research groups over the world in development of conventional as well as in-beam PAS techniques [11] will be utilized. The system as such satisfies basic needs of experimenters at the experimental site and communication with remote laboratories. It also appears to be sufficiently flexible to allow for easy implementation of new PAS techniques in the future.

**References**


[1] K.G. Lynn, J.R. MacDonald, R.A. Boie, L.C. Feldman, J.D. Gabbe, M.F. Robbins, E. Bonderup, and J. Golovchenko, Physical Review Letters 38, 241 (1977)

[2] S. Szapala, P. Asoka-Kumar, B. Nielsen, J.P. Peng, S. Hayakawa, K. G. Lynn, and H.-J. Gossmann, Physical Review B 54, 4722 (1996). A.C. Kruseman, H. Schut, A. van Veen, P.E. Mijnarends, M. Clement, and J.M.M. de Nijs, Applied Surface Science 116 (1997) 192

[3] P. Kirkegaard, N.J. Pedersen, M. Eldrup, PATFIT-88, Risø National Laboratory Report, Risø M-2470, 1989

[4] M. Puska, P.F. Nyber, H. Pauppinen, Technical University Helsinki, Laboratory of Physics

[5] J. Kansy, Nuclear Instruments and Methods in Physics Research A 374 (1999) 235

[6] R.B. Gregory, Y. Zhu, Nuclear Instruments and Methods in Physics Research A 290 (1990) 172

[7] A. Shukla, M. Peter, L. Hofmann, Nuclear Instruments and Methods in Physics Research A 335 (1993) 310

[8] A.H. Deng, B.K. Panda, S. Fung, C.D. Beling, Materials Science Forum 255-257 (1997) 744

[9] H. Schut, A. van Veen, Applied Surface Science 85 (1995) 225

[10] G.C. Aers, P. Marshall, T. Leung, R.D. Goldberg, Applied Surface Science 85 (1995) 169

[11] R. Suzuki, T. Ohdaira, T. Mikado, H. Ohgaki, M. Chiwaki, T. Yamazaki, Applied Surface Science 116 (1997) 187

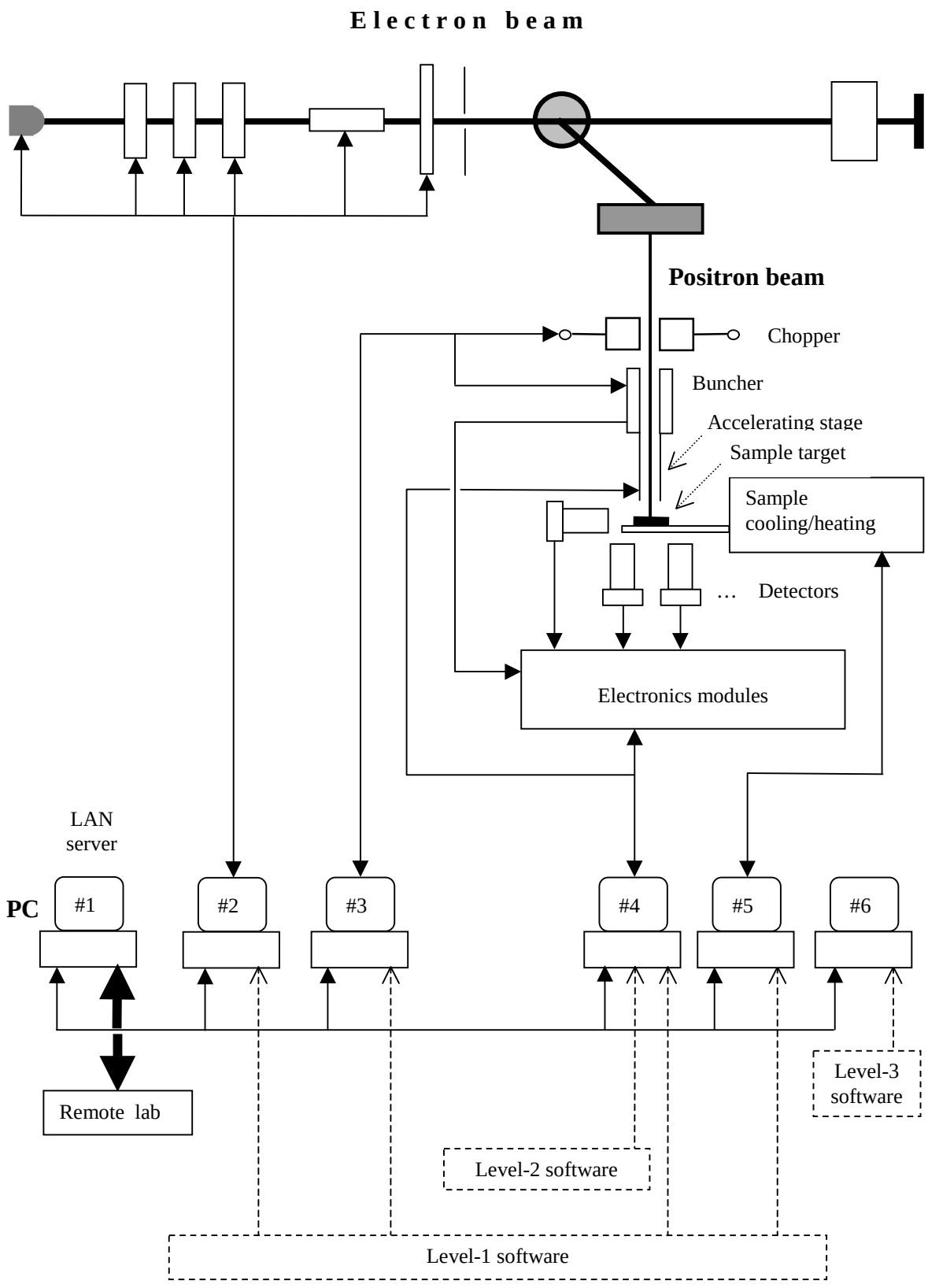


**Figure:** Schematic view of the computerized control and data acquisition system

## 5.2. SURFACE PHYSICS

P.G.Coleman (Bath)

The application of positrons in surface science has been limited principally by the low beam fluxes available and the consequently long data collection times required. (Surfaces in ultra-high vacuum maintain their cleanliness for only ~ 1hour.) An intense beam is thus essential to the realisation and extension of effective positron surface spectroscopies. Examples are outlined below.

**Positron Annihilation-induced Auger Electron Spectroscopy (PAES)**

Low-energy positrons create a hole in the core level of an atom by annihilation rather than by energetic impact: Auger electron emission follows the subsequent atomic rearrangement (figure 1).

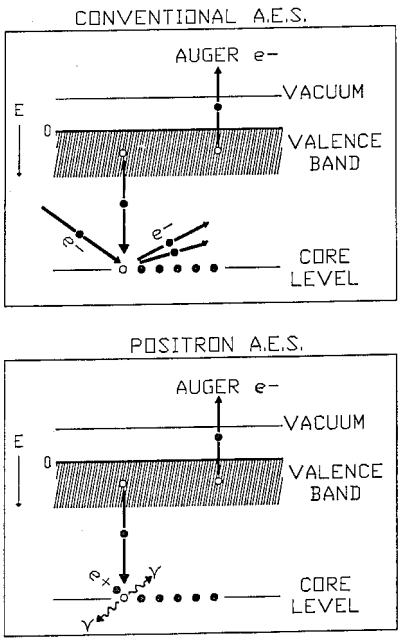


**Fig. 1** Comparison of the core-hole creation mechanism in conventional EAES and PAES. In EAES core electrons are removed by collisions with an energetic electron. The incident electron beam energy must exceed the binding energy of the core electron. In PAES the core hole is created via positron-electron annihilation. The incident positron beam energy can be made arbitrarily low. Auger electron emission follows the creation of the core hole in both cases [1].

The advantages of positron AES over electron AES are: (a) extreme surface sensitivity, (b) reduction of dark noise by Auger electron-annihilation gamma coincidence, (c) vanishingly small secondary electron background, (d) relatively low charge doses and low incident beam energy - both required for studying fragile and insulating systems.

A high flux facility, with cylindrical mirror analyser and/or time-of flight capacity, will permit the performance of PAES at a level currently possible with EAES, but with all the advantages listed above. Time-dependent studies of ultra-thin film growth could be performed, as could higher resolution studies of Auger lineshapes. Higher energy (less probable) Auger peaks could be studied, extending significantly the species amenable to PAES. Very low-energy Auger transitions could be observed, free of the high background common in electron AES. Surface segregation, H-termination and oxidation can all be studied with extreme surface sensitivity. The use of beams of polarized positrons will make possible a new spectroscopy for the study of the magnetic properties of surfaces: Polarized PAES [2]. A positron will annihilate ~558 times faster with an electron with anti-parallel spin than an electron with parallel spin. It is therefore possible to use a polarized beam of positrons to create polarized core holes with a net polarization approximately equal in amount and opposite in direction of the incident positron beam. Selection rules based on the conservation of total spin will permit the study of the polarization of valence electrons by measuring the intensities of Auger transitions in which the core hole is filled by a valence electron. In order to use the PAES signal in conjunction with a positron microprobe (section 6.2) it is necessary to overcome the problem presented by the fact that positrons at the relatively high beam

energies >1000 keV required to form a micro-beam can generate high energy secondary electrons and Auger excitations in the bulk. One proposed solution [2] is to use time-of-flight spectrometry to separate Auger electrons from prompt secondary electrons. If this or another method succeeds then it will be possible to use PAES to obtain a map of the elemental composition of the surface with an in-plane resolution comparable to scanning EAES but with a depth resolution almost an order of magnitude higher.

**Low-Energy Positron Diffraction (LEPD)**

It has been demonstrated that LEPD can have significant advantages as a surface structural probe in systems where LEED has failed to give accurate or conclusive results (e.g. compound semiconductors and hydrogenated surfaces) [3-8]. However, its routine application has been impeded by the low intensity of available laboratory-based positron beams. An intense positron source would allow the use of position-sensitive detectors and energy analysis in geometries reminiscent of more established spectroscopies.

**Re-emitted Positron Energy Loss Spectroscopy (REPELS)**

The differences between positron and electron interactions at solid surfaces are significant enough to make REPELS complementary to the established EELS in the study of vibrational modes on a solid surface [9]. The feasibility of REPELS technique has been demonstrated in the laboratory, but (as for other positron surface spectroscopies) it has not been developed because of lack of beam intensity. An intense source would allow the wider application of REPELS to the study of molecular adsorbates on surfaces.

**Re-emitted positron spectroscopy (RPS)**

The presence of thin overlayers of dissimilar metals can dramatically effect the fraction of positrons reemitted from a metal surface [10]. RPS is thus a sensitive probe of thin metal overlayers (figure 2) [10].

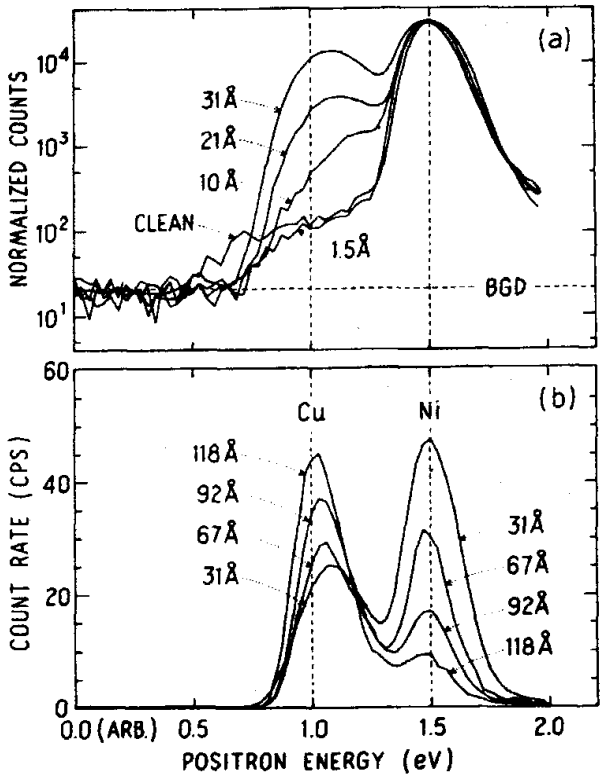


**Fig. 2** Reemitted positron energy spectra for various thicknesses of Cu on Ni (incident energy 4keV). (a) normalised to peak height, (b) to total intensity [10].

RPS is an excellent tool for studying any processes that affect the sum of the bulk chemical potentials, including alloying of the overlayer film; it is insensitive to surface contamination**.** In addition, measurement of the shift

with temperature in the peak of the energy spectrum of elastically-emitted positrons provides a means of measuring thermal volume expansion in thin films [11]. An intense positron beam will make possible the real-time monitoring of the growth and temperature-induced changes in ultrathin films.

**Positron Re-emission Microscopy (PRM)**

The unique contrast mechanism for PRM lies in the sensitivity of the probability for positron re-emission into the vacuum to surface conditions, including the presence of surface defects, adsorbed molecules, different crystal faces, and local charging. PRM complements other microscopies in many areas - for example, (a) direct imaging of bimetallic systems of importance in surface catalysis with high-*Z* substrates - which can swamp TEM signal unless impractically thin, (b) bimetallic systems of similar *Z* or for which TEM contrast is slight, (c) imaging of surface defects - positrons are the most sensitive probe of point defects, (d) imaging of subsurface defects - eg around buried metallic contacts in semiconductors, and (e) non-destructive imaging of biological systems without the need for staining or labelling compounds. An intense positron beam is required to enable studies of well-characterised surfaces in an acceptably short time; real-time image collection is a further possibility, allowing the study of time-dependent processes on surfaces. The resolution limit of a positron re-emission microscope is determined by the deBroglie wavelength of the positron, i.e., ~ 1nm. Information of small surface structures on a scale less than this limit is, however, achievable by holographic means. Chen *et al* [12] have investigated the feasibility of performing positron re-emission holography with a PRM (fig. 3), and find that a $10^{10}$ positrons $s^{-1}$, 1μm beam would in general be required. Tong *et al* have shown, also theoretically, that "...positron diffraction is better suited than electron diffraction for holographic reconstruction because of the positron's weak scattering and large damping in solids" [13].

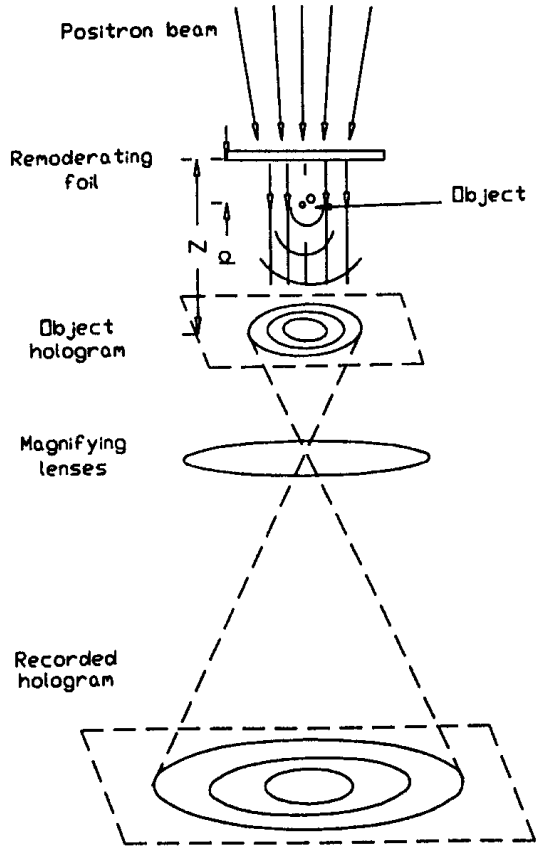


**Fig. 3** Simulated positron holography experiment. Object: two atoms. *d* is the distance between object and moderator foil. *Z* is the distance between object hologram and moderator foil [12].

**Electronic structure of surfaces and thin films**

Angular Correlation of Annihilation Radiation (ACAR) provides high resolution information on the electronic structure of materials not possible with other methods [14]. If controllable-energy positron implantation is used then ACAR can be used to study the electronic structure of surface states (incident positron energies $E \sim 10^2$ eV) or subsurface regions ($E \sim 10^3$ eV). Gamma coincidence rates in standard (bulk) two-dimensional ACAR are low, such that run times of several days are required. If a positron beam is used then intensities $\geq 10^8$ $s^{-1}$ are required in order to make the measurements feasible. An example of one of a very small number of surface 2D-ACAR measurements made to date is shown in figure 4 [15].

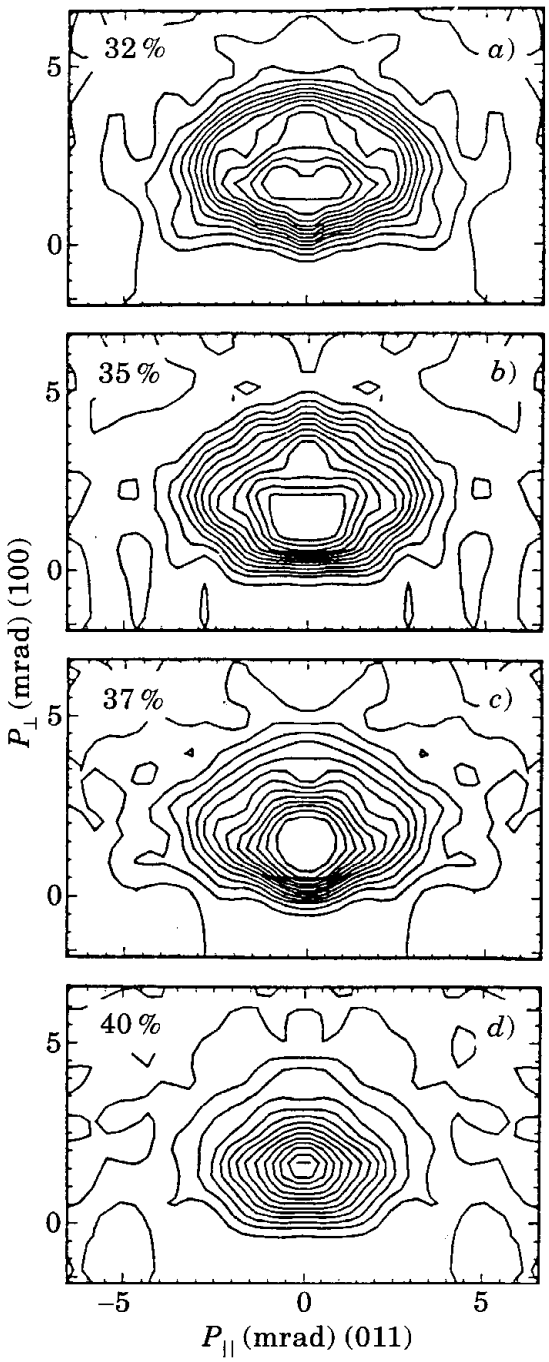


**Fig. 4** 2D-ACAR projections of momentum spectra of Ps emitted from (a) clean Al(100) and after oxygen contamination for (b) 3h, (c) 6h, (d) 9h [15].

**Positronium spectroscopies**

Angle-resolved positronium (Ps) emission spectroscopy is performed using 2D-ACAR, as described above, Several other novel Ps-based spectroscopies of solid surfaces have been proposed but currently cannot be realised because of inadequate beam intensities. Ishii [16-19] has performed extensive theoretical work showing how Ps formation can be used to provide information on solid surfaces in novel ways. Briefly, they are:

**(a)** ***Inverse Ps Formation Spectroscopy*****.** In this technique a beam of Ps atoms impinges on a surface; the electron is given up to an unfilled state and the positron takes away information on the state. The method should be more sensitive to the topmost surface layer than the two existing spectroscopies of unoccupied states, inverse photoelectron spectroscopy and two-photon photoemission [16]. Another advantage should be the strength of the signal.

**(b)** ***Adsorbate studies using Ps formation Spectroscopy*****.** Ishii [17] has shown that the dependence on incident positron energy of Ps formation probability at adsorbate-covered surface is sensitive to the atomic positions of the adatoms. In particular, he shows that the method is sensitive even to hydrogen adatoms, in contrast to the standard angle-resolved photoemission. This method is extended to randomly-positioned adsorbate atoms when Ps formation is accompanied by desorption of the ionised adatom [18].

**(c)** ***Surface barrier potential studies*** **[19].** The dependence of the Ps formation probability on incident positron energy is sensitive to the shape of the electronic surface barrier (see Figure 5). Measurements of this kind, coupled with LEED (for the surface atomic configuration), angle-resolved ultraviolet photoemission spectroscopy ARUPS (for information on electronic states), and LEPD (using the LEED and ARUPS data) for the positronic potential, provides the only method for measuring the electronic surface barrier potential.

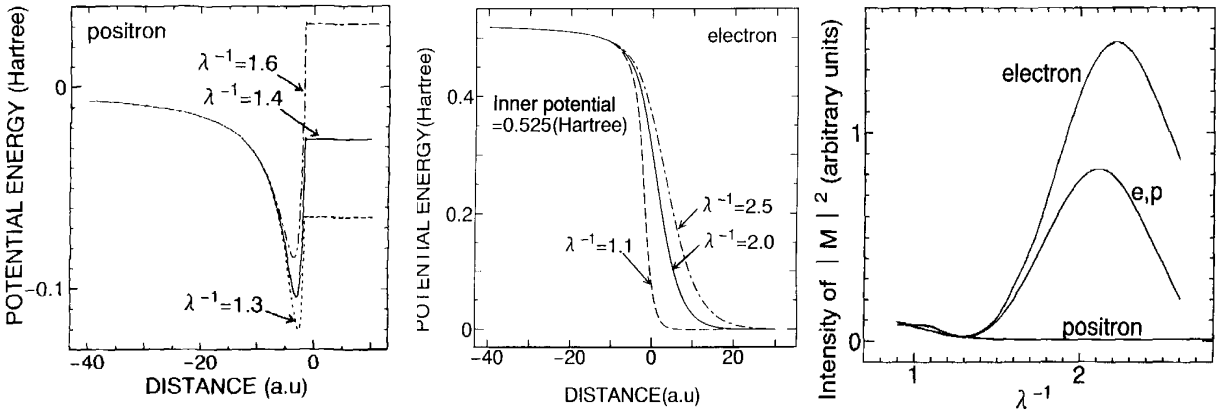


**Fig. 5** (left) Electronic surface barrier potential for different shape parameters λ: (middle) positronic surface barrier potential: (right) Ps formation intensity vs $\lambda^{-1}$ (incident positron energy 40.8 eV: 1 Hartree = 27.2eV). [19]

**References**


1. A. Weiss, D. Mehl, A.R. Koymen, K.H. Lee and Chun Lei, 1990, J. Vac. Sci. Technol A **8**, 2517.
2. A.H. Weiss, 1995, *The Handbook of Surface Imaging and Visualization*, Ed. Arthur T. Hubbard (CRC Press, Boca Raton) pp. 617 - 633.
3. T.N. Horsky, G.R. Brandes, K.F. Canter, C.B. Duke, S.F. Horng, A.Kahn, D.L. Lessor, A.P. Mills, Jr., A. Paton, K. Stevens and K. Stiles, 1989, Phys. Rev. Lett. **62**, 1876.
4. T.N. Horsky, G.R. Brandes, K.F. Canter, C.B. Duke, A.Paton, D.L. Lessor, A. Kahn, S.F. Horng, K. Stevens, K. Stiles, and A.P. Mills, 1992, Phys. Rev. B **46**, 7011.
5. X.M. Chen, K.F. Canter, C.B. Duke, A. Paton, D.L. Lessor, and W.K., 1993, Phys. Rev. B, **48**, 2400.

6. C. B. Duke, A. Paton, and A. Lazarides, D, Vasumathi and K.F. Canter, 1997, Phys. Rev. B **55** 7181.
7. C.B. Duke, D.E. Lessor, T.N. Horsky, G. Brandes, K.F. Canter, P.H. Lippel, A.P. Mills,Jr., A. Paton and Y.R. Wang, 1989, J. Vac. Sci. Technol, A**7** 2030.
8. D. L. Lessor, C. B. Duke, X. M. Chen, G.R. Brandeis, K.F. Canter, and W. K. Ford, J. Vac. Sci. Technol. 1992, A**10** 2585.
9. D.A. Fischer, K.G. Lynn and W.E. Frieze, 1983, Phys. Rev. Lett. **50**, 1149.
10. D.W. Gidley and W.E. Frieze, 1988, Phys. Rev. Lett. **60**, 1193.
11. David W. Gidley, 1989, Phys. Rev. Lett. **62**, 811.
12. X.M. Chen, K.F. Canter and A.P. Mills, Jr., 1991, *Appl. Phys.* A**53**, 203.
13. S.Y. Tong, H. Huang and X.Q. Guo, 1992, *Phys. Rev. Lett.* **69**, 3654.
14. R.N. West, 1995, *Positron Spectroscopy of Solids*, eds. A. Dupasquier and A.P. Mills, Jr. (IOS, Amsterdam), p. 75.
15. D.M. Chen, S. Berko, K.F. Canter, K.G. Lynn, A.P. Mills, Jr., L.O. Roellig, P. Sferlazzo, M. Weinert and R.N. West, 1987, Phys. Rev. Lett. **58**, 921.
16. A. Ishii, 1990, Nucl. Instrum. Methods B **48**, 386.
17. A. Ishii, 1993, Surface Sci. **287/8**, 811.
18. A. Ishii, 1993, Surface Sci. **283**, 462.
19. A. Ishii and T. Aisaka, 1995, Appl. Surf. Sci. **85**, 33.

## 5.3. ATOMIC PHYSICS

## 5.3.1. POSITRON SCATTERING / IONIZATION / BREMSSTRAHLUNG

R. Hippler (Greifswald)

The interaction of antiparticles with atoms, molecules and surfaces is of substantial scientific interest [1-3]. This is in part due to the fundamental nature of the underlying interaction processes, the formation of positronium “atoms” consisting of positrons and electrons and of anti-hydrogen atoms being formed by positrons and antiprotons [4], and the importance of slow positron beams as a tool for solid-state physics and material research [5,6] including positron microscopy [7] and life sciences (medicine, biology).

The interaction of slow, moderated positrons with atoms, molecules and surfaces is basically of similar nature as for electrons. Important differences among other things result because of

- the different charge,
- the different magnetic moment,
- the possibility to distinguish positrons from electrons and
- the ability to form positronium together with electrons, i.e. stable "atoms" or "molecules".

These differences compared to electrons among other things lead to the fact that the scattering of positrons at atoms shows a behaviour in the vicinity of excitation or ionisation thresholds that deviates from that of electrons [8] while exchange effects that sometimes dominate electron scattering cannot occur.

**Single and multiple ionisation of atoms** is dominated by the Coulomb interaction. The exchange interaction providing an additional contribution to the scattering cross section during electron collisions is missing for positron impact. This usually leads to scattering cross sections that become larger for positrons compared to electrons [9-11]. In the proximity of the ionisation threshold $I$ the correlation of the outgoing charged particles among themselves plays an important role, for example, leading to so-called “critical” angles among the outgoing charged particles. Depending on the outgoing charge, the occurring of *cusps* or *anti-cusps* in the ejected particle spectrum at these critical angles and a different threshold behaviour of the ionisation cross section $\sigma$

$$\sigma \propto (E\text{-}I)^n \qquad (1)$$

results. $E$ the projectile energy and $n$ = 1.127 for electrons. A significantly steeper energy dependency is expected for positrons. The predicted $n$ for positron impact varies widely from $n = 2.651$ [16] to $n \approx 3.6 \ldots 3.8$ (e.g., Ref. [17]). Experimental investigations for positron impact confirmed the predicted steeper energy dependence but where at variance with the calculated $n$ [18]. As a possible reason one needs to consider that the

experimental measurements due to limited positron intensities were carried out at excess energy $E - I > 1.5$ eV and thus in an energy range where the validity of the Wannier law is highly questioned (e.g., Ref. [19]).

**Positron scattering off molecules** has also received some interest during the past years. For example, non-dissociative and dissociative ionisation of CO, $CO_2$, and $CH_4$ has been studied by Bluhme et al. [17]. Whereas in non-dissociative scattering the positronium formation channel provides a strong contribution, it appears to be largely suppressed during dissociative ionisation. Distinct differences between positron and electron impact were also noted for vibrational excitation of $CO_2$ [20] and $CF_4$ molecules [21]. A pronounced mode dependence for vibrational excitation of $CO_2$ was found by Kimura et al. [20] where the symmetric stretching mode is 2 … 3 orders of magnitude more likely excited by electron compared to positron impact. Similar investigations for excitation of the asymmetric stretch mode of $CH_4$ as a function of projectile energy also displayed marked deviations between positron and electron impact which are not yet understood [21].

Positron annihilation studies in atomic and molecular gases have been performed by Surko and coworkers [22]. The annihilation rate $\Gamma$

$$\Gamma = \pi r_0^2 c n Z_{eff} \tag{2}$$

where $r_0$ is the classical electron radius, $n$ the number density of atoms or molecules, $c$ the speed of light and $Z_{eff}$ the effective number of electrons per molecule participating in the annihilation process. While for noble gas atoms typical $Z_{eff}$ values range around 1-8, unusually large values of $Z_{eff} \approx 10^4$ have been observed for large organic molecules [22]. A much disputed explanation that has been offered recently [23] to explain for these large $Z_{eff}$ values is based on “virtual” positronium” formation and the formation of “exotic” atomic or molecular states that bind positrons, e.g., Ref. [24], while concluding evidence for any of these mechanisms is still missing.

So far, investigations for ionisation of atoms and molecules by positron impact were largely limited to integral investigations, however. Angle-differential investigations, which could serve the clearing-up of important details leading to a better understanding of the underlying processes, are the exception yet (e.g., Ref. [25]). In particular the occurring of "critical angles" in the scattering at which, depending on the charges of the involved particles, the ionisation processes becomes more effective or ineffective, could be examined thereby in great detail. A particular example of such a critical angle occurs when the colliding positron and the ionised electron run out into the same direction and with approximately the same impulse, eventually leading to the formation of a “cusp” in the spectrum of emitted electrons [25], [26], or by mutual "capture" to the formation of positronium “atoms”.

The exchange interaction plays an important role also during the **excitation of atoms by positron impact.** So far there are to our knowledge no investigations for the excitation of atoms by positrons impact. Such investigations would offer some advantages in comparison to studies with electrons. For example, excitation of helium atoms into a singlet state proceeds via direct excitation, and, for electrons but not for positrons, additionally through the exchange process. The excitation of helium into a triplet state, however, is not possible by direct excitation and, since the exchange process does not operate during positron impact, no excitation of triplet levels by positron impact should occur. Excitation of triplet states by positron impact would, hence, allow for an investigation of magnetic, e.g., spin-spin interaction processes during positron impact and largely undisturbed by other excitation processes.

**The ionisation of inner atomic shells** in the proximity of the ionisation threshold is influenced by the Coulomb effect. This is because charged particles, depending upon the sign of their charge, undergo a deceleration or acceleration in the nuclear field of the target atom. Positrons are decelerated here, whereby the possible impulse and, hence energy transfer to bound electrons is considerably reduced as is the probability for ionisation. The Coulomb effect shows up particularly clearly if the projectile has to penetrate deeply into the nuclear field, as is the case, e.g., for inner shell ionisation. There exist rather few experimental investigations of inner shell ionisation yet. Moreover, these investigations have not yet been carried out close enough to the ionisation threshold to investigate the threshold behaviour in sufficient detail [12].

There exist no experimental investigations so far of **positron-induced bremsstrahlung.** Bremsstrahlung is produced if charged particles are decelerated or accelerated. The strongest acceleration occurs in close proximity to the target nucleus leading with high probability to a total loss at kinetic energy of the projectile. The energy spectrum of bremsstrahlung photons emitted by electrons is constant up to the high-energy limit given by energy conservation where it aborts abruptly. This high-energy edge is, hence, easily observed in the energy spectrum of the bremsstrahlung emitted by electrons. Contrary to electrons, which are strongly

accelerated in the core field, incoming positrons are slowed-down, which is why for bremsstrahlung photons to be emitted only a significantly reduced energy is available. This has the consequence that the energy spectrum of positron-induced x-rays the intensity gradually approaches zero in the high-energy limit, in clear contrast to the sharp high-energy-edge observed for electrons. To our knowledge, no investigations of a positron-induced bremsstrahlung spectrum at keV energies has been performed yet.

**Positronium formation** is an additional ionisation channel in collision with positrons. Similarly as for the capture of electrons by positive ions substantial details of the capture process are still unsettled and, in particular, a complete theoretical description still pending. In addition, new phenomena have been observed, e.g. a strong suppression of positronium formation in double ionisation of rare gas atoms [Helms, Knudsen]. Positronium formation has emerged in recent years as a new branch of positron physics. For example, spectroscopic investigations offer new inside into atomic structure theory. Other aspects of the interaction of positronium with matter or with photons are yet completely unexplored. The interaction of fast positronium with atoms and surfaces is one of the processes taking place during the slowing-down of positrons in matter. For example, scattering of positronium needs to be considered during the diffraction of positrons and of positronium from surfaces and is an essential ingredient in the determination of the range of positrons in matter. Detailed investigations of the interaction of positronium with atoms, molecules, and surfaces would require intense positronium beams which are at present unavailable.

**Energy loss of leptons (positrons, electrons) in matter.** The energy loss of charged particles in matter is both of basic interest and of importance for numerous applications in the material research and in the life sciences (medicine, biology). There exist detailed calculations of the energy loss of leptons in matter [13] which are predominantly based, however, on high-energy approximations (e.g., Bethe-Born approximation). These calculations are accordingly not very reliable at low energies. Even at energies in the 10 keV range and particularly for high-$Z$ materials significant deviations to existing experiments [14] exist whose cause so far is not fully understood [15] but would require further angle-differential investigations to clarify this point.

The investigations executed so far all suffer from the fact that sufficiently intense slow positron sources are not at all or not readily available. This is the principal reason for the fact that numerous investigations were omitted so far or could not yet been performed with the necessary accuracy.

**Proposeded investiagtions:**

1. **Excitation and ionization of atoms and molecules**. Excitation and ionization of atoms and molecules by positrons shall be examined. Measurements of angle-integrated cross-sections for excitation and for single as well as multiple ionisation of atoms are planed from close to threshold up to several times the electronic binding energy. In addition, positronium formation in ionising collisions will be investigated. Ionization of molecules leads also to formation of repulsive molecular states and therby to fragmentation. The various reaction channels in dissociative ionisation of, e.g., $H_2$ molecules may be investigated by time of flight ion spectroscopy of produced fragment ions [Siegmann]. Angle-dfferential measurements providing details about particular excitation and ionisation mechanisms shall be conducted at a later stage. A: Prof. Dr. R. Hippler (Universität Greifswald), Prof. Dr. H. Schneider (Universität Giessen), Prof. C.A. Quarles (Texas Christian University)

2. **Inner shell ionisation and positron-induced bremsstrahlung** experiments are planned to investigate the so-called Coulomb effect which predicts significantly reduced ionisation cross sections in close proximity to the ionisation threshold as well as a decrease of the high-energy portion of the emitted bremsstrahlung spectrum. A Si(Li) or Ge solid state x-ray detector will be employed to detect characteristic and bremsstrahlung photons induced by positron impact. A: Prof. Dr. R. Hippler (Universität Greifswald), Prof. Dr. H. Schneider (Universität Giessen), Prof. C.A. Quarles (Texas Christian University)

3. **Energy loss and scattering of positrons in thin foils.** It is planned to examine the scattering (and backscattering) of leptons after the passage through thin foils in an angle-differential experiment. Previous investigations in forward direction and for heavy targets have revealed significant discrepancies to existing calculations, which are so far not understood. A: Prof. Dr. R. Hippler (Universität Greifswald), Prof. Dr. H. Schneider (Universität Giessen)

4. **Scattering of positronium from atoms, molecules, and surfaces.** It is proposed to develop an intense positronium beam to investigate scattering of positronium “atoms” on other atoms, molecules and surfaces, to investigate the angle-differential scattering and back-scattering of positronium and of the produced positrons and electrons.

5. **Positronium spectroscopy**, e.g., Ley et al. [27], and see **chapter 5.3.2.**

6. **Surface studies**, see **chapter 5.2.**

**References**


[1] D.R. Schultz, R.E. Olson, C.O. Reinhold, J. Phys. B 24, 521 (1991)
[2] E. Morenzoni, In: High-Energy Ion-Atom Collisions (D. Berényi, G. Hock, Eds.), Lecture Note in Physics 376, p. 173 (1990)
[3] H. Knudsen, J.F. Reading, Phys. Reports 212, 107 (1992)
[4] K.Sachs, T.Sefzick, W.Oelert, G.Baur, Spektrum der Wissenschaft 3, 24 (1996)
G. Gabrielse, W. Jhe, D. Phillips, W. Quint, C. Tseng, L. Haarsma, K. Abdullah, J. Gröbner, H. Kalinowsky, Hyperfine Interactions 76, 81 (1993)
[5] A. Weiss, A.R. Koymeh, K.H. Lee, C. Lei, J. Vac. Sci. Techn. A 8, 2517 (1990)
[6] P.J. Schultz, L.R. Logan, W.N. Lennard, G.R. Massoumi, Scanning Microscopy, Supplement 4 (J. Schou, P. Kruit, D.E. Newbury, Eds.), p. 223 (1990)
Coleman, this proposal (chapter 5.2.)
[7] e.g., G.R. Brandes, K.F.,Kanter, A.P. Mills, Phys. Rev. Letters 61, 492 (1989)
[8] R. Hippler, Phys. Letters A 144, 81 (1990)
[9] H. Bluhme, H. Knudsen, J.P. Merrison, K.A. Nielsen, J. Phys. B 32, 5237 (1999)
[10] R. Hippler, S. Helms, U. Brinkmann, J. Deiwiks, R. Hippler, H. Schneider, D. Segers, Can. J. Phys. 74, 373 (1996)
[11] S. Helms, U. Brinkmann, J. Deiwiks, R. Hippler, H. Schneider, D. Segers, J. Paridaens, J. Phys. B 28, 1095 (1995)
[12] H. Schneider, I. Tobehn, F. Ebel, R. Hippler, Phys. Rev. Letters 71, 2707 (1993)
[13] e.g., M.J. Berger, S.M. Seltzer, *Stopping Power of Electrons and Positrons*, NBSIT 81-2550-A, National Bureau of Standards, U.S. Department of Commerce, Washington (1983)
[14] J. Deiwiks, Diplomarbeit, Universität Bielefeld (1994); H. Schneider, I. Tobehn, M. Rückert, U. Brinkmann, R. Hippler, Nucl. Instr. Meth. Phys. Res. B 79, 353 (1993) und Acta Phys. Pol. A 83, 375 (1993)
[15] W.N. Lennard, G.R. Massoumi, P.J. Schultz, P.J. Simpson, G.C. Aers, Phys. Rev. Letters 74, 3947 (1995)
[16] H. Klar, J. Phys. B 14, 4165 (1981)
[17] H. Bluhme, H. Knudsen, J.P. Merrison, M.R. Poulsen, Phys. Rev. Letters 81, 73 (1998); H. Bluhme, H. Knudsen, J.P. Merrison, In: Application of Accelerators in Research and Industry (J.L. Duggan, I.L. Morgan, Eds.), AIP Conference Proceedings 475, 357 (1999)
[18] P. Ashley, J. Moxom, G. Laricchia, Phys. Rev. Letters 77, 1250 (1996)
[19] W. Ihra, J.H. Macek, F. Mota-Furtado, P.F. Mahoney, Phys. Rev. Letters 78, 4027
[20] M. Kimura, M. Takekawa, Y. Itikawa, H. Takaki, O. Sueoka, Phys. Rev. Letters 80, 3936 (1998)
[21] S. Gilbert, R.G. Greaves, C.M. Surko, Phys. Rev. Letters 82, 5032 (1999)
[22] C.M. Surko, A. Passner, M. Leventhal, F.J. Wysocki, Phys. Rev. Letters 61, 503 (1988); T.J. Murphy, C.M. Surko, Phys. Rev. Letters 67, 2954 (1991)
[23] G. Laricchia, C. Wilkin, Phys. Rev. Letters 79, 22412 (1997)
[24] J. Mitroy, G.G. Ryzhikh, Phys. Rev. Letters 83, 3570 (1999)
[25] Á. Kövér, G. Laricchia, Phys. Rev. Letters 80, 5309 (1998)
[26] J. Barakdar, Phys. Rev. Letters 81, 1393 (1998)
[27] D. Hagena, R. Ley, D. Weil, G. Werth, W. Arnold, H. Schneider, Phys. Rev. Letters 71, 2884 (1993)

## 5.3.2. POSITRONIUM PHYSICS AS A TEST OF QED

R. Ley (Mainz)

Positronium (Ps ,$e^+e^-$) is the bound state of an electron and its antiparticle, the positron. Both constituents are pointlike structureless leptons. The absence of structure avoids the difficulties encountered in hydrogen due to the compositeness of the proton. The advantage, compared with muonium ($\mu^+e^-$) , is the absence of an additional free parameter like the muon mass. Positronium is completely described by only two fundamental constants [1], the Rydberg constant

$c \times R_\infty = mc^2\alpha^2/2h$ = 3 289 841 960. 367 5 (250) MHz

and the finestructure constant

$\alpha = \mu_0 ce^2/2h$ = 1 / 137. 035 999 76 (50) .

The weak interaction and quantum chromo dynamics (QCD) play no role at the present level of accuracy.

Moreover positronium is an eigenstate of the charge conjugation operator. As a consequence real and virtual annihilations lead to additional Feynman diagrams which are absent in hydrogen and muonium, but can easily be tested in positronium.

For all these reasons positronium is an ideal candidate for a test of bound state QED. Only the yet uninvestigated system antimuon-muon ($\mu^+\mu^-$) would have comparabel qualities.

The S- and P-state energy levels of positronium have been completely calculated [2] up to the order $R_\infty\alpha^4$ . In the next higher order $R_\infty\alpha^5$ only the leading logarithmic contribution is known. The uncertainty of the theoretical calculations is an estimate of the uncalculated terms which amount to 700 kHz for the ground state and to 90 kHz for the 2S-state, the 2P-states are accurate to 10 kHz.

In table 1 some measured spectroscopic quantities of positronium are compared with theory.

Table 1 : Comparison between experiment and theory for some transition frequencies and energy level differences. The uncertainties of the theoretical calculations are estimates of the yet uncalculated higher order contributions. Where two values are given for the experimental error the first value is only statistical and the second is systematical.

| | Experiment [MHz] | Theory [MHz] [2] |
|---|---|---|
| $1^3S_1 \Rightarrow 2^3S_1$ | 1 233 607 216. 40 (320) [3] | 1 233 607 222. 17 (60) |
| $1^3S_1 \rightarrow 1^1S_0$ | 203 389. 10 (74) [4] | 203 392. 01 (50) |
| $2^3S_1 \rightarrow 2^1S_0$ | Not yet measured | 25 424. 672 (60) |
| $2^3S_1 \rightarrow 2^3P_0$ | 18 499. 65 (120)(400) [5] | 18 498. 246 (90) |
| $2^3S_1 \rightarrow 2^3P_1$ | 13 012. 42 (67)(154) [5] | 13 012. 407 (90) |
| $2^3S_1 \rightarrow 2^3P_2$ | 8 624. 38 (54)(140) [5] | 8 626. 709 (90) |
| $2^3S_1 \rightarrow 2^1P_1$ | 11 180 (5)(4) [5] | 11 185. 372 (90) |
| $\lvert 2^3P_0 - 2^3P_1 \rvert$ | 5 487. 23 (140)(430) [5] | 5 485. 839 (10) |
| $\lvert 2^3P_2 - 2^3P_1 \rvert$ | 4 388. 04 (86)(210) [5] | 4 385. 698 (10) |
| $\lvert 2^1P_1 - 2^3P_1 \rvert$ | 1 832 (5)(4) [5] | 1 827. 035 (10) |

From table 1 it is clearly demonstrated that the experimental uncertainties must be reduced to improve the comparison with theory. The agreement between theory and experiment is satisfactory, with one exception: The measured hyperfine splitting of the ground state is four standard deviations below the theoretical calculation. Therefore a measurement of the hyperfine splittng in the excited state at 25 MHz is desirable. This can be done with the same technique that we used for the other fine structure transitions [5].

Some further transitions are of interest which involve the excited state n = 3 , where a degeneracy between $3^3P_2$ and $3^3D_2$ occurs up to the order $R_\infty\alpha^2$.

Other interesting quantities of positronium are the annihilation rates into gamma quanta. For the decay rate $\lambda_3$ of ortho-positronium into three gamma quanta ($1^3S_1 \rightarrow 3\gamma$) there exists a long lasting and well established discrepancy (more than five standard deviations) between the measurements of the Ann Arbor group [6, 7] and the theory [8]. This discrepancy has triggered an intense search for exotic and forbidden decays of ortho-positronium which resulted in an exclusion limit for such decays much below $10^{-3}$. It is now experimentally proved that exotic decays can not explain the discrepancy in the decay rate of ortho-positronium. On the other hand a group in Tokyo has reported a decay rate measurement in agreement with theory [9]. To overcome the controversial situation completely new experiments are necessary which differ from the old measurements by possible systematic errors. At the moment there exist three proposals (Mainz, Fulda) which all need high positron intensities as produced by a LINAC:

1. Look at the decay of a large ensemble of positronium atoms confined simultaneously in a high vacuum apparatus.
2. Use a Lyman-$\alpha$ photon from the excited state n = 2 as a start pulse for positronium formation in the ground state.
3. Use a fast beam of positronium atoms produced by ionisation of an accelerated beam of negative positronium ions ($Ps^- = e^+e^-e^-$).

Another approach to clarify the situation with the decay of ortho-positronium is proposed by Baryshevsky (Minsk) who will look at the spatial distribution of the decay gamma quanta from polarized positronium.

In table 2 the measured decay rates of ground state positronium and the theoretical predictions are compared. For completeness some data on the positronium negative ion are included.

Table 2 : Comparison between experiment and theory for the decay rates of ortho- and para-positronium. The uncertainties of the theoretical calculations are estimates of the yet uncalculated higher order contributions. Where two values are given for the experimental error the first value is only statistical and the second is systematical. $\lambda_3$ and $\lambda_5$ are the allowed decay rates of ortho-positronium into three and five gamma quanta respectively. $\lambda_2$ and $\lambda_4$ are the allowed decay rates of para-positronium into two and four gamma quanta.

| | Experiment [$s^{-1}$] | Theory [$s^{-1}$] |
|---|---|---|
| $\lambda_3$ ($1^3S_1 \rightarrow 3\gamma$) | 7. 051 4 (14) $\times 10^6$ [6]<br>7. 048 2 (16) $\times 10^6$ [7]<br>7. 039 8 (29) $\times 10^6$ [9] | 7. 039 934 (20) $\times 10^6$ [8] |
| $\lambda_5$ ($1^3S_1 \rightarrow 5\gamma$) | 2. 2 ($^{+2.6}_{-1.6}$)(5) $\times 10^{-6}\ \lambda_3^{(0)}$ [10] | 0.959 1 (8) $\times 10^{-6}\ \lambda_3^{(0)}$ [10] |
| $\lambda_2$ ($1^1S_0 \rightarrow 2\gamma$) | 7. 990 9 (17) $\times 10^9$ [11] | 7. 989 50 (2) $\times 10^9$ [12] |
| $\lambda_4$ ($1^1S_0 \rightarrow 4\gamma$) | 1. 50 (11) $\times 10^{-6}\ \lambda_2^{(0)}$ [13, 14] | 1. 479 3 (18) $\times 10^{-6}\ \lambda_2^{(0)}$ [14] |
| $Ps^- \rightarrow 1\gamma + e^-$ | Not yet measured | 0. 088 [15] |
| $Ps^- \rightarrow 2\gamma + e^-$ | 2. 09 (9) $\times 10^9$ [16] | 2. 090 8 $\times 10^9$ [17, 18] |
| $Ps^- \rightarrow 3\gamma + e^-$ | Not yet measured | 1. 77 $\times 10^6$ [19] |

**References:**


[1] P.J. Mohr, B.N. Taylor, „CODATA Recommended Values of the Fundamental Physical Constants“ in Rev. Mod. Phys. **72** (April 2000), or in: Physikalische Blätter (March 2000)
[2] A. Czarnecki, K. Melnikov, A. Yelkhovsky, Phys. Rev. A **59** (1999) 4316
[3] M.S. Fee et al. , Phys. Rev. Lett. **70** (1993) 1397 and Phys. Rev. A **48** (1993) 192
[4] M.W. Ritter et al. , Phys. Rev. A **30** (1984) 1331
[5] D. Hagena, R. Ley, D. Weil, G. Werth, W. Arnold, H. Schneider, Phys. Rev. Lett. **71** (1993) 2887 and Hyp. Int. **89** (1994) 327
[6] D.W. Gidley et al. , Phys. Rev. A **40** (1989) 5489 : Ann Arbor measurement in gases
[7] D.W. Gidley et al. , Phys. Rev. Lett. **65** (1990) 1344 : Ann Arbor measurement in vacuum
[8] G.S. Adkins, R.N. Fell, J. Sapirstein, Phys. Rev. Lett. **84** (2000) 5086
[9] S. Asai et al. , Phys. Lett. B **357** (1995) 475 : Tokyo measurement in $SiO_2$ powder
[10] T. Matsumoto et al. , Phys. Rev. A **54** (1996) 1947
[11] A.H. Al-Ramadhan, D.W. Gidley, Phys. Rev.Lett. **72** (1994) 1632

[12] A. Czarnecki, K. Melnikov, A. Yelkhovsky, Phys. Rev. Lett. **83** (1999)1135
[13] H. von Busch et al. , Phys. Lett. B **325** (1994) 300
[14] S. Adachi et al. , Phys. Rev. A **49** (1994) 3201
[15] M.-C. Chu, V. Pönisch, Phys. Rev. C **33** (1986) 2222
[16] A.P. Mills, Jr., Phys. Rev. Lett. **50** (1983) 671
[17] Y.K. Ho, Phys. Lett. A **144** (1990) 237
[18] A.M. Frolov, J. Phys. B **26** (1993) 1031
[19] G. Ferrante, Phys. Rev. **170** (1968) 76

## 5.3.3. ANISOTROPIC PHENOMENA IN ORTHO-POSITRONIUM DECAY

V. Baryshevsky (Minsk)

**Introduction**

Hydrogen-like atoms are traditional objects for developing models and methods in quantum mechanics and quantum field theory. At the same time the characteristics measured for these atoms are among the most precisely measured physical quantities in modern science. The lightest hydrogen-like atom positronium (Ps) is the bound electron-positron state and the ideal system for testing the quantum electrodynamics of bound state, because of absent of nucleus. The interaction with nucleus can not be calculated with the necessary accuracy at the present state of theoretical physics.

The measurements of ortho-positronium decay rate, carried out more than 20 years ago, have revealed the disagreement with the theory [1,2]. Up to now any experimental tests using of positronium atom are very interesting because of possibility of other discrepancies.

It is well known, that the decay of particle with spin 1 (like orthopositronium is) is described by three complex decay amplitudes. Orthopositronium decay rate is proportional to the sum of the squared decay amplitudes. Thus, only this value has been measured until now. The difference this amplitudes from each other leads to anisotropy of three-photon decay. Therefore measurements of anisotropic phenomenon in o-Ps decay will allow us to obtain information about orthopositronium decay amplitudes.

The present projects suggest to investigate thoroughly anisotropic (spin-dependent) properties of orthopositronium decay and to measure for the first time the vacuum decay amplitudes.

All fundamental experiments with positronium require high statistics to provide sufficient accuracy that lead to the necessity to have intensively positron beam. Slow positron beam is usually used to reduce the systematic error. It is especially true for the measurements of anisotropic phenomenon in orthopositronium decay because the statistics of such experiments must be approximately 25 time as much as the statistics in the decay rate experiments to reach the same accuracy.

**The project descriptions:**

**a) near future**

**Precision measurements of the positronium decay amplitudes as a new quantum electrodynamics test**

1. **Planned experiment:** We would like to measure the orthopositronium decay amplitudes corresponding to three projections of orthopositronium spin (m=0, ±1) separately. It would allow us to find up which of the annihilation amplitudes (or all together) is responsible to the well-known discrepancy between theoretically calculated and measured orthopositronium decay rate.

2. **Description of the experiment:** It is proposed to measure anisotropy of angular distributions of annihilation photons created by aligned orthopositronium. It would allow us to calculate the ratios of annihilation amplitudes and compare them to the theoretically calculated values.

   The technique of the experiment is like that. Positrons slow down in silica aerogel and create positronium atoms. An external magnetic field quenches the m=0 orthopositronium state. It leads to the difference in the averages numbers of positrons with m=0 and m=±1 spin projections to the magnetic field direction. It is necessary to measure the three-photon coincidence rates under three different perpendicular one to another directions of the magnetic field. The angles between detectors must be different from 120°. Theoretically estimated difference in the count rates in the magnetic field $H \sim 3.5$kG is about 15%. It is necessary to measure the value of the anisotropy with the accuracy not worse than accuracy of the Michigan experiments.

The experimental procedure is described more thoroughly in ref [3].

3. **Planned beamtime:** We are going to use our 32-detector spectrometer "ARGUS" for the measurements of three-photon coincidence rates. It allows us to detect the count rates of 180 suitable triades of detectors simultaneously. We would expect to require about one month and two weeks for the assembling, testing and calibrating of the crystal ball (beam time is not required on this stage of the experiment). It is necessary to have about two-three weeks to obtain a good statistics under the beam intensity about $10^8$ $e^+$/sec.

**Search of CP- and CPT-violations in orthopositronium decay**

1. **Planned experiment:** Measurements of the CP- and CPT-violating correlations in orthopositronium decay in the external electric and magnetic fields.

2. **Description of the experiment:** We would examine possible violation CP- and CPT- symmetry in orthopositronium decay. Previous experiments on CP- and CPT- violation searching were performed by Michigan group [4]. These results can be improve significantly because of - higher intensity of positron beam, - use of crystal ball spectrometer, - performing the experiment in external electric and magnetic fields.

It would be possible to improve the accuracy of the Michigan experiment by 100 times when using a source of ~$10^8$ **polarized** positrons per second and a 30 detector crystal ball set-up.

3. **Planned beamtime:** We would expect to require about two weeks to collect good statistics. The time for the assembling, testing and calibrating of the crystal ball would not be necessary if this experiment performed just after the experiment described above.

**b) far future:**

**Observation of positronium spin rotation in condensed media**

**1. Planned experiment:** Measurements of the frequency, amplitude and dumping of time oscillations in positron annihilation lifetime spectra in condensed media. These oscillations appearing due to positronium spin oscillations in an external magnetic field and anisotropy of the angular distribution of orthopositronium decay quanta. They contain important information about positronium hyperfine interactions in media.

**2. Description of the experiment:** The physical nature of the oscillations under positronium annihilation is like that of the well-known muon spin rotation method. The oscillations have been observed in experiments by our group [5] and by Hong-Kong group [6]. We used silica aerogel as positronium-creative sample because only three-photon decay quanta contain information about the oscillations. It is proposed to measure these oscillations in polymers or in semiconductors where the lifetime of longlived part of the spectra is shorter. Pulsed polarized positron beam would be required. To eliminate the background related to two-photon annihilation it is necessary to use at least two detectors registering decay photons placed at the angle differ from 180° to one another.

**3. Planned beamtime:** The required statistics is about $10^5$ registered three-photon annihilation events per one period of oscillations. It is quite high because the majority of orthopositronium decay through two-photon channel due to pick-off annihilation and ortho-para conversion. We would expect to require about two weeks for testing the equipment. The time for collecting a lifetime spectrum would be about three-four hours. One weak would be enough to collect spectra for different samples and different values of an external magnetic field (different periods of oscillations).

**Exchange splitting of orthopositronium m = ±1 levels in optically polarised gases**

**1. Planned experiment:** Observation of m=±1 orthopositronium levels in optically polarized gases. It has been shown [7] that exchange interaction between electron of positronium and electron of polarized media leads to the splitting of degenerating m=±1 orthopositronium levels. This phenomenon is the atomic analogon of the well-known phenomena of neutron spin rotation by polarized nucleus predicted by Baryshevsky and Podgoretsky and observed by Abraham and Forte.

**2. Description of the experiment:** Positronium was created in polarized state by a laser beam gas. The exchange interaction between electron of positronium and electrons of gas responsible to the ortho-para conversion leads also in the case of polarized gas electrons to the splitting of m=±1 orthopositronium levels. The exchange splitting is the result of coherent exchange interaction between electron of positronium and electron of gas therefore it is much stronger then noncoherent scattering that leads to ortho-para conversion. The value of the splitting depends on the polarization of gas electrons and on the kind of gas used. It is possible to use one of the following techniques for the experiments. In the first one the microwave induced transition between m=0 and m=±1 orthopositronium states in magnetic field would be observed. The second one would require registering of two frequency oscillations in positronium lifetime spectrum in a magnetic field.

**3. Planned beamtime:** It would require about two weaks for set-up and testing. The necessary statistics would be obtained in a day or two.

**References:**


1. A.Rich, Rev.Mod.Phys **53** (1981) 127
2. C.I.Westbrook, D.W.Gidley, R.S.Conti, A.Rich, Phys.Rev.Lett. **58** (1987) 1328
3. V.G. Baryshevsky, O.N. Metelitsa, Acta Physica Polonica **A88** (1995) 73
4. B.K. Arbic, S.Hatamian, M.Skalsey et al., Phys.Rev**. A37** (1988) 3189
5. S.K.Andrukhovich, V.G.Baryshevsky et al., Phys.Lett. **136** (1989) 428
6. S.Fan, C.D.Beling, S.Fung, Phys.Lett, **A216** (1996) 129
7. V.G.Baryshevsky, A.V.Ivashin, Zh. Eksper. Theor. Fiz. **65** (1973) 1467
   (see also: V.G.Baryshevsky, Physica Status Solidi **(b) 124** (1984) 619)

# 6. LAYOUT OF POSITRON LABORATORY

## 6.1. ELBE / Rossendorf

G. Brauer (Dresden)

A general sketch of the ELBE arrangement is presented in Figure 1.

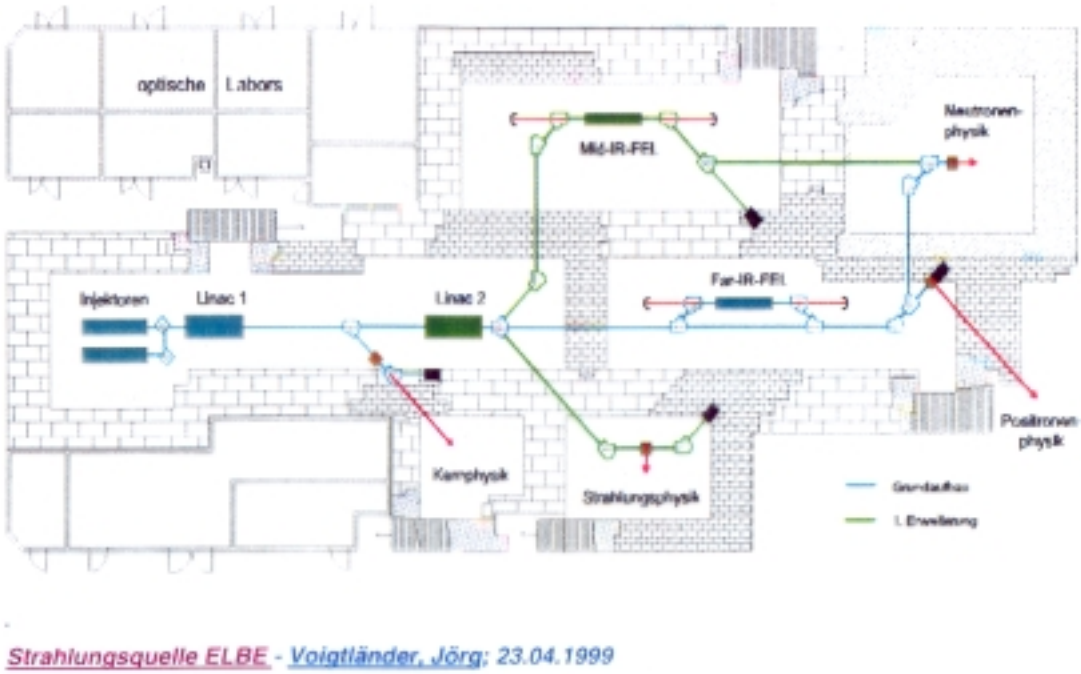


**Fig. 1** Sketch of the ELBE arrangement, with indication of the place to be used for positron physics (Positronenphysik)

Already during 1998, and based on the ELBE plan dated 18.02.1998, the possible location of a positron laboratory and arrangement of the required electron beam line, target chamber and positron beam line have been considered in detail (Figs. 2 and 3).

Starting from a switching magnet, a short electron beam line has to be installed. Thereby a variation of the beam position has to be guaranteed in order to hit the target used for positron production properly. To separate the electron beam line regarding vacuum and electric potential from the target chamber and positron beam line, the electron beam has to travel a short distance in air. At the target chamber, bremsstahlung is produced, and via pair production the positrons are formed. These positrons are to be moderated and formed into a positron beam which has to be guided into the positron laboratory. For more details about this procedure, please, see chapter 3.

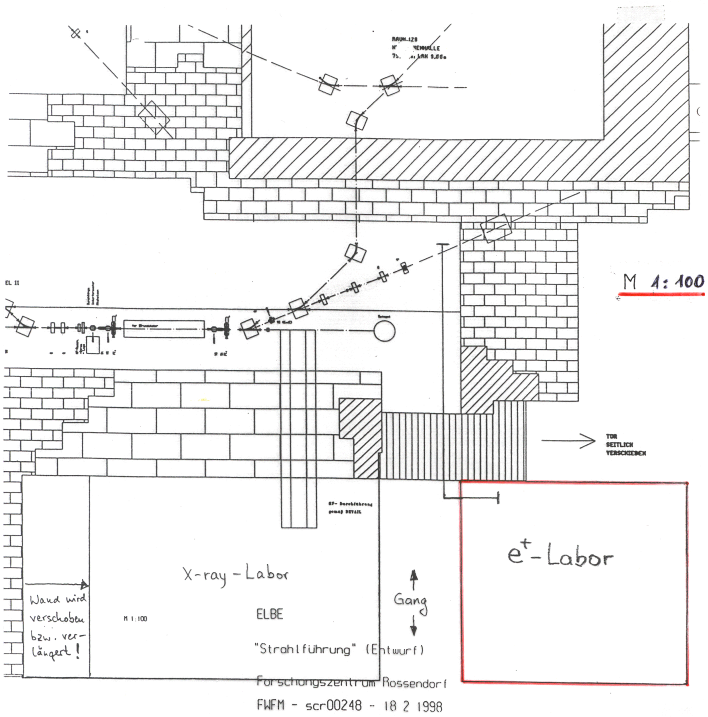


**Fig. 2** Possible location of a positron laboratory at ELBE.

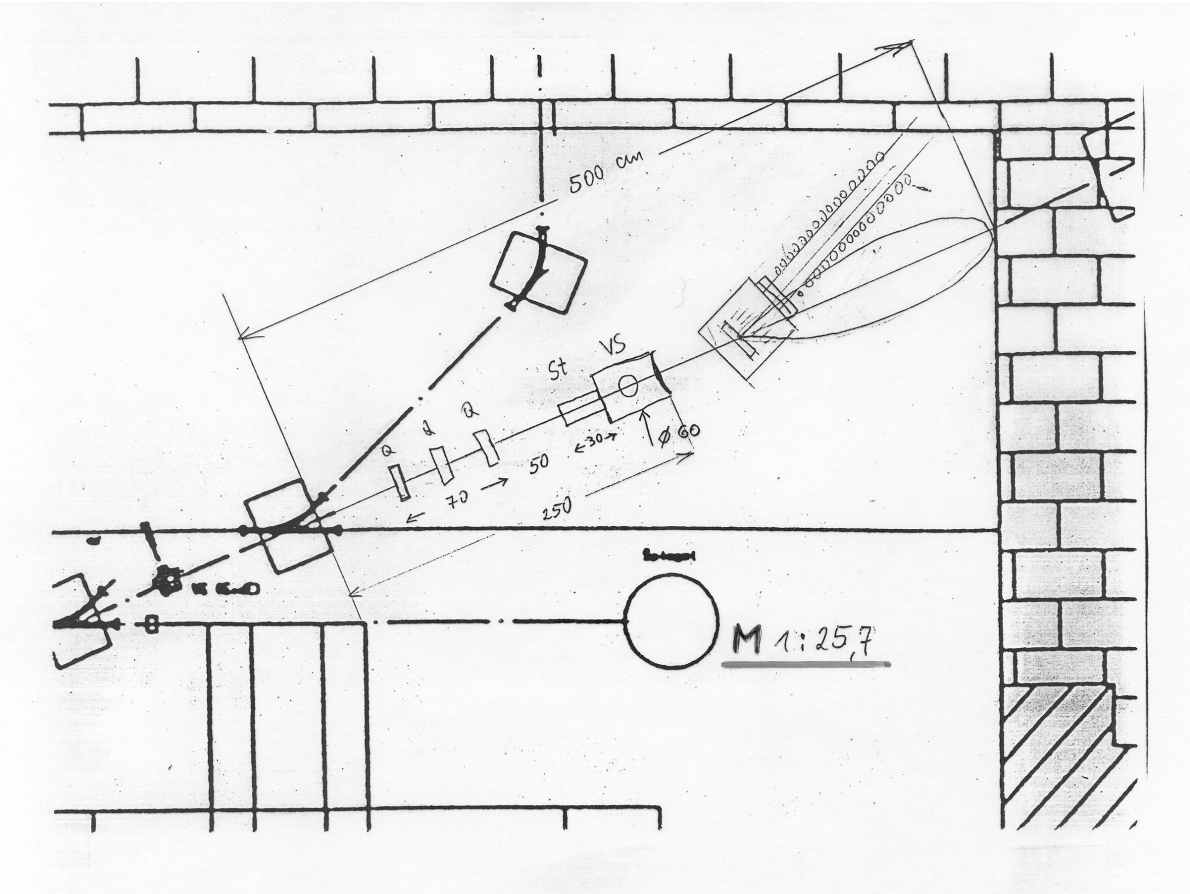


**Fig. 3** Detailed arrangement of separate electron beam line (Q = quadrupole lens, St = steering magnet, VS = view screen), target chamber for positron production (bremsstrahlungs cudgel indicated), and positron beam line with solenoid indicated.

## 6.2. TTF / Hamburg

K. Flöttmann (Hamburg)

The “Tesla Test Facility” (TTF) at DESY Hamburg is a superconducting linear accelerator serving as a test bed for the future TESLA project [1] (TeV Energy Superconducting Linear Accelerator, an electron-positron collider with an integrated free-electron laser in the X-ray wavelength range). In its final stage the 300m long linear accelerator will provide a very intense electron beam to drive a VUV FEL. The electron beam has a planned energy of 1 GeV and a power of 72 kW. The TTF will serve an FEL user facility, hence it is intended to run also after the completion of TESLA. Fig. 1 shows the overview of TTF as a top view.

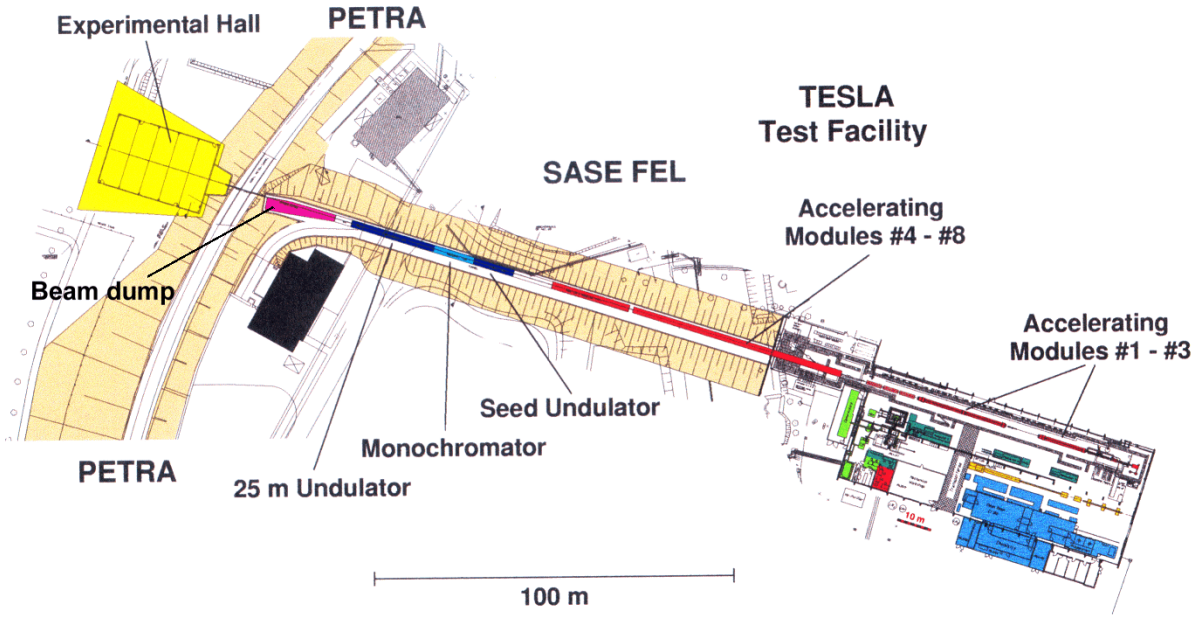


**Fig. 1** An overview of the “Tesla Test Facility” (TTF) at DESY, Hamburg. The assembly of the system is completed for the first three accelerating stages and is in an advanced state for the remaining part. The TTF Experimental Hall is used as exhibition hall for the EXPO 2000 until the end of October 2000. The electron beam is fed after the 25m long undulator into the beam dump where the slow positron beam line may start.

The electron beam will be stopped in the beam dump where positrons are generated by pair production. A possible slow-positron beam must be generated in a moderator stage in this beam dump area (see Chapter 3). The experimental setup could be arranged in the FEL Experimental Hall (yellow in Fig. 1) or in Bldg. 49 (black in Fig. 1) close to the TTF tunnel. However, it should be noted that presently a slow positron source is not a part of the TTF project.

[1] see “Conceptual Design Report for the TESLA Test Facility (TTF) Linac”, Version 1.0, available at http://tesla.desy.de/TTF_Report/CDR/TTFcdrTab.html
[2] further information under http://tesla.desy.de/

## 7. RADIATION PROTECTION AT THE POSITRON LABORATORY

W. Anwand (Dresden)

The positron beam hitting a solid (sample or moderator) emits high energy γ rays. Those ionizing γ rays need to be shielded. The calculation of the required shielding is based on the following assumptions:

- activity of the beam 1 GBq ($10^9$ $e^+$/s)
- energy of the annihilation radiation 511 keV
- exposure rate behind the shielding 1 µSv/h
- Pb as material of the shielding
- a point source of radiation.

Secondary or scattered γ ray in the attenuating material is not taken into account because of the small influence of these effects on the thickness of the radiation shielding.

The exposure rate *R* due to a point source is proportional to the energy of emitted γ photons. The exposure rate decreases as the inverse of the square of the distance from the radiation source. A simple formula to calculate the exposure rate in free space is given in [1]:

$$R = \frac{const \times C \times E_\gamma}{d^2} \qquad (1)$$

where *R* is the exposure rate, *C* is the activity, $E_\gamma$ is the photon energy and *d* is the distance from the radiation source. The coefficient *const* depends on the measures used. In the presence of attenuating materials, the equation becomes:

$$R(mSv/h) = \frac{0.151 \times C(GBq) \times E_\gamma(MeV)}{d^2(m^2)} \times e^{-\mu\rho t} \qquad (2)$$

where $\mu$ is the total $\gamma$ray mass attenuation coefficient, $\rho$ is the density of the shielding material, and *t* its thickness. The measures used for the calculations are given in the brackets.

In case of Pb $\mu$ is equal to 0.140 $cm^2/g$ and $\rho = 11.34$ $g/cm^{-3}$. Using equation (2), and assuming a maximum exposure rate *R* = 1 µSv/h (about 4 x natural exposure rate) the thickness *t* of the Pb shielding was calculated in dependance on the distance *d* from the area of the radiation creation as shown in fig.1.

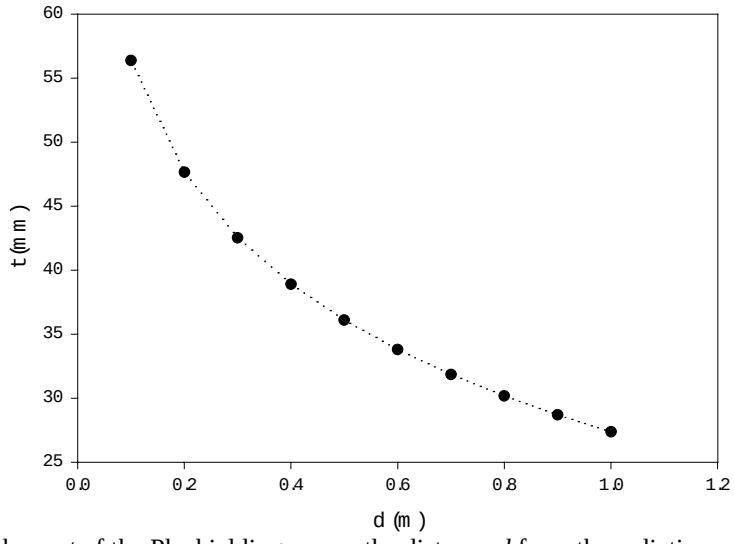


Fig.1 Calculated thickness *t* of the Pb shielding versus the distance *d* from the radiation source

It is seen that a Pb shielding of less than 60 mm (about 14 half width's) is completely sufficient to weaken the γ radiation to an acceptable value. In case of the sample chamber it is necessary to realize a greater distance

between sample and wall of the chamber in order to avoid that reemitted positrons contribute to the measurements. For this reason, a thinner Pb shielding of 48 mm (11 half width‘s) can be used.

The radiation protection at the site of the positron production has not been considered in the frame of this contribution. This has to be done later as such a calculation requires information about the geometry and the design of the positron source, the target region, and about the used materials which is not avaible at this early phase of the conceptional report.

At least two problems are seen:

- the activation of the material in the surrounding of the location of positron production,

and

- the creation of ozone in the target region (information from Gießen, H. Schneider).

**References**

[1] J.Shapiro, Radiation Protection (Harvard University Press, Massachussettes, 1972)

# 8. ESTIMATION OF FINANCIAL REQUIREMENTS

G. Brauer (Dresden)

A prerequisite to start any positron project at ELBE would be the provision of a positron laboratory („positron hut“) in the ELBE building, i.e. a room having the assumed dimension (basic area) of about 50 $m^2$ and a height of about 3.50 m. The costs to build such a positron hut, including air conditioning and provision of media, like electricity, water, and may be pressurized gases, may vary in the limits 300-500 DM/$m^3$. As the room having the assumed dimensions contains 175 $m^3$, one will arrive at costs in the limits 52.500-87.500 DM. In other words, assuming **100.000 DM** necessary for building the **positron hut** one would be on the safe side.

Costs for the stretch from **magnetic switch to target chamber** (electron beam line) have been evaluated to be about **150.000 DM**. This estimate is based on the assumption that standard parts available for vacuum tubes and LINAC construction from the Rossendorf project group ELBE will be used. Production and assembly then should be coordinated by this group too. Doing the construction of the required electron beam line this way would have the advantage of being part of the maintenance scheme of the whole LINAC, i.e. no separate service at extra costs will be required. Any other solution would cost more money and efforts for later maintenance.

Costs for the stretch **target chamber to positron laboratory** have roughly been estimated to be about **350.000 DM**. The design of the target chamber and the positron beam line is known and almost fixed in principle although still several simulations and evaluations for optimization of the design have to be performed. After final fixing of the construction, manufacturing will be arranged by contract elsewhere in industry.

The realization of this part of the project is the most challenging and critical one as it is the basis of any further application of the intense positron beam. Costs and efforts to establish this at TTF should be more or less of the same order, i.e. about **600.000 DM** as a minimum. It is thought that the realization will be possible within **18 months**.

Having an intense positron beam available in a positron hut, the suggested experiments in atomic physics (see chapter 5.3.) can be performed easily. The necessary equipment will be provided by the potential users for the duration of their experiments and is already available, i.e. has to be moved to the corresponding location where the intense positron source will be constructed.

More difficult, but mostly desired, will be the construction of an efficient user facility for materials science (see chapter 5.1.). As there is no complete equipment commercially available, it has to be build up in the frame of one or more separate projects where potential users share efforts and costs. It seems to be realistic to assume for this period a duration of at least **24 months**, at costs of at least **500.000 DM**. Hereby it has to be considered and debated if costs for e.g. beam line, beam switching, vacuum generation and control, etc. have to be considered as basic investment or part of a certain experimental setup to be constructed for a given user facility/experiment. Such investment costs might be requested and to be covered from the host institution (FZ Rossendorf or DESY) and would add to the costs required for building a ‚positron hut‘.

It has been discussed and considered very useful to have an active positron group working in materials science at the location where the intense positron beam is installed. This fact would favour a realization at FZ Rossendorf (ELBE), as at DESY (TTF) no positron group exists and no plans to install such a group in the future are known.

The installation of very sophisticated equipment required for surface studies (see chapter 5.2.) would be relatively easy as all parts are commercially available. For example, plain investment costs would be around **300.000 DM** for assembling a positron reemission microscope, whereas an up-to-date installation for PAES would cost around **700.000 DM**. However, it should be noticed that such type of extremely sensitive equipment might not be operated as a user facility without having at least one permanent specialist at the location who cares for operation and maintenance. Furthermore, beam switches in the positron laboratory need to be build and installed if several users and equipments will be permanently installed. This will require some extra costs and manpower once which have not been considered yet.

As a general conclusion it has to be stated, that based on agreement among the positron community a certain project of a user facility has to be worked out now which has to be discussed and agreed with the future potential host institutions (FZ Rossendorf or DESY). And only by such a detailed project one can be more specific regarding definite requirements of finances and manpower for its realisation. Expected costs may be higher than roughly estimated above but should not increase by an order of magnitude.

## 9. ADDRESSES OF CONTRIBUTORS


**Anwand**
Institut für Ionenstrahlphysik und
Materialforschung
Forschungszentrum Rossendorf
Postfach 51 01 19
01314 Dresden
Germany

**V. Baryshevsky**
Institute of Nuclear Problems
Belorussian State University
Bobruiskaya 11
Minsk 22 00 50
Republic of Belarus

**C.D. Beling**
Department of Physics
University of Hong Kong
Pokfulam Road
Hong Kong
P.R.China

**G. Brauer**
Institut für Ionenstrahlphysik und
Materialforschung
Forschungszentrum Rossendorf
Postfach 51 01 19
01314 Dresden
Germany

**R.S. Brusa**
Istituto Nazionale di Fisica della Materia
Dipartimento di Fisica
Universita‘ di Trento
38050 Povo TN
Italy

**P.G. Coleman**
Department of Physics
University of Bath
Claverton, Down Bath BA2 7AY
U.K.

**K. Flöttmann**
DESY
Notkestr. 85
22603 Hamburg
Germany

**P. Hautojärvi**
Laboratory of Physics
Helsinki University of Technology
P.O.Box 1100
02015 Hut
Finland

**R. Hippler**
Institut für Physik
Ernst Moritz Arndt Universität Greifswald
Domstr. 10a
17487 Greifswald
Germany

**G.P. Karwasz**
Istituto Nazionale di Fisica della Materia
Dipartimento di Fisica
Universita‘ di Trento
38050 Povo TN
Italy

**G. Kögel**
Institut für Nukleare Festkörperphysik
Universität der Bundeswehr München
85577 Neubiberg
Germany

**R. Krause-Rehberg**
Fachbereich Physik
Martin - Luther - Universität Halle-Wittenberg
06099 Halle (Saale)
Germany

**R. Ley**
Institut für Physik
Johannes Gutenberg - Universität Mainz
Postfach
55099 Mainz
Germany

**K. Maier**
Institut für Strahlen- und Kernphysik
Universität Bonn
Nußallee 14-16
53115 Bonn
Germany

**A. Osipowicz**
Fachbereich Elektrotechnik
Fachhochschule Fulda
Marquardtstr. 35
36039 Fulda
Germany

**I. Prochazka**
Department of Low Temperature Physics
Charles University
V Holesovickach 2
18000 Prague 8
Czech Republic

**H. Schneider**
Institut für Kernphysik - Strahlenzentrum
Justus - Liebig - Universität Giessen
Leihgesterner Weg 215
35392 Giessen
Germany

**D. Segers**
Department of Subatomic and Radiation Physics
University Gent
Proeftuinstraat 86
9000 Gent
Belgium

**P. Sperr**
Institut für Nukleare Festkörperphysik
Universität der Bundeswehr München
85577 Neubiberg
Germany

**H. Stoll**
Max-Planck-Institut für Metallforschung
Heisenbergstr. 1
70569 Stuttgart
Germany

**A. Zecca**
Istituto Nazionale di Fisica della Materia
Dipartimento di Fisica
Universita‘ di Trento
38050 Povo TN
Italy